1-1-2010

Nanoporous High Surface Area Silicas With Chelating Groups For Heavy Metal Ion Adsorption From Aqueous Solution

Kothalawalage Nuwan Kothalawala
Eastern Illinois University

THESIS MAINTENANCE AND REPRODUCTION CERTIFICATE

TO: Graduate Degree Candidates (who have written formal theses)

SUBJECT: Permission to Reproduce Theses

The University Library is receiving a number of request from other institutions asking permission to reproduce dissertations for inclusion in their library holdings. Although no copyright laws are involved, we feel that professional courtesy demands that permission be obtained from the author before we allow these to be copied.

PLEASE SIGN ONE OF THE FOLLOWING STATEMENTS:

Booth Library of Eastern Illinois University has my permission to lend my thesis to a reputable college or university for the purpose of copying it for inclusion in that institution's library or research holdings.

Author's Signature

05/05/10

Date

I respectfully request Booth Library of Eastern Illinois University **NOT** allow my thesis to be reproduced because:

_____

_____

_____

_____ _____

Author's Signature Date

This form must be submitted in duplicate.

Nanoporous high surface area silicas with chelating groups

for heavy metal ion adsorption from aqueous solution

(TITLE)

BY

Kothalawalage Nuwan Kothalawala

THESIS

SUBMITTED IN PARTIAL FULFILLMENT OF THE REQUIREMENTS
FOR THE DEGREE OF

Masters in Chemistry

IN THE GRADUATE SCHOOL, EASTERN ILLINOIS UNIVERSITY
CHARLESTON, ILLINOIS

2010

YEAR

I HEREBY RECOMMEND THAT THIS THESIS BE ACCEPTED AS FULFILLING
THIS PART OF THE GRADUATE DEGREE CITED ABOVE

4/27/10	5/4/10
THESIS COMMITTEE CHAIR — DATE	DEPARTMENT/SCHOOL CHAIR OR CHAIR'S DESIGNEE — DATE
4/27/10	
THESIS COMMITTEE MEMBER — DATE	THESIS COMMITTEE MEMBER — DATE
04/27/10	4/27/10
THESIS COMMITTEE MEMBER — DATE	THESIS COMMITTEE MEMBER — DATE

Abstract

NANOPOROUS HIGH SURFACE AREA SILICAS WITH CHELATING GROUPS FOR HEAVY METAL ION ADSORPTION FROM AQUEOUS SOLUTION

Nanoporous high surface area silicas are an ideal substrate for the design of materials with useful properties via chemical surface modification. The adsorption of heavy metals for contaminated water detoxification is one potential application. In this work we have used three different kinds of silica substrates with varying pore structures; commercially available narrow pore and wide pore silica gels, as well as surfactant templated mesoporous SBA-15 exhibiting a relatively narrow pore size distribution. These silicas have each been subjected to post-synthesis modification with an organosilane consisting of ethylenediamine triacetic acid functionalities for chelation/adsorption of metal ions from aqueous solution. The surface modified materials have been characterized by N_2 adsorption for the determination of surface area and pore size distribution and FTIR spectrometry to probe metal ion - surface bonding interactions with the help of computational calculations. Metal ion adsorption isotherms for Hg(II), Cd(II), Cu(II), Sr(II) and Cr(III) are reported. Previous studies have shown that post-synthesis modification of narrow pore silicas results in a significant reduction of surface area, with dramatically reduced adsorption capacity. In this work chemical surface modification has been achieved with little to no reduction in surface area, thus adsorption capacity remains high even for narrow pore silicas. Very large adsorption capacities,

approaching one gram Hg(II)/gram of silica have been achieved. Diffuse reflectance FTIR spectrometry show changes after metal adsorption indicating specific metal - organosilane interactions are responsible for adsorption.

Nanoporous high surface area silicas with chelating groups for heavy metal ion adsorption from aqueous solution

A Thesis

Submitted to the Faculty of Eastern Illinois University

in partial fulfillment of the requirements

for the degree of

Masters in Chemistry

Department of Chemistry

by

Kothalawalage Nuwan Kothalawala

Eastern Illinois University

Charleston, Illinois

2010

Supervisor: Dr. Jonathan P. Blitz

Table of Content

Chapter 3: Metal ion adsorption behavior of modified silica

List of Tables

Chapter 01: Introduction

Chapter 02: Modification and Characterization of Silica

Chapter 03: Metal ion adsorption behavior of modified silica

List of Figures

Chapter 03: Metal ion adsorption behavior of modified silica

Acknowledgement

I would like to express my deepest appreciation to my research advisor, Dr Johnathan Blitz for giving me the opportunity to work on this exciting project. Without his guidance and persistent support, this thesis would not have been possible. His intellectual and personal guidance influence me to think and work as a scientist in my career.

Also sincerely thank goes to the members of my defense committee, Dr S A Peebles, Dr S M Mitrovski and Dr D J Sheeran for taking the time to review this work. I would like to thank to the past and present members of Dr Blitz's group for the utmost support given to maintain the high quality research. Special thanks goes to Dr S M Mitrovski, Dr R F Semenuic and Dr M Jaroniec for the support given in experimental and data analysis.

My heartiest gratitude goes to my parents, and to my loving wife Vihara and her parents, for the encouragement given me especially during unbearable times in my life. Also I want to thank Dr Periyannan and all of my friends at Eastern Illinois University especially for Gishanthi, Dilani, Pramodha, Bimali and Laleen for the positive influence and assistance given to me throughout these years.

Finally I want to thank each and every individual of the Department of Chemistry at Eastern Illinois University for the tremendous support, guidance and the encouragement given to me.

Chapter 01

Introduction

1.1 Heavy metals and their impact on humans

It has been well established that mineral elements are essential for functioning of animal life. Beyond carbon, hydrogen, oxygen and sulfur or elements supplied by water, carbohydrates, lipids, fats and proteins, a lot of mineral elements play a distinct role in human and animal life (O'Dell & Sunde, 1997). These elements function as structural, catalytic and in signal transduction systems in humans (Metian, Warnau, HÃ©douin, & Bustamante, 2009). Depending on the requirement of these elements, they can be classified as macro and micro elements. Table 1.1 shows a list of macro and micro elements essential for our body with their importance (O'Dell & Sunde, 1997).

Most of these elements are metals. Even though these metals are essential to the human body, presence in elevated amounts can cause disease conditions (Thomas G. Spiro, 1980). Also some of these essential metals are known to be heavy metals. According to IUPAC classifications, heavy metals are also known as toxic metals (Duffus, 2002). They are individual metals that can affect negatively on people's health. It is very clear that these toxic metals play a great role in our day today life. Almost all of the toxic metals are bio-accumulators. This means that the concentration of these metals increase in the biological system over time. When the metals are taken in to the biological systems, they are stored much faster than they are either metabolized or excreted out of the cell. Toxic metals can replace other essential metals from enzyme binding sites. As a result of this, thousands of enzyme reactions are altered by either inhibiting or stimulating the enzymes. Further, these metal ions can substitute for the substances in other tissue

Element	Function
Macro elements	
Calcium	Structure of bone and teeth.
Phosphorous	Structure of bone and teeth. Used for ATP.
Sodium	Major electrolyte in extracellular fluids. Maintain osmotic balance and pH
Chloride	Major electrolyte in extracellular and intracellular fluids. Maintain osmotic balance and pH
Potassium	Major electrolyte in intracellular fluids. Maintain osmotic balance and pH
Magnesium	Structure of bone.
Micro elements	
Iron	Present in hemoglobin and myoglobin, which is required for oxygen transport.
Copper	Structural element in many enzymes.
Manganese	Major component in mitochondrial antioxidant enzymes.
Iodine	Required for the production of thyroxine, which is important in metabolic rate.
Zinc	A component in most of enzymes.
Selenium	Contained in anti oxidant enzymes.
Fluorine	Hardens tooth enamel and dentine.
Cobalt	Contained in Vitamin B 12.
Molybdenum	Contained in enzyme Xanthine oxidase.
Chromium	A cofactor needed for the regulation of sugar levels

Table 1.1 Macro and micro elements with their functions in humans (O'Dell & Sunde, 1997).

structures and are weakened by replacement process. They may also help to develop unwanted fungal, bacterial and viral infections (Goyer, 1997).

Toxic metal ions can enter into the human body by food, water, air or by absorption through the skin. So bioaccumulation of heavy metals in to the food chain begins with either fresh water or marine plants. Therefore toxic metal pollution in eco systems is becoming increasingly important in the 21st century.

1.2 How toxic metals come into the environment

Even though most of the toxic metals are found in the earth's crust, environmental pollution by these metals mainly takes place by human activities. They can reach to the environment through a variety of ways, as acid leaches of soil, smelting, electroplating, power generating, mining, by consumer products and by pigment industries. In the aquatic environment metals can exist as ionic, hydrated, sorbed, salts, or by complexes with a variety of naturally occurring organic acids. Normally the most toxic form of the metal is the ionic form. The metal ion concentration in aquatic environments will depend on the pH, suspended particles, other complexing materials, and the redox potential of the water (Adams, Chapman, & Landis, 1988). Among these toxic metals, this work focuses on Hg(II), Cd(II), Cr(III), Sr(II) and Cu(II) in this thesis.

1.3 Toxic metals

By looking at the toxic metal abundance and the effect from them on nature, the following metals have been used to find a method to eliminate them from the environment. Main characteristic features of these toxic metals have been summarized in

Table 1.2.

1.3.1 Mercury

Mercury is found naturally in the environment which comes from degassing of the earth's crust by volcanic emissions. It can exist in three forms, elemental mercury, organic and inorganic mercury. Mercury is a heavy metal that releases to the environment mainly on burning of coal for electric power generation. In addition, chloralkali plants and paper industries are significant producers of mercury (Fuhrmann, 1996). Trace amounts of mercury in coal, which does not burn but is volatile (i.e. enters the gas phase), is transported via lakes and rivers. This will allow the bioaccumulation of mercury in the food pyramid reaching toxic exposure to humans if they consume mercury contaminated fish. This is why there are warnings on eating too much large tuna for instance. Mercury affects the nervous system, cardiovascular system, immune system and reproductive system in the human body. Mercury is responsible for over 7000 diseases and can cause permanent brain and kidney damage, blindness, hearing, polyneuropathy, seizures, tremors and extreme shyness (Frackelton & Christensen, 1998).

1.3.2 Cadmium

Cadmium is a byproduct of the mining and smelting of lead and zinc. Mining and smelting, metal finishing, plastic industry, microlectronics, battery manufacture, and phosphate fertilizer production are the major industries that release cadmium to the environment. Nowadays three fourth of all cadmium is used to make batteries. Mainly cadmium can be found as Cd^{2+} in the aquatic environment. Cadmium, in particular, is

Element	Natural source	Anthropogenic source	Common forms in aquatic environment	Risks and disease conditions
Hg	Native metal (Hg), cinnabar (HgS), degassed from Earth's crust and oceans	Burning of coal, chloralkali plants, paper industries, electrolysis industry, plastic industry, refuse disposal/landfills and fungicides	Hg^{2+}, Hg_2^{2+}, Organo-Hg complexes	permanent brain kidney damage, blindness, deaf, polyneuropathy, seizures, tremors, birth defects and extreme shyness
Cd	Zinc carbonate and sulfide ores, copper carbonate and sulfide	Mining and smelting, metal finishing, plastic industry, microlectronics, battery manufacture, phosphate fertilizer	Cd^{2+}	respiratory track liver and kidney failure, osteomalacia, osteoporosis, hyphophosphatemia, arthritis, hyperuricemia, hyperchloremia and cancers
Cu	Native metal (Cu), chalcocite (Cu_2S) and chalcopyrite ($CuFeS_2$)	Mining and smelting, metal finishing, microelectronics, wood treatment, refuse disposal and landfills, pyrometallurgical industry, swine manure, pesticides and scrapheaps	Cu^{2+}, Cu^{+1}	hepatic or neurological diseases. Wilson disease, Oral large doses of copper is fatal
Sr	Celite and strontianite	Alloy industry, glass industry and nuclear by product	Sr^{2+}	necrosis lesions and cancers of bone and adjacent cells. High doses destroy the born marrow
Cr	Chromite ($FeCr_2O_4$) and eskolaite (Cr_2O_3)	Metal finishing, plastic industry, wood treatment, pyrometallurgical industry, landfills, scrapheaps	Cr^{3+} complexes with organic/inorganic ligands	larger quantities can be moderately harmful

Table 1.2: Summary of toxic metals studied here with their sources, common forms and health effects.

located just below zinc in the periodic table of the elements, so its atomic structure is very similar to that of zinc. It almost fits perfectly in the zinc binding sites of critical enzymes such as RNA transferase, carboxypeptidase, alcohol dehydrogenase and alters their function in the body. Target organs are the liver, kidneys, placenta, brain, lungs, and bones. The common effects and side effects are respiratory track, liver and kidney failures sometimes fatal, osteomalacia, osteoporosis, hyphophosphatemia, arthritis, hyperuricemia and hyperchloremia. In addition, this is a carcinogenic metal which can cause cancers (Asagba & Obi, 2005; Nogawa, Kobayashi, Okubo, & Suwazono, 2004).

1.3.3 Copper

Most of the copper metals are extracted from large open pit mines as copper sulfides that contain 0.4 to 1.0 percent of copper. Copper is mainly released to the environment from mining and smelting, metal finishing, microelectronics, wood treatment, refuse disposal and landfills, pyrometallurgical industry, swine manure, pesticides and scrapheaps. Divalent and monovalent copper are the most common forms of copper in the aquatic environment. Copper is not as toxic as mercury or cadmium. But this happens mainly due to the accumulation of copper in the liver and other organs resulting in hepatic or neurological diseases. Wilson disease, a common disease condition, is also a result of accumulation of copper in the body tissues. Oral large doses of copper are fatal (Raja, Hazarey, Peters, & Warnakulasuriya, 2007).

1.3.4 Strontium

Strontium is an alkaline earth metal which occurs naturally only with other elements due to its high reactivity with water and oxygen. Celite and strontianite are the commercially important minerals that contain strontium. Strontium is used in alloy and glass industries and it also releases to the environment as a nuclear by product. There are two forms of strontium isotopes, i.e. stable isotopes and radioactive isotopes. There is no direct evidence that the stable strontium is toxic to the human under normal exposures. But exposure of the radioactive isotopes can cause necrosis lesions and cancers of bone and adjacent cells. High doses of this metal can destroy the bone marrow. The radioactive isotope has half of 29 years. Being in the same group and carrying similar characteristics to calcium, easily replaces calcium in bones, which causes very serious health conditions. (Miledi, 1966).

1.3.5 Chromium

Chromium is an essential trace element needed for the human body. Therefore trivalent chromium in minor amounts does not cause serious damage to the body tissues. But hexavalent chromium is extremely harmful to humans even in minor quantities. The role of trivalent chromium in glucose and lipid metabolism is well known. But few studies have addressed the toxicity of trivalent chromium in humans (Kusiak, Ritchie, Springer, & Muller, 1993).

Therefore it is very important to remove these metal ions from the environment, especially from contaminated water. Therefore materials which have a large capacity and large partition coefficient for removing these metal ions play an important role.

1.4 Current knowledge on available methods to remove toxic metals

Finding treatments for the removal of toxic metals from polluted water bodies became a great challenge in the last few decades of the 20th century. Therefore several new materials and techniques originated to treat heavy metal contaminated water. Nowadays, most common techniques for removal of heavy metals include precipitation, ion exchange, adsorption, filtration, electrodeposition and reverse osmosis (Kumar, Rao, & Kaul, 2000). But every single method has its own drawbacks when comparing the cost and time. Table 1.3 summarizes each of these methods by comparing the advantages and disadvantages.

Toxic metal waste removal by precipitation methods is very simple, but the resulting voluminous metal alkaline sludges need to be disposed in an environmentally safe manner; or further treatments are needed. In addition, this treatment technique requires large tanks. Ion exchange methods are relatively expensive and time consuming, but metals can be recovered. Filtration methods are mostly used in small scale treatments. Some toxic metals can be recovered from electrodeposition processes using insoluble anodes. The major advantage of this method is that this can recover the pure metal that has an economic value. But this has its own drawbacks being very costly and has low efficiency at lower metal concentrations. Most commonly, reverse osmosis is used in metal finishing industries to recover the plating chemicals. This method is good to selectively recover the metals. But fouling and the lesser durability of the membrane are the main disadvantages. Adsorption at the solid solution interface is playing an important role for controlling the metal pollution. This technique is highly effective for removing

metal ions to a very low concentration. The major disadvantage of this technique is the disposal of solid waste after adsorption (Bulut & Tez, 2007; Lewinsky, 2007).

1.5 Modified silica for the removal of metal ions

Materials that have the ability to adsorb metal ions onto its surface through complexation are very effective for removing metal ions. Surface modified silicas have received considerable attention because of its success of heavy metal removal. Silica gels are an amorphous, inorganic matrix which contains internal siloxane groups with silanol groups distributed on the surface given in Figure 1.1(Cestari & Airoldi, 1997).

Silica provides many advantages as a surface for modification, i.e. inert, good adsorption and cation exchange capacity, easily and inexpensively prepared, and high mechanical as well as thermal stability (Budiman, Fransiska, & Setiawan, 2009). The silanol groups of silica gel have the ability to react with agents containing different functional organosilanes. These modifications enhance the adsorption and ion exchange capability of silica gels at the solid solution interface (I.P. Blitz, Blitz, V.M., & Sheeran, 2006)

Various chemical groups which contain donor atoms such as sulfur, nitrogen, oxygen can be attached to the silica surface through this process. The principal success of modifying silica with organofunctional silane groups is the immobilization of the desired reactive group which gives the opportunity to handle various functions and abilities on the modified silica surfaces. Therefore modified silica gel can be used in various areas of chemistry such as heterogeneous catalysis, as a stationary phase in chromatography, enzyme catalysis, biotechnology, electrochemistry, metal ion pre-concentration and

Process	Method/Energy	Advantages	Disadvantages
Chemical precipitation	Precipitant/flocculant, acid, base, mixing and fluid handling	Simple, low metal concentration in the effluent are achieved	Voluminous alkaline metal sludge disposal problems, higher amount of chemical needed, high capital cost
Electrochemical	Electrical energy	Recovered pure metal has economic value	High energy usage, high capital cost, reduced efficiency at lower concentration
Adsorption	Adsorption	removing metal ions to a very low concentration	Solid waste disposal problems
Ion exchange	Ion exchange	removing metal ions to a very low concentration	High cost, solid waste disposal problems, time consuming
Reverse osmosis	Ion selective membrane	Selective metal removal	Fouling and lesser durability of membranes

Table 1.3: Current knowledge in methods available for removal of toxic metals

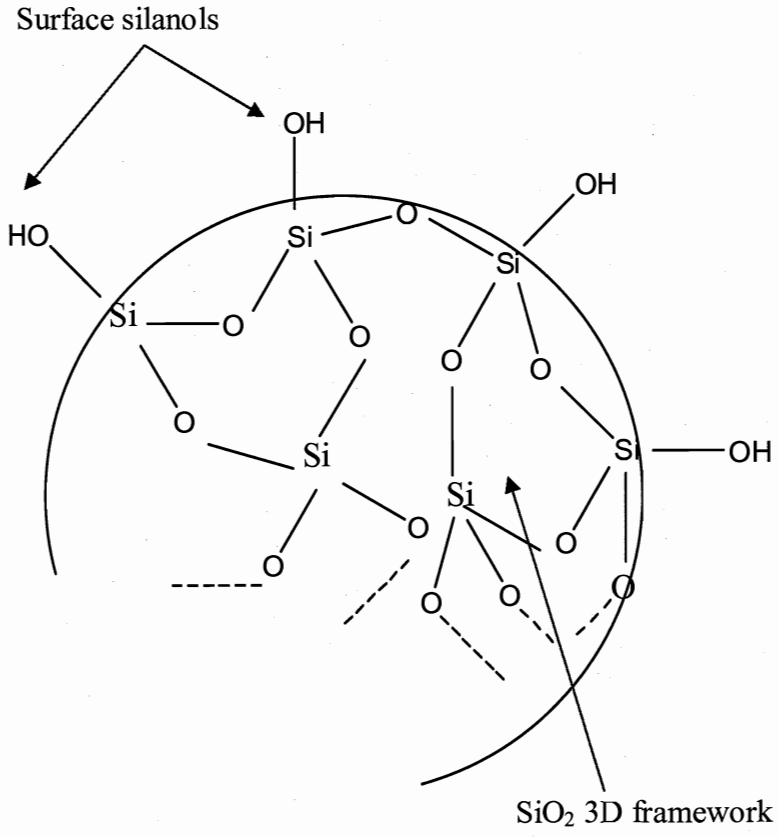

Figure 1.1 Silica 3D structure and surface silanols.

removal of toxic metal ions (Prado & Airoldi, 2001). Many advantages are seen when organic functional silanes are attached to the silica surface and involve in toxic metal ion adsorption. These advantages include high surface area to increase the adsorption capacity, high mechanical stability and donor ability, which can be selectively change according to the toxic metal ion affinity (Ian P. Blitz, Blitz, Gun'ko, & Sheeran, 2007).

1.6 Sections of the Thesis

The overall goal of my research is to synthesize and study the properties of new materials, which can be used to clean up wastewater in order to remove toxic heavy metal pollutants.

Chapter Two describes the modification of silica using organosilanes and characterization them using N_2 adsorption and diffuse reflectance FTIR spectrometry. Chapter Three describes the adsorption capacity and the affinity of these modified silicas for various metals, including mercury, by atomic absorption spectrometry and electrochemical (cyclic voltammetry) measurements. Further, this chapter suggests possible metal ion - surface bonding interactions on some complexes predicted by using diffuse reflectance FTIR spectrometry and by computational calculations. Finally Chapter Four summarizes the thesis with suggestions for future work.

1.7 Reference

1. Blitz, I. P., Blitz, J. P., Gun'ko, V. M., & Sheeran, D. J. (2007). Functionalized silicas: Structural characteristics and adsorption of Cu(II) and Pb(II). *Colloids and Surfaces A: Physicochemical and Engineering Aspects, 307*(1-3), 83-92.
2. Blitz, I. P., Blitz, J. P., V.M., G., & Sheeran, D. J. (2006). Functionalized surfaces: silica structure and metal ion adsorption behavior *surface chemistry in biomedical and environmental science* (pp. 337-348): Springer Netherland.
3. Budiman, H., Fransiska, S. H. K., & Setiawan, A. H. (2009). Preparation of Silica Modified with 2-Mercaptoimidazole and its Sorption Properties of Chromium(III). *E-Journal of Chemistry, 6*(1), 141-150.
4. Bulut, Y., & Tez, Z. (2007). Removal of heavy metals from aqueous solution by sawdust adsorption. *Journal of Environmental Sciences, 19*(2), 160-166.
5. Cestari, A. R., & Airoldi, C. (1997). Chemisorption on Thiol-Silicas: Divalent Cations as a Function of pH and Primary Amines on Thiol-Mercury Adsorbed. *Journal of Colloid and Interface Science, 195*(2), 338-342.
6. Duffus, J. H. (2002). "Heavy metals" a meaningless term? (IUPAC Technical Report). *Pure Appl. Chem., 74*(5), 793-807.
7. Goyer, R. A. (1997). Toxic and essential metal interactions. *Annual Review of Nutrition, 17*(1), 37-50.
8. Kumar, A., Rao, N. N., & Kaul, S. N. (2000). Alkali-treated straw and insoluble straw xanthate as low cost adsorbents for heavy metal removal - preparation, characterization and application. *Bioresource Technology, 71*(2), 133-142.

9. Lewinsky, A. A. (2007). *Hazardous Materials and Wastewater.* New York: Nova science publishers.

10. Metian, M., Warnau, M., HÃ©douin, L., & Bustamante, P. (2009). Bioaccumulation of essential metals (Co, Mn and Zn) in the king scallop Pecten maximus: seawater, food and sediment exposures. *Marine Biology, 156*(10), 2063-2075.

11. O'Dell, B. L., & Sunde, R. A. (Eds.). (1997). *Handbook of nutritionally essential mineral elements.* New York: Marcel Dekker, Inc.

12. Prado, A. G. S., & Airoldi, C. (2001). Adsorption, preconcentration and separation of cations on silica gel chemically modified with the herbicide 2,4-dichlorophenoxyacetic acid. *Analytica Chimica Acta, 432*(2), 201-211.

13. Adams, W. J., Chapman, G. A., & Landis, W. G. (1988). *Aquatic toxicology and hazard assesment* (Vol. 10). Ann Arbor, MI.

Chapter 02

Modification and Characterization of Silica

2.1 General introduction

2.1.1 Importance of inorganic supporting materials

In water metal ions can exist in either the ionic or hydrated forms. In order to convert these metal ions in to extractable species, some or all valence orbitals must be filled with electrons and some or all the water molecules involved in hydration must be replaced. Therefore the primary concept of the removal of metal ions from water is to use a functional group or any atoms with a pair of electrons ready for donation, which can form a complex with the metal ions in the solution. Various chemical groups which contain donor atoms such as sulfur, nitrogen and oxygen can be used as a ligand to the metal ions. The donor nature can be satisfied by using organic chemical groups such as phenol, carbonyl, carboxylic, hydroxyl, ether, phosphoryl, amine, nitro, nitroso, azo, diazo, nitrile, amide, thiol, thioether, thiocarbamate, bisulphate and forming complexes may not be difficult to separate from the water.

Incorporation of a suitable specific functional group into the polymeric matrix support may overcome the separation problem. Mainly there are two types of polymeric supports, i.e. inorganic based supports and polymeric resins. High mass exchange characteristics, no swelling (Alimarin, Fadeeva, Kudryavtsev, Loskutova, & Tikhomirova, 1987), greater resistance to organic solvents and very high thermal resistance (Arakaki, Nunes, Simoni, & Airoldi, 2000; Sarkar, Datta, & Sarkar, 1996) are some of the advantages of using the inorganic supports in place of polymeric resins

(Deorkar & Tavlarides, 1997). Due to its high surface and mechanical stability, silica gels are one of the inorganic supports that have received great attention as a supporting material for many ligands in chromatography, for extraction of cations from aqueous and non-aqueous solvents, for catalytic or ion-exchange reactions, in electronics, in ceramics and also in bioengineering (Davis, 1997; Tong, Akama, & Tanaka, 1990; Wasiak & Urbaniak, 1997).

2.1.2 Silica

Silica consists of inter-linked SiO_4, in a tetrahedral fashion with a basic chemical formula of SiO_2. Silica is the most abundant mineral in the earth's crust. It exists as sand or quartz, cell walls in diatoms and in plants such as bamboo, rice and barley (Iler, 1978). The properties of silica make it promising to use in a number of industries such as soda-lime glass, optical fibers, ceramics, portland cement, food additives and in microelectronics. Most of the time silicas used in chemical applications are of synthetic origin. They can be divided into two classes, i.e. crystalline silica and amorphous silica.

Amorphous silica has become a key base material for metal ion adsorption due to its mechanical resistance, porosity, high surface area and the selectivity for chemical modifications. But the most interesting property is the high porosity, which introduces a large surface area inside the particles. Amorphous silica can be fabricated as fibers, sheets, powders, sols and gels depending on their relevance.

Pore size, volume, active surface area, particle size and hardness are some of the unique properties of silica, each of varying importance in specific applications. These properties can be controlled during preparation and all the chemical and physical features

of amorphous silica will depend on these above factors. Therefore silica classification is based on these properties. According to the IUPAC classification of pore sizes, there are four types of amorphous silica described in Table 2.1. These pores explain the availability of the reactive sites on the silica surface. In addition, it is directly proportional to the surface area of the silica. Pores can have different shapes such as cylinder, slit-shape, cone-shape, ink-bottle, rhomboid, elliptical and square. And these pore shapes are related to the sorption characteristics of silica (Zdravkov, Čermák, Šefara, & Janků, 2007).

2.1.3 Silica surface species

The active silica surface with silanols, and the large specific surface area both play an important role in adsorption studies. There are three different classes of silanols at the silica surface. That is isolated silanols, vicinal silanols and geminal silanols as shown in Figure 2.1. In the isolated or the free silanols, the surface silica has three bonds directed towards the inside of the bulk silica and the remaining bond attached to a hydroxyl group. In vicinal silanols, two single silanol groups, attached to a different silicon atoms, are bonded to each other through H bonding. Geminal silanols consist of two hydroxyl groups that are attached to the same silicon atom but not hydrogen bonded to each other, because hydroxyl groups are too far way to form a hydrogen bond. The surface of silica, chemically defined by these silanol groups are the key factors, which help to modify the silica (Vansant, Van der voot, & Vrancken, 1995).

Name	Pore Diameter (nm)
Micropores	0-2
Mesopores	2-50
Macropores	50-7500
Megapores	>7500

Table 2.1: IUPAC classification of pores (Iler, 1978)

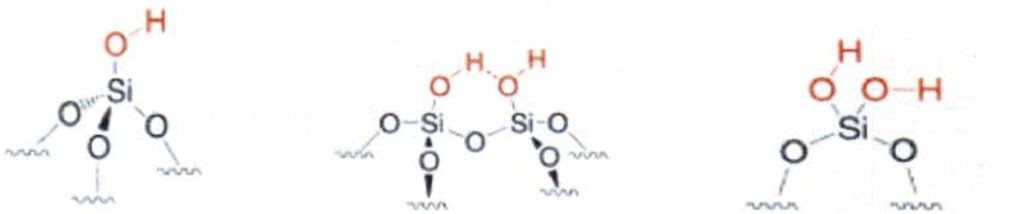

Figure 2.1: Three types of silanols at the silica surface (Downloaded from http://192.207.64.1/rungroj/index.htm)

2.1.4 Surface modification

Chemical surface modifications can be defined as the bonding of molecules or molecular fragments to a surface, in order to change its chemical or physical properties in a controlled way. The purpose of chemical modification is to combine the mechanical and structural properties of a pure substrate with dedicated intermolecular interactions. Normally modified materials can be classified according to the field that they going to be applied. In the sense of metal ion adsorption, attachment of organic groups to silica surfaces can be called surface modification. There are several advantages that these two combinations have gained over past few decades (Jal, Patel, & Mishra, 2004).

Surface modification via various functional group immobilization provides unique properties to the silica surface. Also the chemical bonding of functional groups offers a unique advantage making the modified surface more robust due to a strong covalent bond of the molecule to the substrate (Bogus, *et al.*, 1998). It is very easy to attach an organo-functional group by a simple reaction on to the silica surface compared to other polymers. Silica, having a high specific surface area with a constant composition enables easy analysis. (Arakaki, et al., 2000).

Coupling agents can be defined as materials that improve chemical resistance of the bond across an interface (Plueddemann, 1982). Organofunctional silanes are the best for this purpose because organosilanes have a good potential for bonding through several mechanisms. The common formula of an organosilane is R_n-Si-$X_{[4-n]}$. R is the organic group and X is the hydrolysable ligand. Even though X represents acyloxy, amine, halogen or alcoxy, the most common X groups are ethoxy, methoxy and chlorine (Vansant, et al., 1995). Conventional methods of silica surface modification involve

coupling of a surface hydroxyl group with the organo-silanes. Normally, these silylating agents react with the surface silanol groups in two step resulting in an Si---O---Si---C moiety by removing a water molecule as shown in Figure 2.2 (Ian P. Blitz, et al., 2007).

2.1.5 Cross linking

Generally cross linking refers to the bond between two or more organosilanes to form oligomers and polymers on the silica surface. Cross linking of organosilanes on silica significantly affects its porosity. Organo-silanes which possess one hydrolysable group are unable to make a cross link. But organo-silanes which have two or three hydrolysable groups are able to form cross links as shown in Figure 2.3. These cross links can be directly related to the metal ion adsorption capacity of the modified silica. It can increase the metal ion adsorption capacity due to the presence of larger amounts of functional groups at a shorter distance between one another, and due to greater flexibility of the cross linked functional groups (Ian P. Blitz, et al., 2007).

2.1.6 Characterization of modified silica

Specific surface area, porosity and Fourier Transform Infrared Reflectance spectroscopy (FTIR) characterization to confirm the attachments of organo-silanes to silica surface are the three major parameters, which we focus on this chapter. Porosity characterization includes specific pore volumes and the distribution of pore sizes or pore area. The first two major parameters, specific surface area and the porosity are directly related to the accessibility of adsorption sites, which is the active site (Vansant, et al., 1995).

(a) $(R)_3SiOH + Si(s)\text{-}OH \rightarrow Si(s)\text{-}O\text{-}Si(R)_3 + H_2O$

(b)

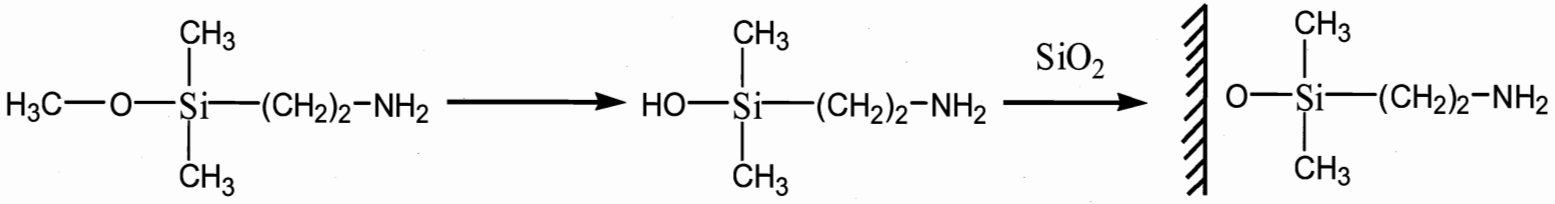

Figure 2.2: (a) General reaction for modification of silica (b) Example for a surface modification reaction with amino silane.

(a)

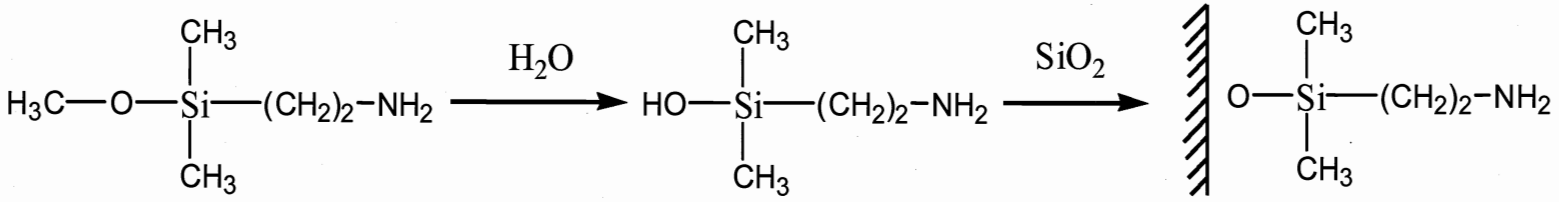

(b)

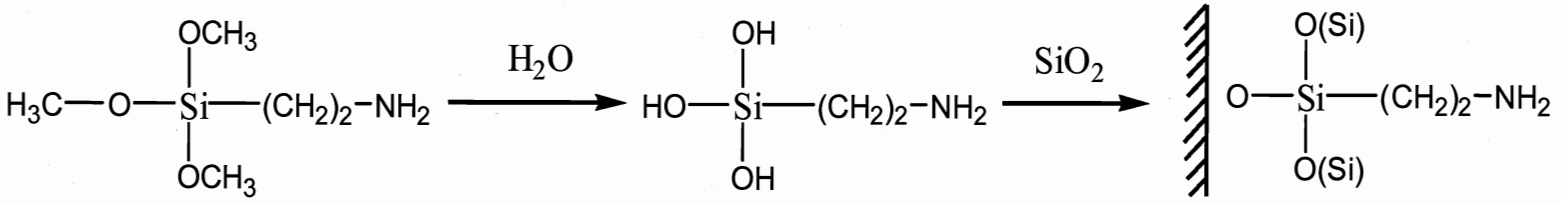

Figure 2.3: Cross linking of modified silica (a) Organosilanes with one hydrolysable group are unable to cross link (b) Organosilanes with three hydrolysable groups are able to cross link

Binding of significant amounts of organo-silanes on to the surface of the silica sometimes alter the metal ion adsorption capacity by occupying a volume inside the pore space. Therefore the adsorbent surface area and the average pore diameter may be very important in the sense of metal ion adsorption. Normally BET method is used to calculate the above parameters. This is based on nitrogen adsorption capacity to the silica surface, and these nitrogen molecules adsorbed preferentially to silanols where as shows a weak adsorption on to organic surfaces compared with bare silica surfaces. The decrease in the specific surface area by nitrogen adsorption indicates that the silica bare surfaces are covered with the modified groups (Ian P. Blitz, et al., 2007; I.P. Blitz, Blitz, V.M., & Sheeran, 2006; Jal, et al., 2004).

FTIR spectroscopy reveals the energies of possible stretching and deformation vibrations within the surface of the modified silica. By assigning these vibrations to specific chemical groups allows for qualitative and quantitative identify the chemical components of the modified silica surface. That will confirm the attachment of organo-silanes to the silica surface (Al-Oweini & El-Rassy, 2009).

2.2 Experimental methods

2.2.1 Silica gels

The nanoparticulate fumed silica gels HP39(Crosfield), 200DF(Crosfield) and SBA15(Kent State University , Ohio) were modified as received, by using several organosilanes. The organosilane structures are given in Table 2.2. All the materials used are summarized in Table 2.3.

Structure	Name/Acronym
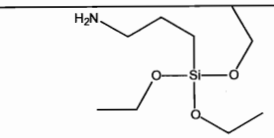	**APTS** **3-aminopropyltriethoxysilane**
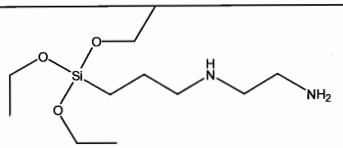	**Diamino** **N-(2-aminoethyl)-3-aminopropyltriethoxysilane**
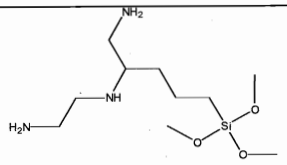	**Triamino** **3-(trimethoxysilylpropyl)diethylenetriamine**
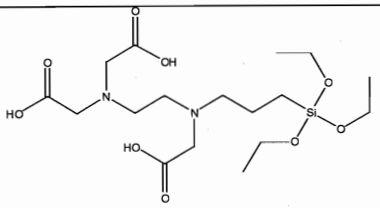	**EDTA** **N-(triethoxysilylpropyl)ethylenediaminetriacetic acid**
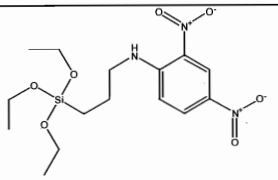	**DPPS** **3-(2,4-dinitrophenylamino)propyltriethoxysilane**
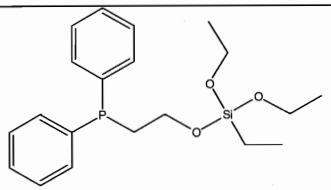	**Phosphino** **2-(diphenylphosphino)ethyltriethoxysilane**

Table 2.2: Organosilane structures

Silica type	Modified group
HP39	3-aminopropyltriethoxysilane **(APTS)** N-(2-aminoethyl)-3-aminopropyltrimethoxysilane **(Diamine)** 3-(trimethoxysilylpropyl)diethylenetriamine **(Triamine)** N-(triethoxysilylpropyl)ethylenediaminetriacetic acid **(EDTA)** 3-(2,4-dinitrophenylamino)propyltriethoxysilane **(DPPS)**
200DF	3-aminopropyltriethoxysilane **(APTS)** N-(2-aminoethyl)-3-aminopropyltrimethoxysilane **(Diamine)** 3-(trimethoxysilylpropyl)diethylenetriamine **(Triamine)** N-(triethoxysilylpropyl)ethylenediaminetriacetic acid **(EDTA)**
SBA15	N-(triethoxysilylpropyl)ethylenediaminetriacetic acid **(EDTA)**

Table 2.3: Silica types and modified groups

2.2.1.1 HP39

The HP 39 silica was modified by using 3-aminopropyltriethoxysilane (APTS), N-(2-aminoethyl)-3-aminopropyltrimethoxysilane(Diamine), 3-(trimethoxysilylpropyl) diethylenetriamine(Triamine), N-(triethoxysilylpropyl) ethylenediaminetriacetic acid (EDTA) and 3-(2,4-dinitrophenylamino) propyltriethoxysilane(DPPS)(Gelest).

2.2.1.2 200DF

The 200DF silica was modified by 3-aminopropyltriethoxysilane(APTS), N-(2-aminoethyl)-3-aminopropyltrimethoxysilane(Diamine), 3-(trimethoxysilylpropyl) diethylenetriamine (Triamine),), N-(triethoxysilylpropyl) ethylenediaminetriacetic acid (EDTA) (Gelest).

2.2.1.3 SBA15

The SBA15 silica was modified by using N-(triethoxysilylpropyl) ethylenediaminetriacetic acid (EDTA)(Gelest).

2.2.2 Syntheses of modified silicas

2.2.2.1 Preparation of APTS, Diamine and Triamine modified silica

A sample of 4.0 g of silica was refluxed with 20 mmol of the organosilane in 200 mL of toluene for 2 hours. The slurry was filtered and washed with toluene, and dried at 150 ^{0}C in vacuum for 2 hours. All reactions were carried out in the presence of 100 μL of n-butylamine as catalyst. The modified silica was resuspended in Millipore water for 30 min and filtered. Then solid was dried again in a vacuum (~0.1 mm Hg) at 150 ^{0}C to facilitate cross linking (Ian P. Blitz, et al., 2007).

2.2.2.2 Preparation of EDTA and Phospeno modified silicas

A sample of 4.0 g of silica was refluxed with 20 mmol of the organosilane in 200 mL of water for 2 hours. The slurry was filtered and washed with water, and dried at 150 ^{0}C in vacuum for 2 hours (Ian P. Blitz, et al., 2007).

2.2.2.3 Preparation of DPPS silica

A sample of 4.0 g of silica was refluxed with 20mmol of the organosilane in 200 mL of toluene for 2 hours. The slurry was filtered and washed with toluene, and dried at 150 ^{0}C in vacuum for 2 hours. All reactions were carried out in the presence of 100 µL of n-butylamine as catalyst. The prepared 3-(2,4-dinitrophenylamino) propyltriethoxysilane silica underwent solid phase reduction to form DPPS modified silica by using metallic Sn and diluted HCl (as shown in Figure 2.4), with continuous shaking for two hours (Basu, Das, & Das, 2005). Then the DPPS modified silica was resuspended in Millipore water for 30 min, filtered and dried in vacuum at 150 ^{0}C to facilitate the cross linking.

2.2.3 Preparation of SBA15 silica (Prepared at Kent State University, OH)

SBA-15 MW2 sample was synthesized under acidic conditions using poly(ethylene oxide)-poly(propylene oxide)-poly(ethylene oxide) triblock copolymer ($EO_{20}PO_{70}EO_{20}$, Pluronic P-123, BASF) as a template and tetraethyl orthosilicate (TEOS, Aldrich) as the silica source. The molar composition used was 1 TEOS: 0.0167 P123: 190 H_2O: 5.82 HCl. The entire synthesis was carried out in a microwave oven (initial gel formation and hydrothermal treatment). In the first step, the synthesis mixture was stirred using magnetic bars for two hours at 40°C. After the initial stage, temperature was

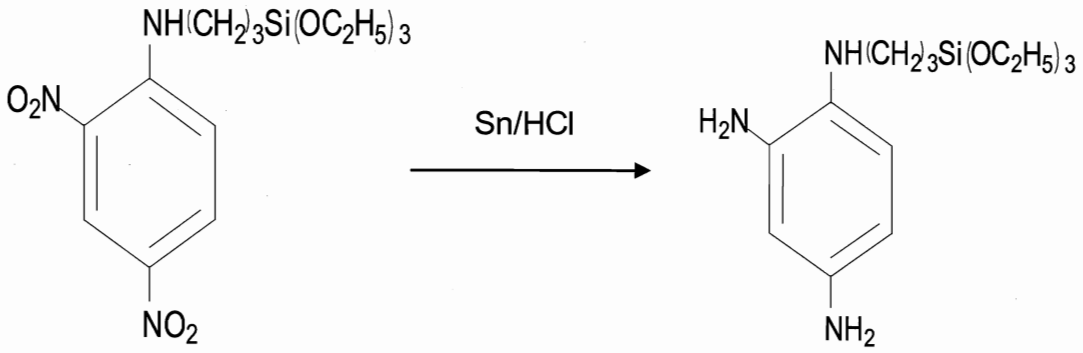

Figure 2.4 The conversion of 3-(2,4-dinitrophenylamino) propyltriethoxysilane silica to 3-(2,4- diaminophenylamino) propyltriethoxysilane using solid phase reduction

increased to 140°C and was kept for six hours; the magnetic stirring was off during this stage. The resulting as-synthesized composites were filtered, washed with deionized water, and dried overnight at 80 °C. Next the sample was calcined at 540 °C for four hours under air atmosphere with a heating rate of 5 °C min^{-1}.

2.2.4 Characterization of Modified silica

2.2.4.1 FTIR Characterization

Surface modification was verified using FTIR spectroscopy depending on the availability of the functional group frequencies of characteristic NH_2, NO_2, and COO^- groups. Reflectance infrared spectra were obtained using a Digilab FTS 3000 FT-IR equipped with a narrow band MCT detector. Diffuse reflectance spectra were obtained using a "praying mantis" diffuse reflectance accessory from Harrick Scientific. N_2 gas was purged into the sample compartment in order to remove interference of the spectra from water vapor. All integrations were done using standard instrument software. The samples were prepared by mixing 20 mg of modified silica with 200 mg of dried, preground (~5 μm) KCl.

2.2.4.2 Nitrogen adsorption data collection and surface area analysis (done at Kent State, OH, and SABIC, Baltimore, MD)

A sample of approximately 0.3 g was out gassed at 110 ^{0}C prior to the analysis. Nitrogen adsorption-desorption isotherms were recorded at 77.35 K using a Micromeritics ASAP 2010 adsorption analyzer at p/p_0 10^{-6} to 10^{-5}, where p and p_0 denote the equilibrium pressure and saturation pressure of nitrogen at 77.35 K, respectively. The specific surface area (S_{BET}) was calculated using the standard BET method (Gregg S.J.,

1982). The pore volume (Vp) was estimated from the nitrogen adsorption at $p/p_0 \sim 0.98$-0.99. Pore size distributions (PSDs) with respect to the pore volume and surface areas were calculated with Micomeritics DFT software. Another data analysis method was used based on an equation described in detail elsewhere (Ian P. Blitz, et al., 2007). %N data was obtained by combustión analysis at the UIUC microanalysis lab.

2.3 Results and discussion

2.3.1 Characterization of Modified silica using Nitrogen adsorption data collection and surface area analysis

2.3.1.1 Unmodified silica

The three silica types have different characteristics. Silica gel 200DF has mainly micropores and narrow mesopores with pore radii R<2 nm, since contribution of broad mesopores at 2 nm<R<25 nm and macropores at R>25 nm are low, given in the Figure 2.5. The nitrogen adsorption desorption isotherm in 200DF unmodified silica shows three hysteresis loops P/P_0 in between 0.4 and 1.0 (Figure 2.6 and 2.6.b). The third small hysteresis loop $P/P_0 > 0.94$ belongs to the textural porosity at R>25nm. The comparatively large second hysteresis loop at $0.6 > p/p_0 > 0.9$ and the small hysteresis loop at $0.4 > P/P_0 > 0.6$ is due to the narrow pores. In contrast to the silica gel 200DF, HP39 and SBA15 silica gels are mainly mesopores materials (Figure 2.5). Nitrogen adsorption desorption isotherm for HP39 unmodified silica at $0.7 > P/P_0 > 1.0$ large hysteresis loop in Figure 2.6 as well as enlargement in 2.6.c confirm this idea. In addition to this main loop belongs to the mesopores at 2 nm<R<20 nm, HP39 is characterized by a

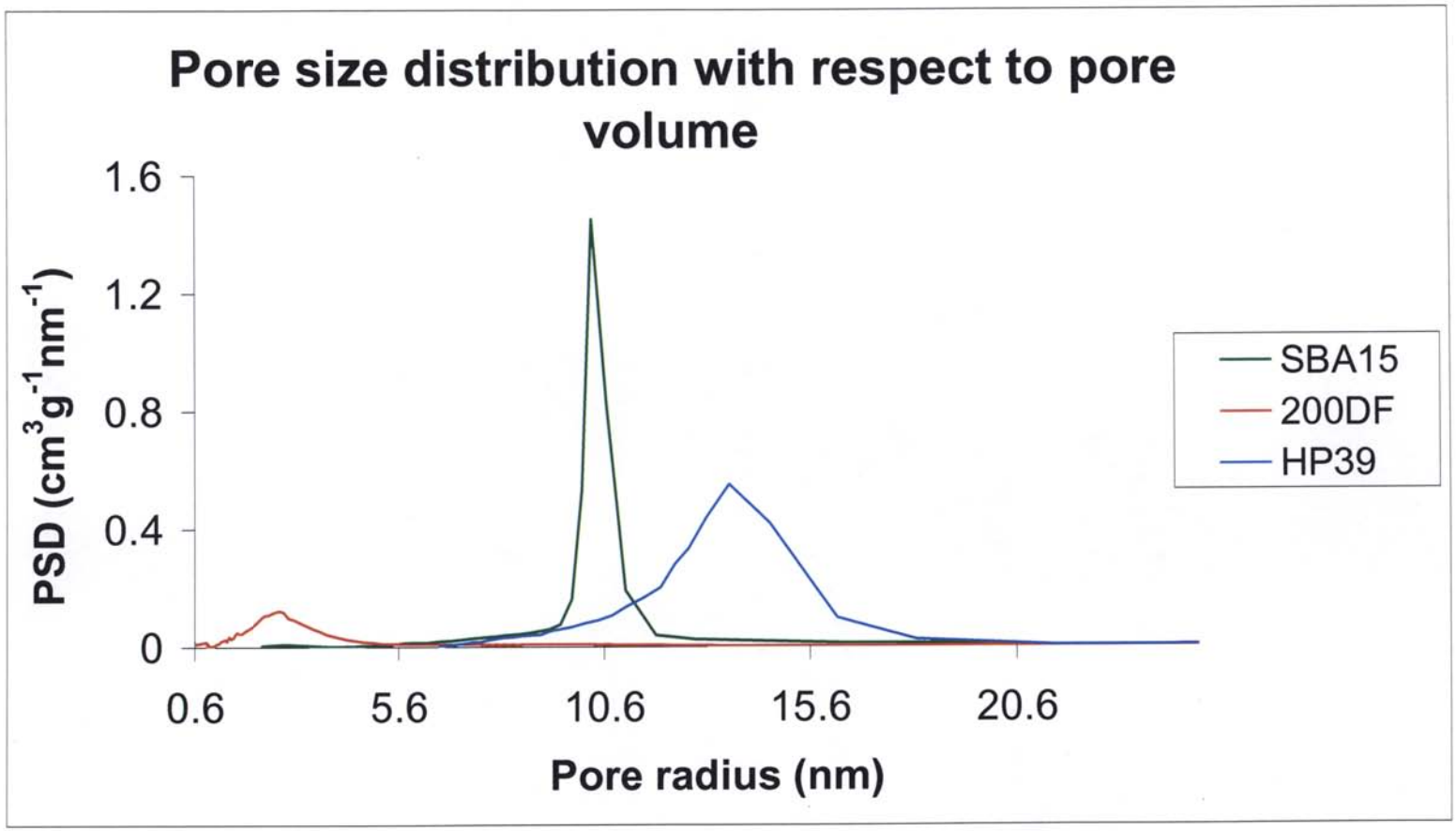

Figure 2.5 Pore size distribution compared to the pore volume for initial silica gel SBA15, 200DF and HP39

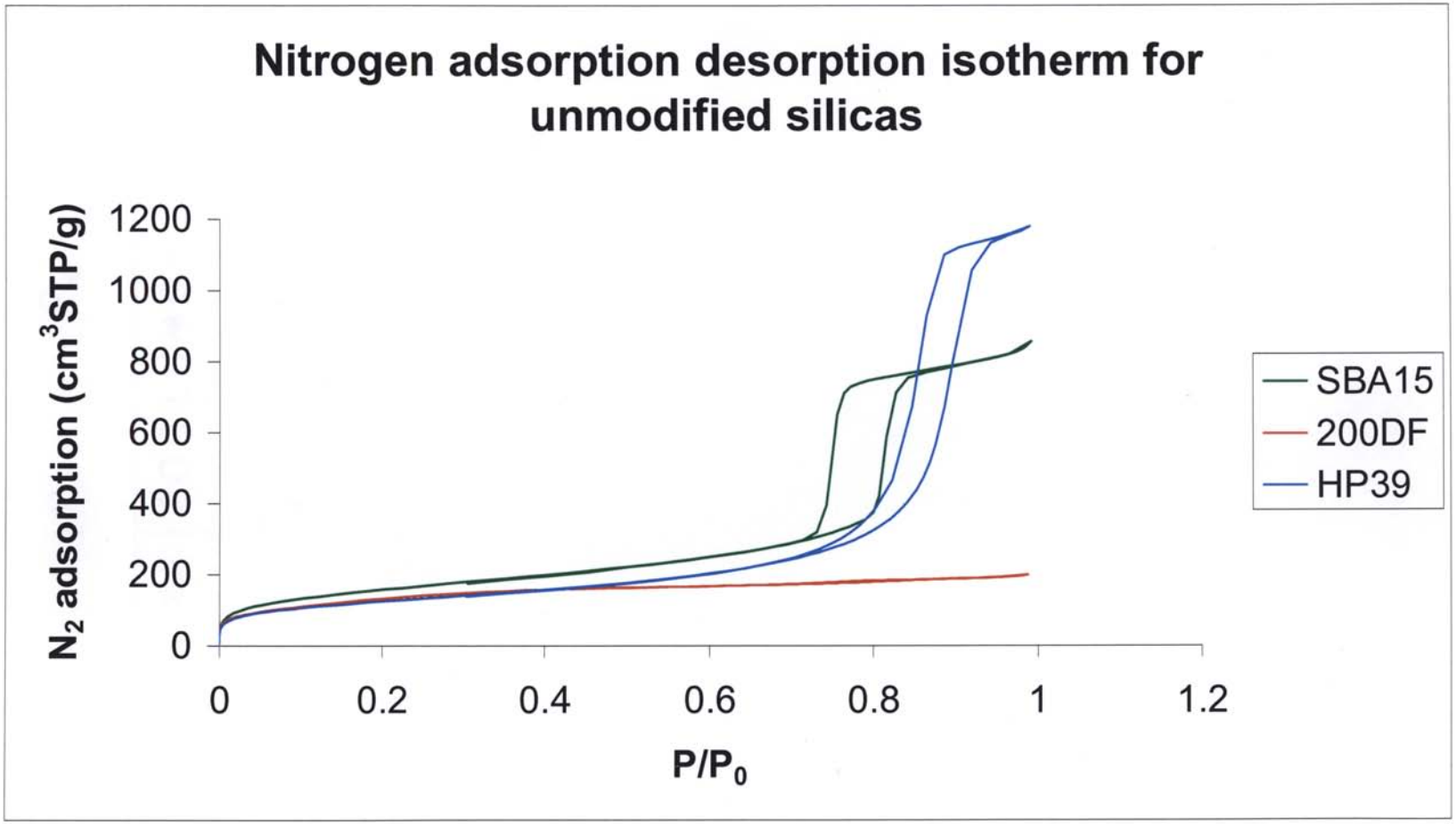

Figure 2.6 Nitrogen adsorption desorption isotherm for unmodified silica SBA15, 200DF and HP39

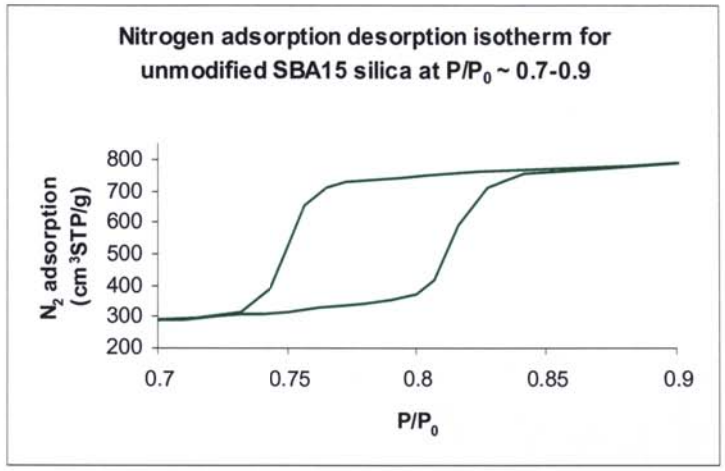

Figure 2.6.a N_2 adsorption desorption isotherm for Unmodified SBA15 silica at $P/P_0 \sim 0.7$-0.9

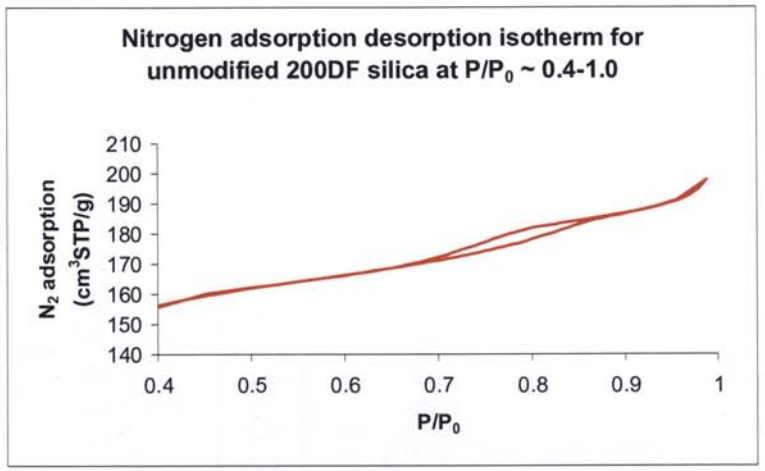

Figure 2.6.b N_2 adsorption desorption isotherm for Unmodified 200DF silica at $P/P_0 \sim 0.4$-1.0

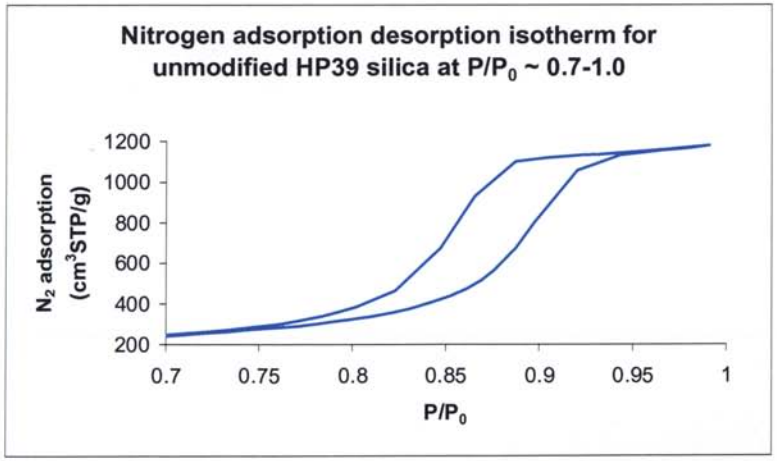

Figure 2.6.c N_2 adsorption desorption isotherm for Unmodified HP39 silica at $P/P_0 \sim 0.7$-1.0

small contribution of micropores at R>1 nm and macropores because of textural porosity at R>25 nm (Ian P. Blitz, et al., 2007). In SBA15 silica narrow mesoporous nature is confirmed by the hysteresis loop at $0.75 > P/P_0 > 0.95$ at nitrogen adsorption desorption isotherm given in Figure 2.6 and enlargement 2.6.a (Kruk, Jaroniec, Ko, & Ryoo, 2000).

2.3.1.2 Modified Silica

According to Table 2.4, in all cases it is clear that the surface modification results in reduction in surface area. Clogging of pores by grafted silanes upon surface modification complicated by cross linking are the direct causes for this. When considering the percentage of surface area reduction in each silica after modification, (Table 2.4) dramatic change can be found in the 200DF silica which has a reduction percentage of 63.22%. This is because the micropores of 200DF silica are easily clogged by surface modification as well as cross linking compared to the other two mesoporous silicas. The reduction of PSD in nitrogen adsorption desorption isotherms for unmodified and EDTA modified silica (Figure 2.7.a ,b and c) also illustrate this phenomenon.

But it is interesting to see that compared to the reduction of surface area pore volume is not significantly reduced, especially in 200DF and SBA15 silicas (Table 2.4). In addition, for all three types of silicas pore width are increasing, sometimes dramatically, compared to the initial values This idea is further verified by curves belonging to the pore size distribution with respect to pore volume given in Figure 2.8.a.b.c. That is, in all three types of silicas, pore radius is shifted to higher values after surface modification. Especially in 200DF silica, a fair amount of micropores turn into mesopores.

Sample	S_{BET}, m^2g^{-1}	V_t, ccg^{-1}	w_{KJS}, nm	N%	%reduction S_{BET}
200DF	484	0.30	2.64		
200DF-EDTA	178	0.25	5.71	-	63.22
HP39	449	1.96	15.97		
HP39-EDTA	246	0.81	18.21	0.44	45.21
SBA15	577	1.34	10.87		
SBA15-EDTA	286	0.89	11.55	1.28	50.43

Table 2.4. Adsorption parameters for the silica and EDTA-modified silica samples studied.
S_{BET} – BET specific surface area
V_t – single point pore volume
w_{KJS} – pore width

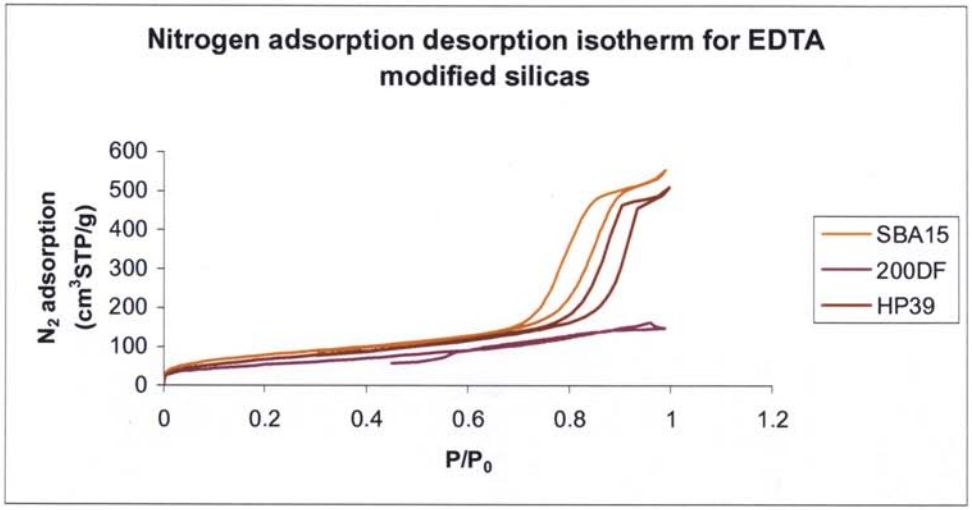

Figure 2.7 N_2 adsorption desorption isotherm for modified silica SBA15, 200DF and HP39

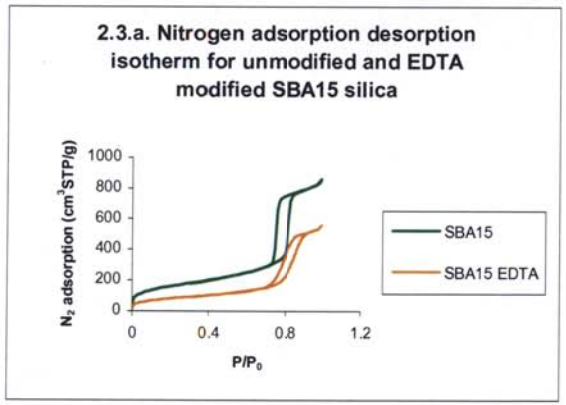

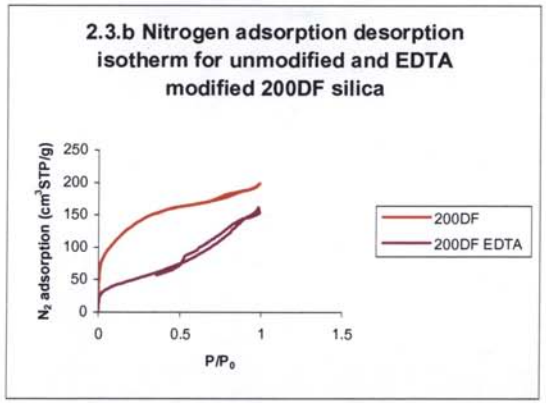

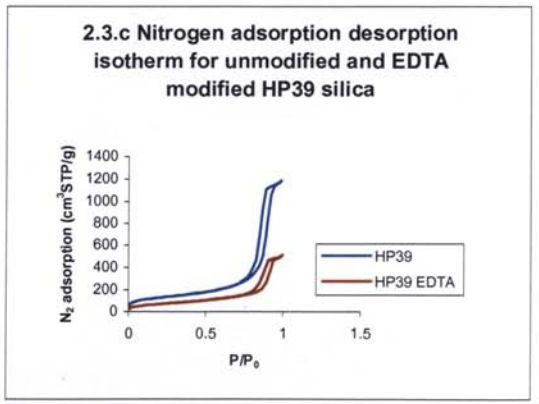

Figure 2.7.a N_2 adsorption desorption isotherm for EDTA modified and unmodified SBA15 silica
Figure 2.7.b N_2 adsorption desorption isotherm for EDTA modified and unmodified 200DF silica
Figure 2.7.c N_2 adsorption desorption isotherm for EDTA modified and unmodified HP39 silica

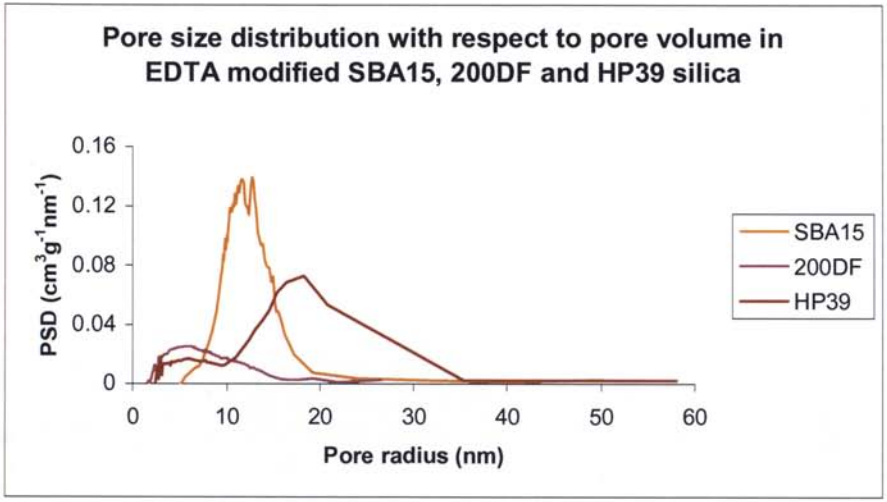

Figure 2.8 Pore size distribution with respect to the pore volume EDTA modified SBA15, 200DF and HP39 silica

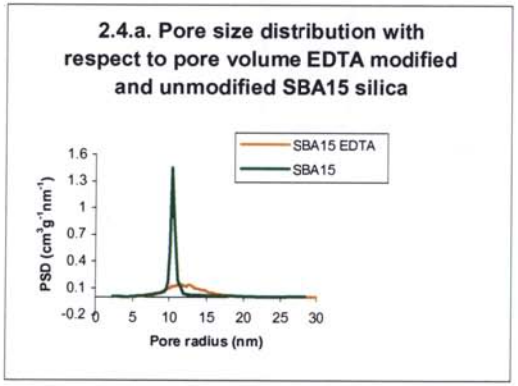

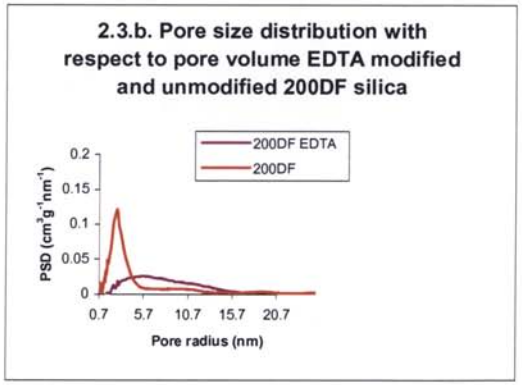

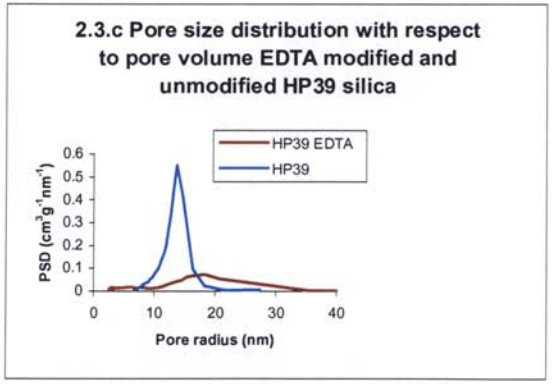

Figure 2.8.a. Pore size distribution with respect to the pore volume EDTA modified and unmodified SBA15 silica
Figure 2.8.b. Pore size distribution with respect to the pore volume EDTA modified and unmodified 200DF silica
Figure 2.8.c. Pore size distribution with respect to the pore volume EDTA modified and unmodified HP39 silica

This phenomenon is not common in modification of silica by other organo-functional silanes. Previous studies indicated that after modification of 200DF silica by APTS, pore volume decreased by 82.4% which is huge. Further HP39 silica modification with APTS, pore volume decreased by 36.6% and the percentage drop of pore volume of HP39 and 200DF silica after modification with amino functional silanes are given in the Table 2.5. According to these studies, it is clear that the surface modification reduced the surface area, pore volume and the pore diameter considerably compared to the EDTA modified silicas. (Ian P. Blitz, et al., 2007; I.P. Blitz, et al., 2006). The reason for this is solubility of amorphous silica at high pH. Especially from pH 9.0 to 10.7, there is an apparent increase in the solubility of amorphous silica given according to Figure 2.9. Further this solubility depends on other factors including temperature of the solution. Normally it is found that the solubility of amorphous silica is 30% higher at 100 °C compared to the room temperature. In addition silica solubility is depends on the impurities, organic matters in the solution including organo-silane and the particle size of the amorphous silica (Iler, 1978).

In our method of modification of silica 20.0 mmol EDTA silane is reacted with 4.00 g of silica in 200 mL of water. In this case pH of the reaction mixture exceeds 10. The reason for this is the EDTA silane is a salt of strong base and a weak acid. Therefore basicity of this salt increases the pH of the solution. In addition refluxing of the reaction mixture in water for more than two hours increases the temperature of the solution to 100 °C. Because of this high pH, as well as high temperature dissolving the silica particles and corroding pores results in an increase in pore volume as well as pore width. But the disadvantage of this procedure is some amount of silica dissolving causes a drop of

(a) $(SiO_2)_x + 2H_2O \longrightarrow Si(OH)_4 + (SiO_2)_{x-1}$

$Si(OH)_4 + OH^- \longrightarrow Si(OH)_5^- + (\text{or } HSiO_3^-)$

(b)

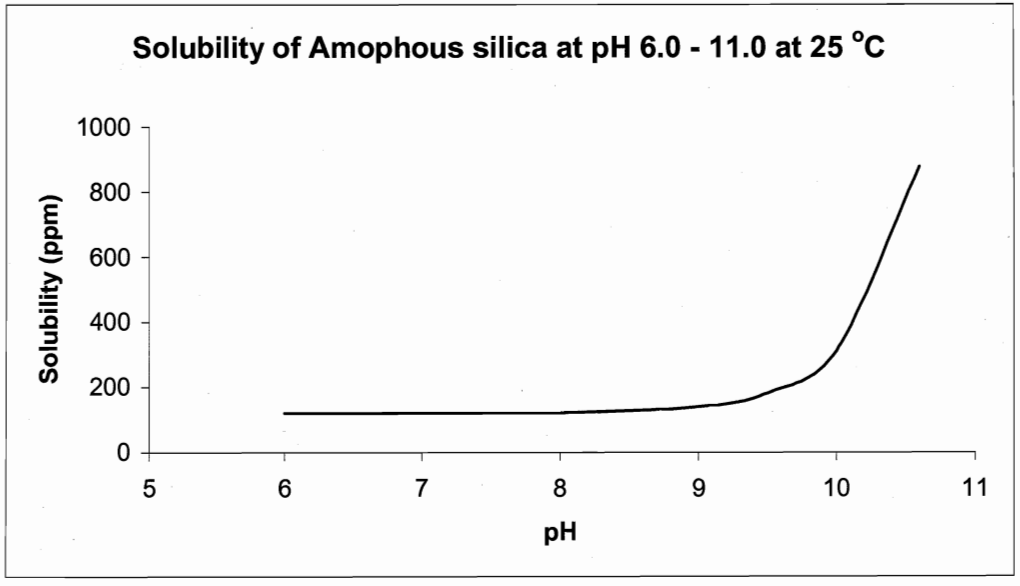

Figure 2.9 (a) Solubility of silica

(b) Solubility of amorphous silica at 25°C according to the pH increment.

Sample	Vp(cm^3/g)	((Vp-Vp,o)/Vp,o) * 100%
200DF	0.34	
APTS	0.06	-82.4
Diamine	0.02	-94.1
Triamine	0.002	-99.4
HP39	1.91	
APTS	1.21	-36.6
Diamine	0.98	-48.7
Triamine	0.89	-53.4

Table 2.5. Modified silica's and their pore volume , percentage of pore volume drop compared to unmodified silica (Ian P. Blitz, et al., 2007)

percent yield of the surface modification reaction.

2.3.2 Characterization of Modified silica using FTIR Spectroscopy

The main idea of surface modification is to introduce different functional groups into the silica surface by chemical reactions. These different functional groups can be readily identifiable through FTIR spectroscopy which gives a better understanding of the modifications.

The FTIR spectra of HP39 silica and other modified HP39 silica with EDTA, diamino and nitro are shown in the Figure 2.10. The broad peak at 1550 cm^{-1} to 1650 cm^{-1} EDTA modified silica represent the asymmetrical stretching of $-COO^-$ groups (Ian P. Blitz, et al., 2007; Hodgson, Shen, & Sale, 2000). The weak band at 3300 cm^{-1} and 3360 cm^{-1} belongs to the asymmetrical N–H stretch and the symmetrical N–H stretch respectively in Diamino modified silica (Ooya & Yui, 1999). The N–O stretching vibrations in nitro groups occur at 1525 cm^{-1} and 1450 cm^{-1} in nitro modified HP39 silica (Grube, Muter, Strikauska, Gavare, & Limane, 2008).

2.4 Conclusion

The EDTA modified silica and other silicas were successfully synthesized. The surface modified EDTA silica characterization by N_2 adsorption was able to conclude that little to no reduction observed on the surface area by surface modification. The FTIR characterization of some of the modified silica reveals that the surface modification was successful.

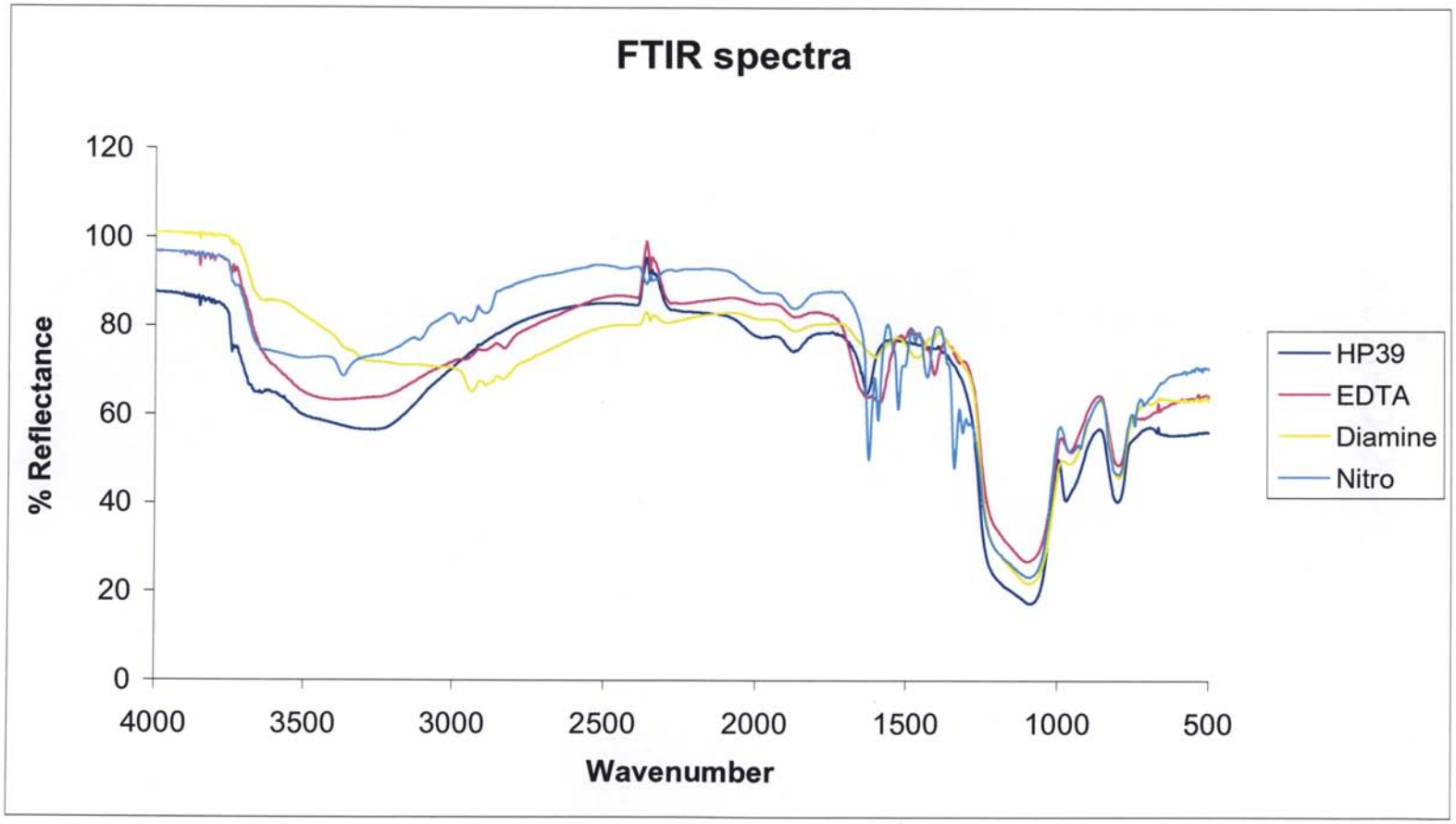

Figure 2.10 FTIR spectrums of HP39 silica and EDTA, Diamine, Nitro, Phospeno modified HP39 silica

2.5 Reference

1. Al-Oweini, R., & El-Rassy, H. (2009). Synthesis and characterization by FTIR spectroscopy of silica aerogels prepared using several Si(OR)4 and R"Si(OR')3 precursors. [doi: DOI: 10.1016/j.molstruc.2008.08.025]. *Journal of Molecular Structure, 919*(1-3), 140-145.

2. Alimarin, I. P., Fadeeva, V. I., Kudryavtsev, G. V., Loskutova, I. M., & Tikhomirova, T. I. (1987). Concentration, separation and determination of scandium, zirconium, hafnium and thorium with a silica-based sulphonic acid cation-exchanger. [doi: DOI: 10.1016/0039-9140(87)80013-9]. *Talanta, 34*(1), 103-110.

3. Arakaki, L. N. H., Nunes, L. M., Simoni, J. A., & Airoldi, C. (2000). Ethyleneimine Anchored on Thiol-Modified Silica Gel Surface--Adsorption of Divalent Cations and Calorimetric Data. [doi: DOI: 10.1006/jcis.2000.6842]. *Journal of Colloid and Interface Science, 228*(1), 46-51.

4. Basu, B., Das, P., & Das, S. (2005). Transfer hydrogenation using recyclable polymer-supported formate (PSF): Efficient and chemoselective reduction of nitroarenes. [10.1007/s11030-005-8106-1]. *Molecular Diversity, 9*(4), 259-262.

5. Blitz, I. P., Blitz, J. P., Gun'ko, V. M., & Sheeran, D. J. (2007). Functionalized silicas: Structural characteristics and adsorption of Cu(II) and Pb(II). *Colloids and Surfaces A: Physicochemical and Engineering Aspects, 307*(1-3), 83-92.

6. Blitz, I. P., Blitz, J. P., V.M., G., & Sheeran, D. J. (2006). Functionalized surfaces: silica structure and metal ion adsorption behavior *surface chemistry in biomedical and environmental science* (pp. 337-348): Springer Netherland.

7. Bogus, lstrok, Buszewski, a., Jezierska, M., Miros, We, a., et al. (1998). Survey and Trends in the Preparation of Chemically Bonded Silica Phases for Liquid Chromatographic Analysis. *Journal of High Resolution Chromatography, 21*(5), 267-281.

8. Davis, S. S. (1997). Biomédical applications of nanotechnology -- implications for drug targeting and gene therapy. [doi: DOI: 10.1016/S0167-7799(97)01036-6]. *Trends in Biotechnology, 15*(6), 217-224.

9. Deorkar, N. V., & Tavlarides, L. L. (1997). Zinc, Cadmium, and Lead Separation from Aqueous Streams Using Solid-Phase Extractants. [doi: 10.1021/ie960415m]. *Industrial & Engineering Chemistry Research, 36*(2), 399-406.

10. Gregg S.J., S. K. S. W. (1982). *Adsorption, Surface Area and Porosity* (second ed.). London: Academic press.

11. Grube, M., Muter, O., Strikauska, S., Gavare, M., & Limane, B. (2008). Application of FT-IR spectroscopy for control of the medium composition during the biodegradation of nitro aromatic compounds. [10.1007/s10295-008-0456-0]. *Journal of Industrial Microbiology and Biotechnology, 35*(11), 1545-1549.

12. Hodgson, S. N. B., Shen, X., & Sale, F. R. (2000). Preparation of alkaline earth carbonates and oxides by the EDTA-gel process. [10.1023/A:1004826324526]. *Journal of Materials Science, 35*(21), 5275-5282.

13. Iler, R. K. (1978). *The Chemistry of Silica*. New york: Wiley-Interscience

14. Jal, P. K., Patel, S., & Mishra, B. K. (2004). Chemical modification of silica surface by immobilization of functional groups for extractive concentration of metal ions. [doi: DOI: 10.1016/j.talanta.2003.10.028]. *Talanta, 62*(5), 1005-1028.

15. Kruk, M., Jaroniec, M., Ko, C. H., & Ryoo, R. (2000). Characterization of the Porous Structure of SBA-15. [doi: 10.1021/cm000164e]. *Chemistry of Materials, 12*(7), 1961-1968.

16. Ooya, T., & Yui, N. (1999). Synthesis of theophylline-polyrotaxane conjugates and their drug release via supramolecular dissociation. [doi: DOI: 10.1016/S0168-3659(98)00163-1]. *Journal of Controlled Release, 58*(3), 251-269.

17. Plueddemann, E. p. (1982). *Silane coupling agents*. New york: Plenum publishing corporation.

18. Sarkar, A. R., Datta, P. K., & Sarkar, M. (1996). Sorption recovery of metal ions using silica gel modified with salicylaldoxime. [doi: DOI: 10.1016/0039-9140(96)01953-4]. *Talanta, 43*(11), 1857-1862.

19. Tong, A., Akama, Y., & Tanaka, S. (1990). Selective preconcentration of Au(III), Pt(IV) and Pd(II) on silica gel modified with [gamma]-aminopropyltriethoxysilane. [doi: DOI: 10.1016/S0003-2670(00)82778-6]. *Analytica Chimica Acta, 230*, 179-181.

20. Vansant, E. F., Van der voot, P., & Vrancken, K. C. (1995). *Charachterization and chemical modification of silica surface* (1 ed. Vol. 93). Amsterdam: Elsevier.

21. Wasiak, W., & Urbaniak, W. (1997). Chemically bonded chelates as selective complexing sorbents for gas chromatography V. Silica chemically modified by Cu(II) complexes via amino groups. [doi: DOI: 10.1016/S0021-9673(96)00683-8]. *Journal of Chromatography A, 757*(1-2), 137-143.

22. Zdravkov, B., Čermák, J., Šefara, M., & Janků, J. (2007). Pore classification in the characterization of porous materials: A perspective. [10.2478/s11532-007-0017-9]. *Central European Journal of Chemistry, 5*(2), 385-395.

Chapter 03

Metal ion adsorption behavior of modified silica

3.1 General introduction

Heavy metals have many useful applications in day to day life but they are harmful to living organisms especially when they are discharged into aquatic systems. In recent decades heavy metal adsorbents have been prepared with high surface area silica by attaching organic chelators to remove these toxic metals. The advantages of silica as a base material and organo-functional silanes as modifying groups are summarized in Table 3.1. The adsorption capacity and affinity for these modified silica for various metals can be studied by obtaining adsorption isotherms.

3.1.1. Adsorption Isotherms

The word adsorption was first introduced by Kayser in 1881. Adsorption is the accumulation of gases, liquids or solutes on the surface of a solid or liquid. Adsorption can be divided into two classes: physisorption and chemisorption. Physical adsorption is based on Van der Waals interactions and chemical adsorption arises from specific from specific intermolecular forces result during the adsorption process. (Lavrich, Wetterer, Bernasek, & Scoles, 1998)

The first classification of adsorption isotherms is introduced by Brunuer, Deming, Deming and Teller (BDDT) in 1940. According to the IUPAC classification there are six isotherm types given in Figure 3.1. These isotherms are closely related with pore characteristics of the material. Especially in silicas this adsorptive behavior dependent on

Material	Advantages
Silica as base material	1. Functional group immobilizations. 2. Easy to attach organo-functional groups into the silica surface. 3. Silica has high specific surface area. 4. Silica has high mass exchange characteristics 5. No swelling. 6. Silica support has great resistance to organic solvents 7. Very high thermal resistance. 8. Rapid sorption of metal ions.
Organo silane as modifying group	1. Potential for bonding through several mechanisms to the surface. 2. Availability with variety of functional groups therefore high selectivity. 3. Cross linking can be achieved

Table 3.1. Advantages using silica as a base material and organofunctional silane as modifying group

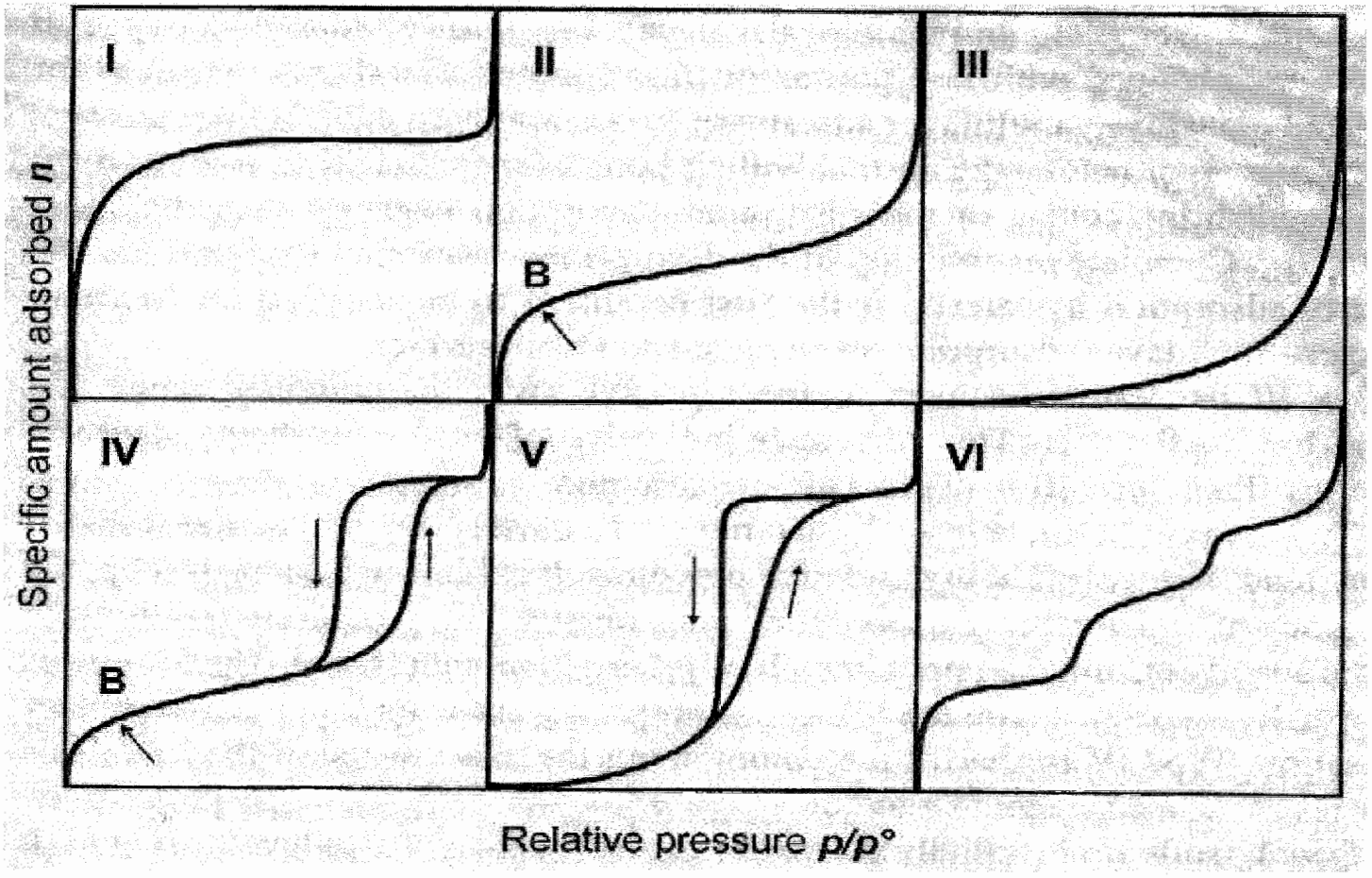

Figure 3.1 IUPAC Classification of Adsorption Isotherms (*www.nuigalway.ie/chem/Donal/Surfaces1.ppt)*

whether the material contains micropores, mesopores or macropores. Sometimes the desorption band does not follow the adsoption band, shown as a hysteresis loop in Figure 3.1 indicated by arrows (Schneidcer, 1995). By using these adsorption isotherms the affinity of various metals to modified silica can be studied with the help of atomic absorption spectrometry and electrochemical (cyclic voltammetry) measurements.

3.1.2. Atomic Absorption Spectrometry

In AAS, an element in its atomic form is introduced into a light beam of appropriate wavelength causing the atom to absorb light and enter an excited state. The reduction of the intensity of the light beam can be directly correlated with the concentration of the element that is going to be analyzed. This unknown concentration then can be measured by using a calibration curve. Normally a nebulizer is used to introduce elements into the flame in something close to an atomic form, which is called flame atomic absorption. In this method flame temperature can be varied according to the fuel that is going to be used in the flame. Hollow cathode lamps are used as light beams, the cathode is made up of the same element to be analyzed. The advantages and disadvantages of this method is described in Table 3.2 (Narin, Soylak, Elçi, & Dogan, 2000).

3.1.3 Anodic Stripping Voltammetry for determination of Hg(II)

By using AAS some metal atoms such as mercury can't be analyzed directly through the flame ionization method. But with the help of vapor generation accessory coupled to an AAS instrument, hydride-forming elements can be measured to very low levels (Vuchkova & Arpadjan, 1996). But there are major drawbacks in this method. The

Advantages	Disadvantages
1.The principles of measurement are straightforward 2. The technology is relatively inexpensive and the equipment is relatively easy to use 3. Results are highly reproducible 4. There are relatively few matrix and other interference effects 5. Satisfactory detection limits and linear dynamic ranges for some elements	1. Handles only liquid samples 2. Flame is a source of noise 3. Wastes sample solution 4. Analysis is usually limited to metals 5. AAS is a sequential, that is, one element at a time

Table 3.2. Advantages and Disadvantages of AAS

susceptibility to interferences from transition metals and hydride-forming elements, the instability of the expensive reduction reagent, and the dependence of the efficiency of hydride generation on the oxidation state of the analyte and on the reaction medium are major disadvantages of this wet hydride generation method (Denkhaus, Beck, Bueschler, Gerhard, & Golloch, 2001). In addition, techniques such as X-ray fluorescence, UV spectrophotometry, Inductively Coupled Plasma Atomic Emission Spectrometry (ICP-AES) and Inductively Coupled Plasma Mass Spectrometry (ICP-MS) become preferred method of determine mercury, but each has its own inherent disadvantages (Zejli, et al., 2007).

Therefore comparatively precise and sensitive electrochemical methods have gained much attention for mercury determination. Anodic Stripping Voltammetry is the most suitable technique for this purpose because of its high sensitivity. The major phenomenon behind this technique is, the longer the metal ions are under cathodic potential in an electrolyte solution, the more of that metal ion is reduced and deposited on the cathode. Therefore anodic peak current is depending on both sweep current and the potential. That is slower sweep rates and more negative switching potentials give larger anodic currents. So by deposition of metals under known potentials and constant time under the cathodic potential, and then measuring the anodic peak currents at the anodic sweep, developed into a sensitive analytical technique called Anodic Stripping Voltammetry. Under this technique measurements can be made in the parts per billion range (Zejli, et al., 2007).

3.1.4 Characterization of surface metal bonding interactions

The interaction of the surface species with the metal ion depend on many factors. Those are surface properties such as nature of the ligand, as well as the metal properties such as coordination number, oxidation number and ionic radius etc.(Jal, et al., 2004). One of the best ways to probe these interactions is by FTIR spectroscopy. This technique reveals the energies of possible stretching and deformation vibrations within the solid network. The assignment of these vibrations to specific chemical groups allows the identification of the chemical components of the solid network and therefore a better explanation of the surface metal bonding interactions can be obtained in different environments. In addition, structural changes according to the metal ion concentration can be readily identified by analyzing the frequency shift of functional groups.

Further, these kinds of interactions can be possible modeled by using computational calculations. After geometry optimizations of the selected metal ligand complexes, the minimum energy conformer help to probe the nature of the interactions as well as other details such as bond lengths, angles and shape of the overall coordination sphere.

3.2 Experimental methods

3.2.1 Metal ion adsorption data collection and analysis

Various concentrations (10 mL) of metal ion solutions were exposed to 0.025 g of modified SiO_2 in sealed conical flasks for 16h in a wrist action shaker. The slurries were centrifuged. The supernatant was then analyzed by Atomic Absorption spectrometry (Perkin –Elmer 2380) for metal ions Cu(II), Cd(II) and Cr(III). The Sr(II) was determined

by Atomic emission spectrometry and the Hg(II) was determined by the anodic stripping voltammetry (Zejli, et al., 2007). In all atomic absorption and emission experiments acetylene and air were used to generate the flame. The Cu(II), Cd(II), Cr(III), Sr(II) metals were analyzed at wavelengths of 324.8nm, 228.8nm, 357.9nm, 460.7nm respectively.

3.2.2 Determination of Hg^{2+} by Anodic Stripping Voltammetry

3.2.2.1 Electrodes, electrochemical cells and reagents

The working electrode (WE) used in all the measurements was a thin-film of Au film deposited onto a glass substrate. The WE was fabricated by electron beam deposition of thin-film Au (100 nm) on glass substrate (5 x 25 mm) that was pre-coated with a 15 nm thick Ti adhesion layer (Temescal Six Pocket E-beam Evaporation Systems). Prior to deposition, the glass slides were cleaned in a freshly prepared "piranha" solution (concentrated H_2SO_4 : 30 % H_2O_2 = 3:1 vol.) for 10 min, after which they were rinsed with copious amounts of 18 MΩ deionized water (Millipore Systems), and dried in a stream of nitrogen.

A Gold coated alligator clip was used for contact between the WE and the WE connection of the potentiostat. Pt-wire was used as an auxiliary (counter) electrode (CE) and the reference electrode (RE) was Ag/AgCl (3 M NaCl).

All experiments were performed with a CHI 660C potentiostat/galvanostat (CH Instruments). Two standard three-compartment electrochemical cells with RE and CE compartments separated from the WE chamber were used.

All experiments were performed in 0.1 M NaBr electrolyte solution.

3.2.2.2 Electrochemical Procedure

Prior to each measurement, the electrolyte in the cell was deaerated by purging with 99.999 % purity inert gas (Ar or N_2) for 30 min. During all the electrochemical measurements, the inert gas was continuously flown above the solution. The procedure consisted of four consecutive steps: electrode cleaning, electrode activation, Hg-deposition and Hg-stripping.

Electrode Cleaning: The WE was first activated by two 30 s pulses, first at 0.6 V and then at –0.3 V after which a cyclic voltammogram in this potential range was recorded. If traces of Hg were present, the electrode was anodically polarized again at 0.6 V for 30 s. In order to prevent further deposition of Hg under open circuit conditions, the electrode was taken out of the Hg-containing electrolyte under potential and rinsed copiously with millipore water.

Activation: The WE was activated by a 30 s pulse at –0.2 V after which it was taken out of the electrolyte under potential and transferred immediately to a second electrochemical cell filled with the Hg-containing electrolyte. The electrode was immersed in solution at 0.6 V (potential at which no Hg deposition occurred).

Deposition: Following the activation pulse, Hg deposition was performed by stepping the potential to –0.2 V and holding it for 30 s. The electrode was then taken out of solution, rinsed copiously with Millipore water and immediately transferred to the other electrochemical cell and immersed into the electrolyte at an immersion potential E = –0.2 V.

Stripping: Anodic stripping was performed –0.2 V to 0.6 V at a potential scan rate of 100 mV/s.

The Hg content was determined from a standard calibration line that was constructed by plotting the stripping peak currents vs. Hg concentration.(Zejli, et al., 2007)

3.2.3 Characterization of surface metal bonding interactions

3.2.3.1 FTIR characterization

The nature of the surface metal bonding interactions were investigated in metal EDTA modified silica complexes by using Reflectance infrared spectra. Various concentrations (10 mL) of metal ion solutions were exposed to 0.025 g of modified SiO_2 in sealed conical flasks for 16h in a wrist action shaker. The slurries were centrifuged. The precipitates were dried at 110 ^{0}C in vacuum for 2 hours. Reflectance infrared spectra were obtained using a Digilab FTS 3000 FT-IR equipped with a narrow band MCT detector. Diffuse reflectance spectra were obtained using a "praying mantis" diffuse reflectance accessory from Harrick Scientific. N_2 gas was purged into the sample compartment in order to remove interference of the spectra from water vapor. All integrations were done using standard instrument software. The samples were prepared by mixing 20mg of metal EDTA modified silica complexes with 200mg of dried, preground (~5μm) KCl.

3.2.3.2 Computational calculations

The nature of the metal EDTA complexes were modeled by using Gaussian® 03 and Gauss view 4.1 program packages. The calculations were done by Molecular Mechanics(MM) and Universal Force Field (UFF). The major parameters used for these calculations are included in the supplementary section.

3.3 Results and discussion

3.3.1 Hg(II) adsorption data and analysis

In our research we gave much attention to mercury because of its toxicity and the fact that it is everywhere, because of their industrial use and burning of coal. (http://mercurypolicy.org/) Therefore preparation of materials that can adsorb large amounts of mercury has become a primary target for adsorptive materials. In addition, choosing (or developing) a technique to determine the amount of mercury in solution more precisely is important to carry out these studies. Techniques that are sensitive as well as precise enough for quantitative determination of mercury such as wet hydride generation, X-ray fluorescence, UV spectrophotometry, Inductively Coupled Plasma Atomic Emission Spectrometry (ICP-AES) and Inductively Coupled Plasma Mass Spectrometry (ICP-MS) are mostly not available at EIU.

Therefore, Dr. Svetlana Mitrovski generously helped to develop an electrochemical technique. The developed new Anodic Stripping Voltammetric technique using a gold electrode was checked under laboratory conditions and succeeded with high reproducibility, very low detection limits, good linear dynamic range and high sensitivity. The obtained calibration curve with these properties is given in Figure 3.2. The maximum stripping peak current compared to the background in cyclic voltammetric curves given under Figure 3.3 was used to draw this calibration curve. The advantages and disadvantages of this technique are summarized in Table 3.3.

The ability of the modified surface to bind mercury from aqueous solution was evaluated by acquiring an adsorption isotherm. Under equilibrium conditions, at the solid/liquid interface metal cations can be adsorbed onto the silica surface. The extent of

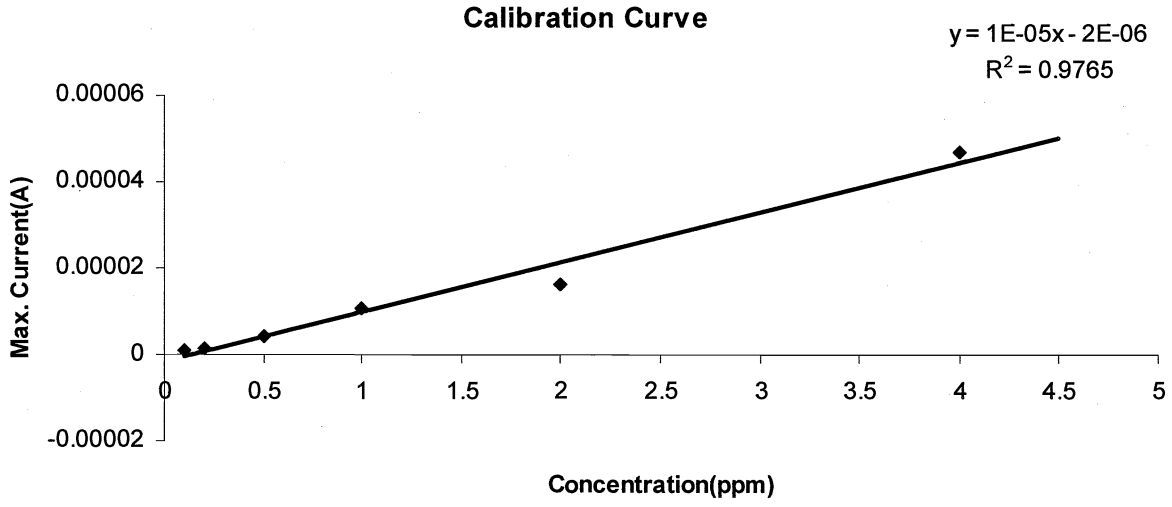

Figure 3.2 The Calibration Curve obtained for the newly developed Anodic Stripping Voltammetric technique.

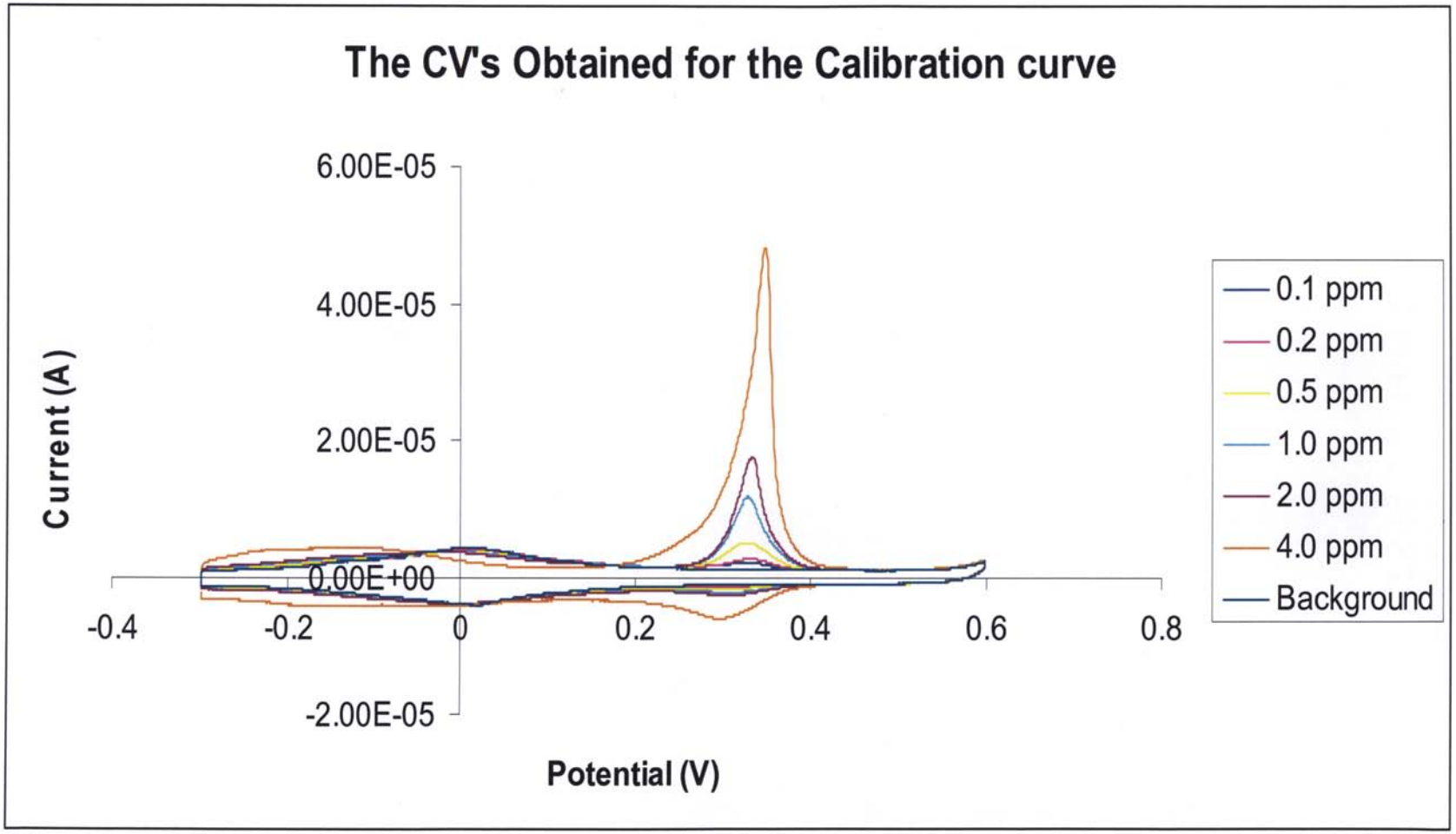

Figure 3.3 The CV's obtained for the Calibration curve

Advantages	Disadvantages
1. Mercury ions can be measured down to 10 ppb in aqueous Solutions 2. High reproducibility of results 3. High sensitivity 4. Good linear dynamic range 5. Method is simple and straightforward 6. Low cost 7. Most suitable for batch type of determinations 8. one electrodes can be used in several determinations 9. The errors of the measurements are readily detectable compared to other techniques	1. Overall measurement procedure has five steps, therefore time consuming compared to the techniques such as AAS 2. The dilutions of solutions and preparation of electrolytes time consuming 3. Cleaning of electrochemical cells needs specific strong oxidizing agents which is hazardous and time consuming 4. The electrolytes well as analyte have to be very clean therefore have to use specific filtration method which is time consuming. (Specially removal of small silica particles is very difficult)

Table 3.3 The advantages and disadvantages of Anodic Stripping Voltammeric technique

this adsorption can be mathematically evaluated by using the numbers of moles adsorbed per gram of support. This value was calculated from subtracting the equilibrium number of moles of metal ion at equilibrium from the initial number of moles added, and then dividing that number by the mass of silica support in grams. By plotting this calculated value versus equilibrium concentration results in an adsorption isotherms. All these calculations are given at supplementary section. (Jal, et al., 2004) In this work pH is fixed at pH ~ 5 to avoid effects of pH on metal ion speciation. (Ian P. Blitz, et al., 2007)

After characterization of EDTA modified HP39, 200DF and SBA15 silica by nitrogen adsorption and FTIR methods, we thought that these materials should have a high metal ion adsorption capacity for two reasons. There was much less reduction in surface area than expected compared to other modified silicas, and the pore volume in some cases actually increased. The EDTA silane has ability to adsorb one metal ion per molecule, both properties were considered to be potentially helpful to increase the metal ion adsorption capacity.

The three adsorption isotherms observed for the Hg(II) ion adsorption on to the EDTA modified HP39, 200DF and SBA15 silica are given in Figure 3.4 and Hg(II) adsorption at low concentration is given in Figure 3.5. As expected these material show the ability adsorb very high amounts of Hg(II). From the three types of modified silicas used for mercury adsorption, HP39 silica has the maximum adsorption capacity. When considering the molar percent adsorbed by each silica given in Table 3.4 all three types of silicas have good adsorption capacity percentages in lower concentrations as well as higher concentration. At very low concentrations sometimes adsorption percentage is

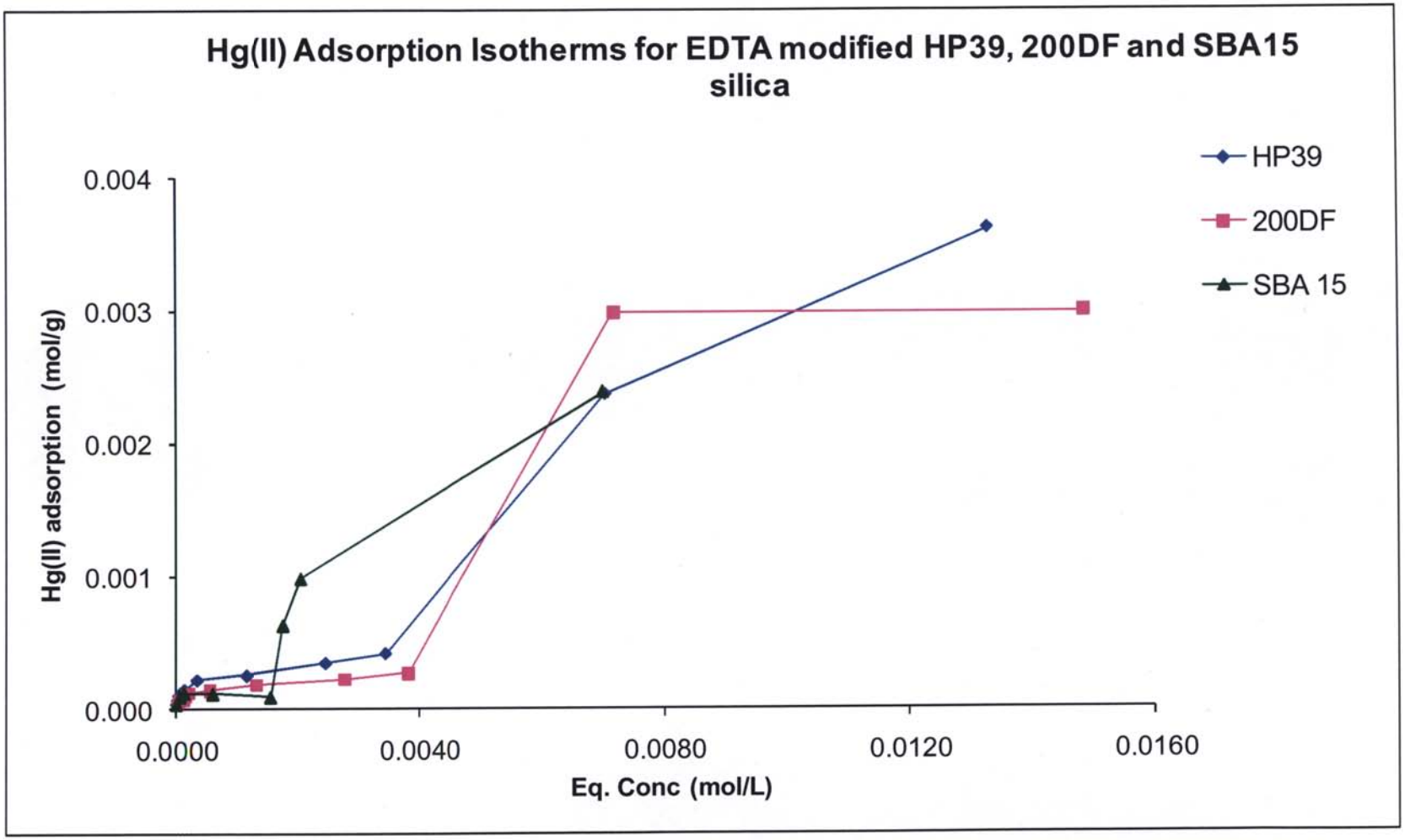

Figure 3.4 Hg(II) Adsorption Isotherm EDTA modified HP39, 200DF and SBA15 silica

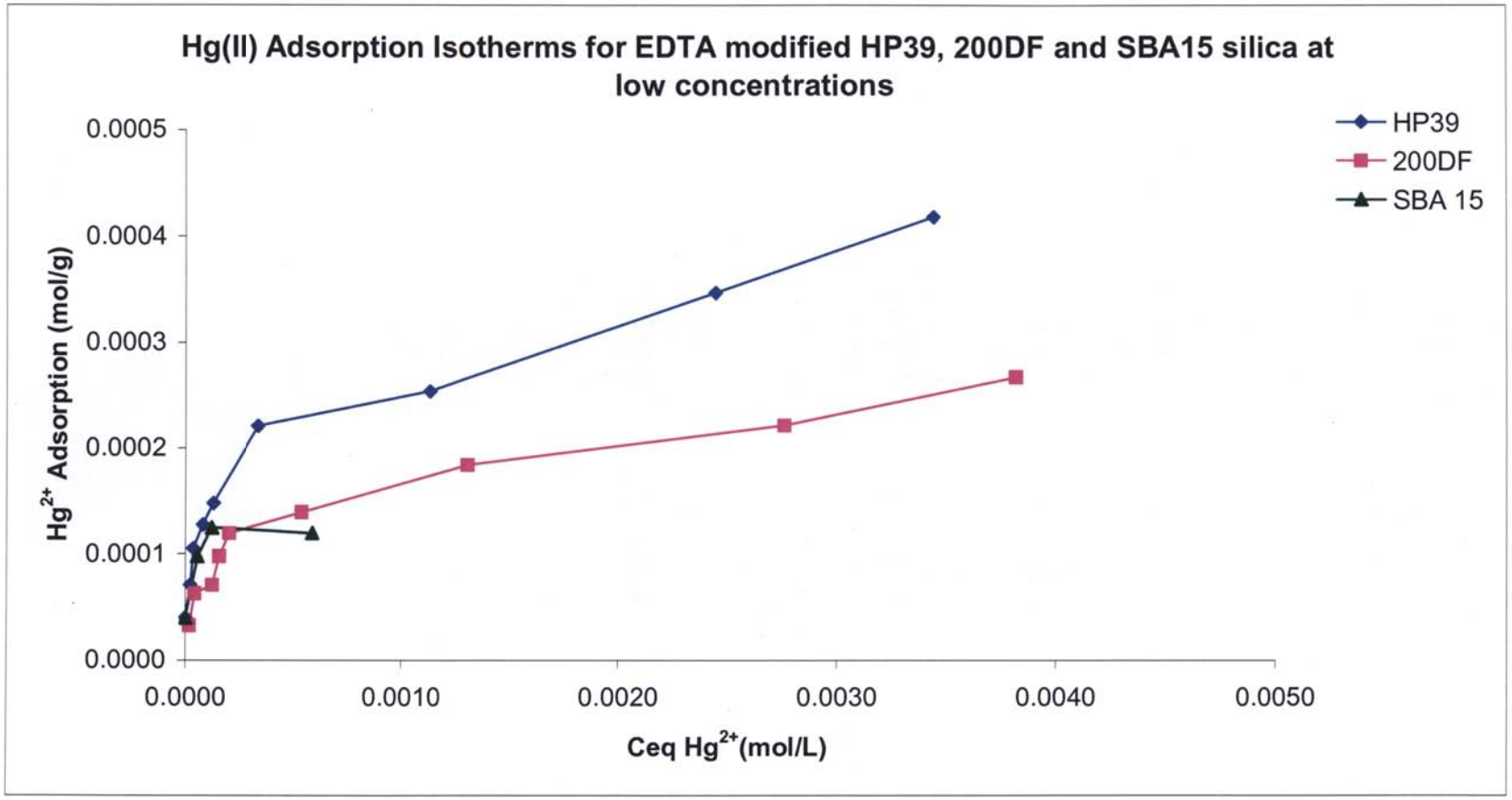

Figure 3.5 Hg(II) Adsorption Isotherm EDTA modified HP39, 200DF and SBA15 silica at low concentrations

Initial concentration of Hg(II) solution (ppm)	Molar percent adsorbed into HP39 silica	Molar percent adsorbed into 200DF silica	Molar percent adsorbed into SBA15 silica
20	100.0	81.4	100.0
40	88.8	78.4	-
60	87.8	58.9	81.5
80	79.9	61.2	-
100	74.1	59.9	72.2
178	62.2	39.2	33.7
355	35.8	26.0	13.2
665	26.1	16.7	47.5
900	23.3	14.9	54.6
2600	45.6	50.9	46.0
4478	40.5	33.5	-

Table 3.4 The percentages of Hg(II) adsorbed by each silica

100% (i.e., within the limits of detection). In some of our mercury adsorption experiments with HP39 silica showed 1: 1 adsorption capacities. That is for each gram of material approximately one gram of mercury can be removed from a water solution. This adsorption capacity is greater than any material that we are aware of.

The Langmuir plots observed for the EDTA modified HP39, 200DF and SBA15 silica for metal ion Hg(II) suggest that at low concentrations these adsorption isotherms behave according to the Langmuir equation. If the high concentration data is include, the Langmuir equation no longer fits. The major assumption of the basic Langmuir type isotherm is adsorption takes place only at specific localized sites on the surface and saturation coverage corresponds to the complete occupancy of sites (Esposito, Del Nobile, Mensitieri, & Astarita, 1996). That is, this equation is defined for monolayers. Therefore, the fact that the data does not fit the Langmuir equation at higher Hg(II) concentrations is not surprising. There may be a multitude of factors that influence this. If there are any structural changes, these can be potentially identified using FTIR spectroscopy (Prasad, Agrawal, & Sharma, 2003). So to check any structural changes of the surface species with increasing Hg(II) ion concentration on EDTA modified silica, we used FTIR diffuse reflectance spectroscopy.

Figure 3.7 includes FTIR spectra observed for the EDTA modified silica after adsorbing metal ion Hg(II) at different concentrations. In these spectra, we focused on the region 1700–1500 cm^{-1} because the most distinguishable feature in the spectra of the EDTA compounds for our purposes are those attributable to the carboxyl groups, being the strongest bands in the mid-IR range (Lanigan & Pidsosny, 2007). In this region the carboxylate C=O stretch can be seen.

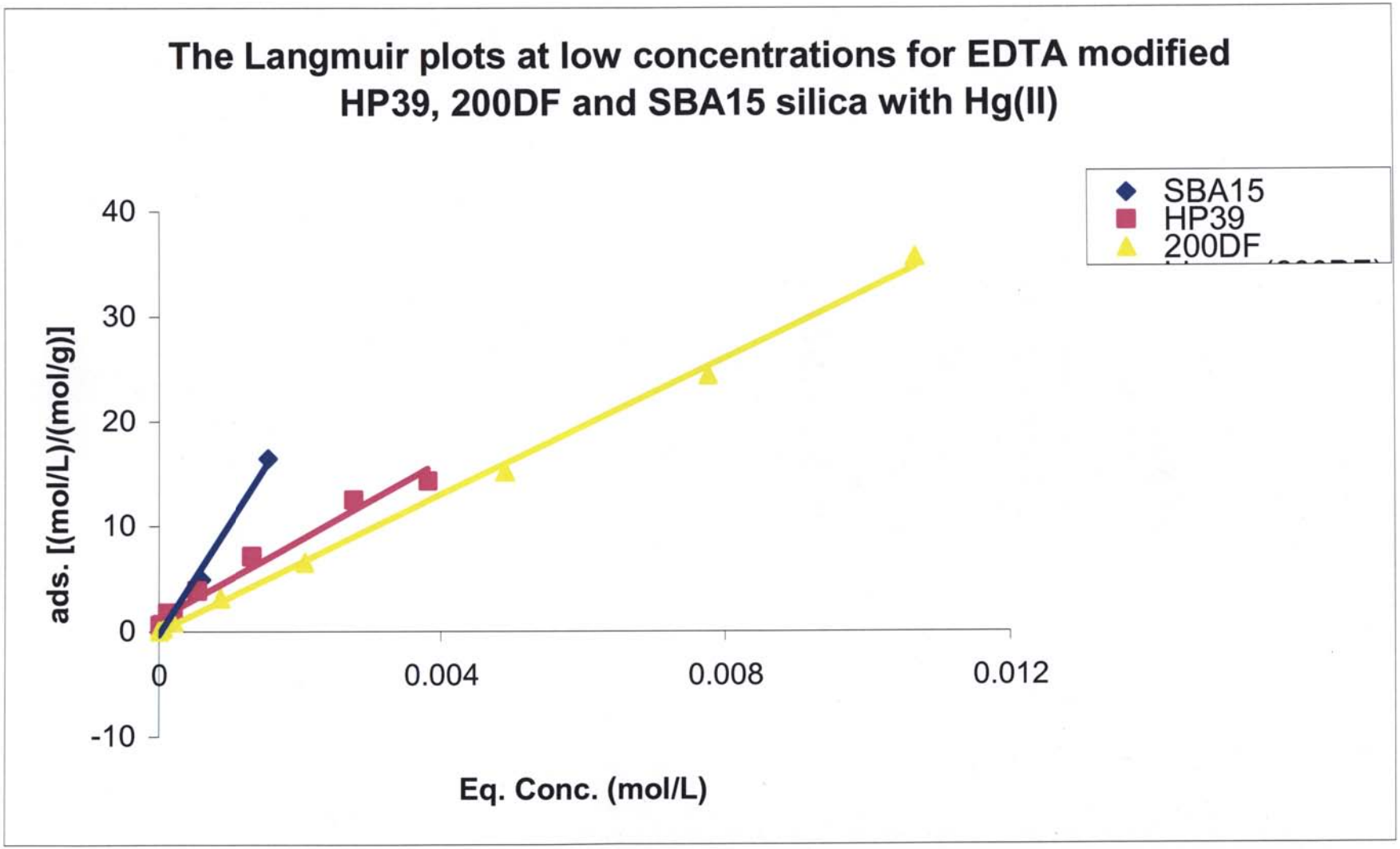

Figure 3.6 The Langmuir plots at low concentration for EDTA modified HP39, 200DF and SBA15 silica with Hg(II)

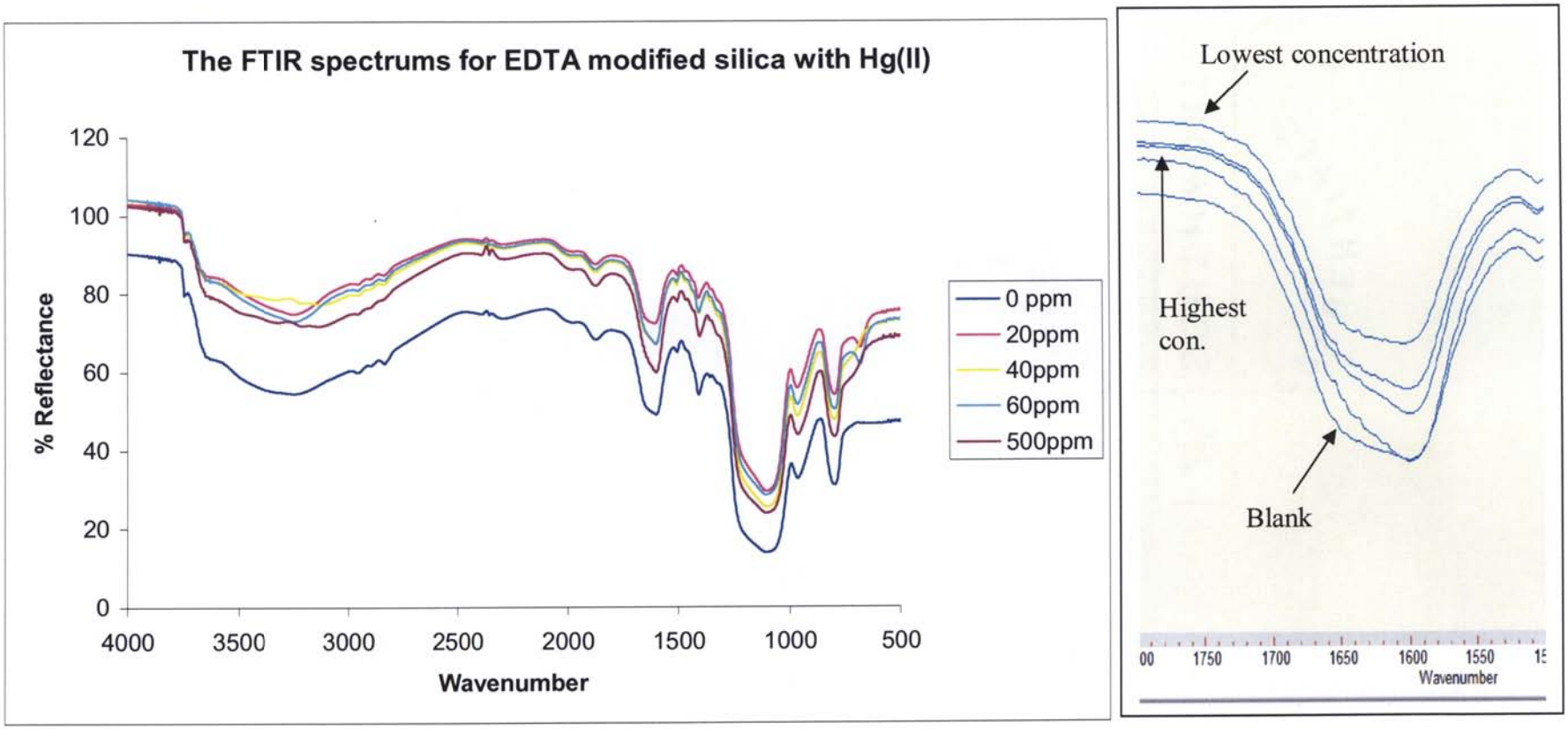

Figure 3.7 FTIR spectrums observed for the HP39 EDTA modified silica after adsorbing metal ion Hg(II) at different concentration

The carboxylate stretching frequency has been shown, in free compounds, to correlate with metal electronegativity. The argument has been that the more electronegative atom pulls electron density from the carbonyl oxygen, decreasing the need for conjugation and thus increasing the stretching frequency. But the observed spectra in Figure 3.7 behave the opposite way. That is, with increasing metal ion concentration the carboxylate frequency appears to shift towards lower energy. This is not understood, except to point out the obvious that solution chemistry does not necessarily extend to surface species.

Normally, in metal-ethylenediaminetetraacetic (M-EDTA complexes) complexes as the metal ion becomes larger the coordination numbers tend to become higher. Some metal ions such as Hg(II) and Ag(I) may tend to be exceptions to this rule. These metal ions tend to have low coordination numbers sometimes, as low as two. In addition these complexes, N-M-N bond angle becomes larger compared to the other larger metal ion complexes (Martell & Hancock, 1996). The major difference in between the ethylenediaminetetraacetic acid molecule and N-(triethoxysilylpropyl) ethylenediaminetriacetic acid silane modified silica is the EDTA silane has three carboxylic group and EDTA molecule has four carboxylic groups when considering the reactive centers given in Figure 3.8. Therefore the above observations are consistent with EDTA modified silica interacting with the metal ion Hg(II).

In Hg(II) EDTA complexes, the metal ion coordinated with the two nitrogen atoms of EDTA generates a five membered ring. If the metal coordinated with the carboxylic group another five membered ring would have to be formed. That is, the

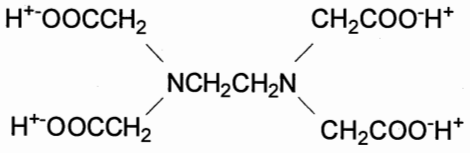

ethylenediaminetetraacetic acid

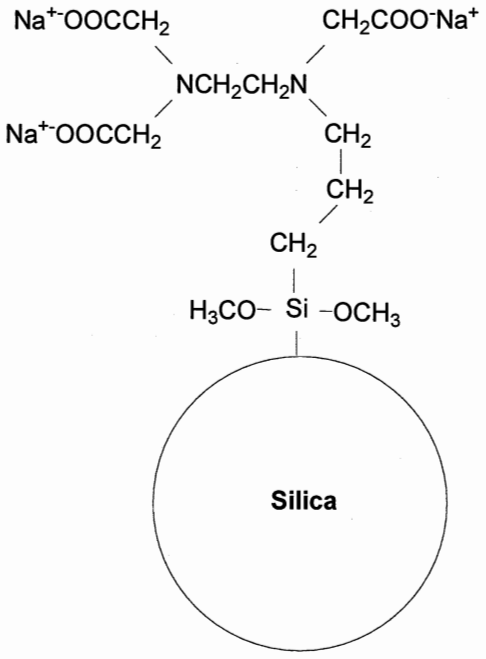

N-(triethoxysilylpropyl)ethylenediaminetriacetic acid

silane modified silica

Figure 3.8 ethylenediaminetetraacetic acid molecule and N-(triethoxysilylpropyl)ethylenediamine silane modified silica

number of five membered rings increases with the coordination number. It is very clear that the strain of these five membered rings will primarily depend on the ionic radius of the metal ion. As mentioned earlier, Hg(II) has low coordination numbers with EDTA. This is because if the Hg(II) approaches in-between two nitrogen atoms, a reasonable assumption, it is best fit into the five membered ring with its large ionic radius (Martell & Hancock, 1996). In addition because of this larger ionic radius, the Hg(II) does not coordinate with the carboxylic groups, since additional rings will further destabilise the complex by increasing the ring strain. This idea is easily verified by performing simple molecular mechanics calculations.

Performing these types of calculations at a level greater than molecular mechanics proved to be too time consuming, because the whole molecule is comparatively large, and Hg(II) has a large number of electrons. Thus electronic effects were not taken into account, only geometry optimizations were completed. If a good force field is available for the molecule under study, the optimized structure by molecular mechanics will more closely match experimentally determined structures than other computational chemistry techniques (Hinchliffe, 2003).

The concern of force field is very important to perform a molecular mechanics optimization because different force fields have been developed for different molecular types. We chose Universal Force Field (UFF) to perform our calculations, the reasons are it extends throughout entire periodic table, and UFF geometry optimizations are based on element, hybridization, and connectivity (Casewit, Colwell, & Rappe, 1992).

The geometry optimized structures are given in Figure 3.9 by using molecular mechanics through the UFF. According to the computational calculations it is very clear that, when increasing the number of rings, the energy of Hg(II) EDTA complexes is increased (Table 3.5). Therefore low coordination numbers can be expected in Hg(II) EDTA complexes.

But the question remains as to why C=O frequencies of the Hg(II) EDTA modified silica complexes shift to lower energy with increasing metal ion concentration. It was previously discussed that increasing the number of rings, increases the energy of Hg(II) EDTA complexes. But in the surface, the coordination can be achieved without forming rings. As indicated in the Figure 3.10 the carboxylic group at molecule 1 can coordinate with the Hg(II) EDTA complex because molecule 1 can freely rotate to achieve the correct orientation. When the metal ion concentration increases most sites are filled with the trapped Hg(II) ions, and a five membered ring is generated at the each site. Then with the ring strain, the ability of the free rotation around bonds are decreased and the correct orientation of the carboxylic group towards the Hg(II) can't be easily achieve. Therefore no of sites that have carboxylic metal bond decreased when increasing the metal ion concentration. So, C=O frequencies of the Hg(II) EDTA modified silica complexes move into lower region when increasing the metal ion concentration. While these computational results are highly speculative, they provide a framework for future study.

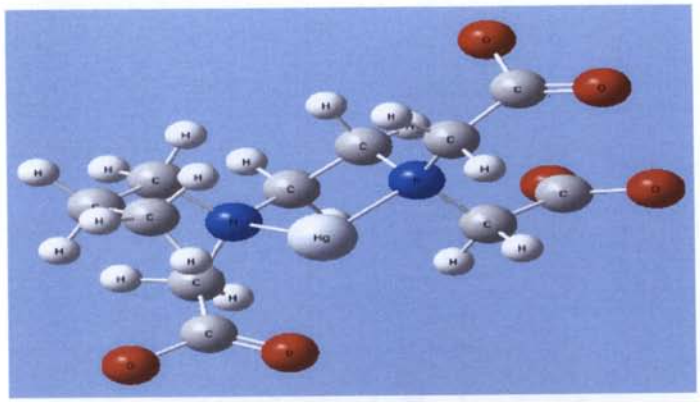

Hg(II) EDTA complex (C.N. 2)

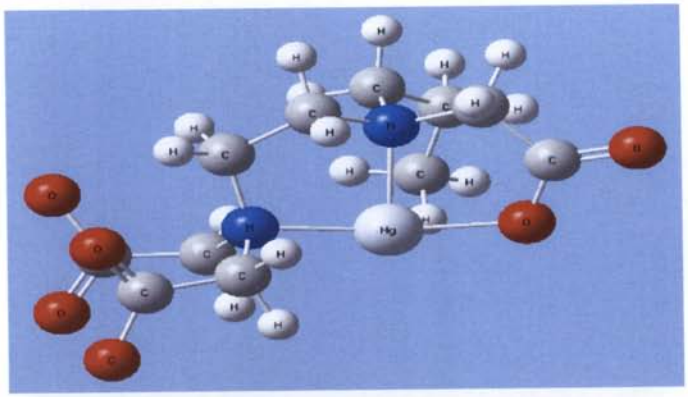

Hg(II) EDTA complex (C.N. 3)

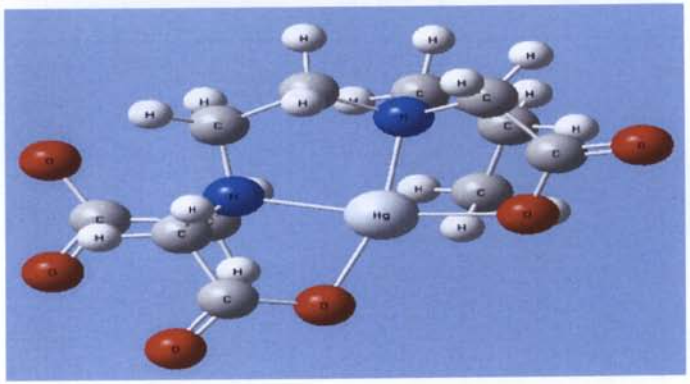

Hg(II) EDTA complex (C.N. 4)

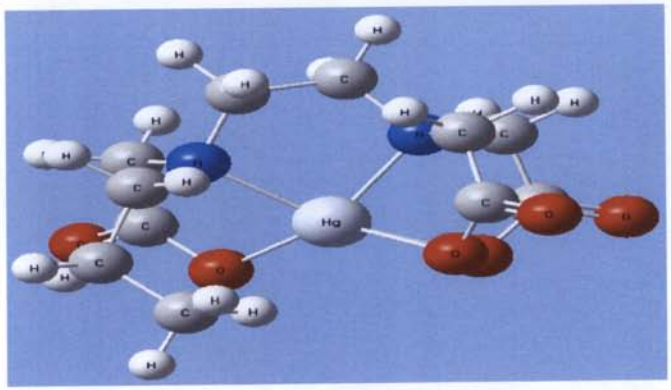

Hg(II) EDTA complex (C.N. 5)

Figure 3.9 Structures obtained after the geometry optimization of Hg(II) EDTA modified silica complexes

No.of Rings	Coordination number	Minimum calculated energy (a.u)
1	2	0.10835820
2	3	0.15943687
3	4	0.24287332
4	5	0.38261557

Table. 3.5 Calculated Energy values for each Hg(II) EDTA complex

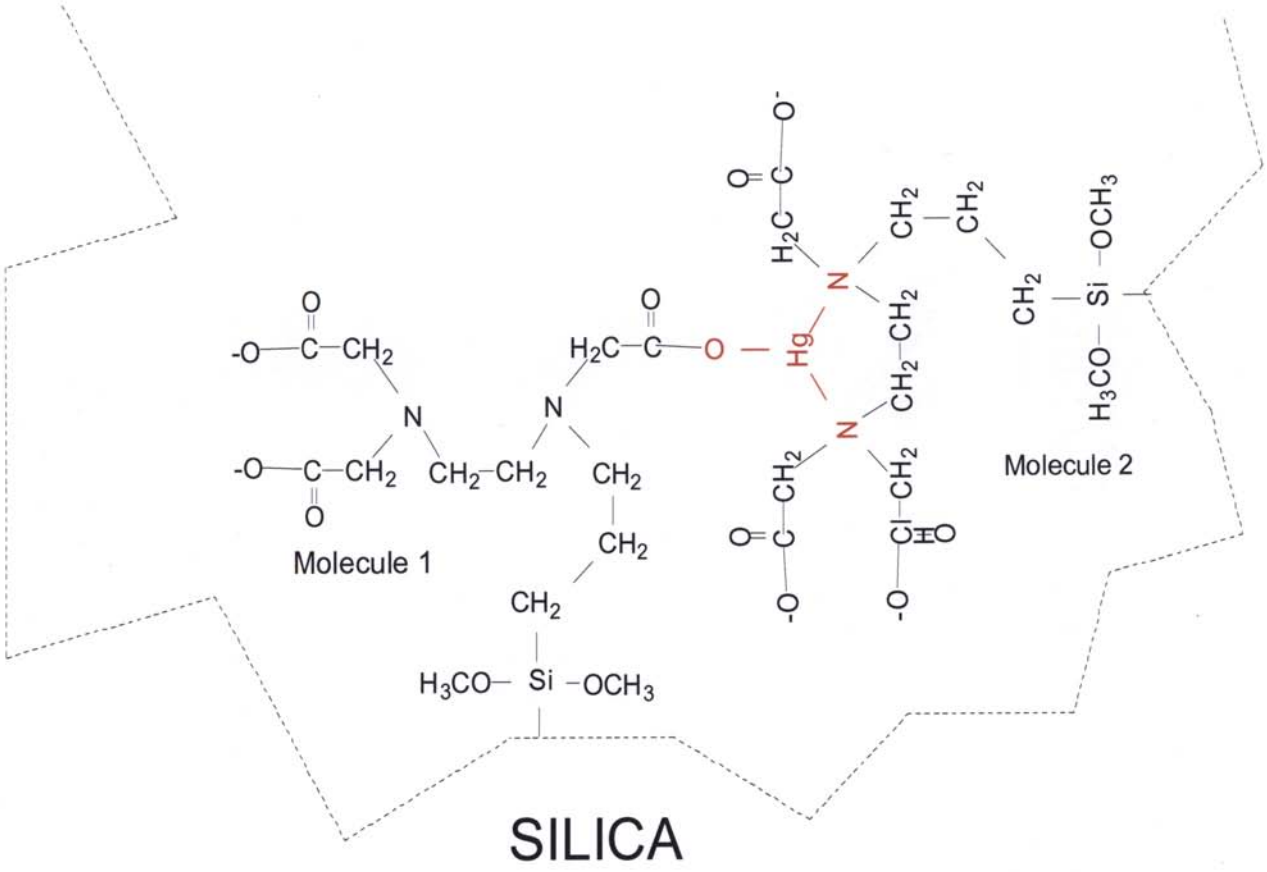

Figure 3.10 One Coordination possibility of Hg(II) with EDTA modified silica.

3.3.2 Cr(III) adsorption data and analysis

In Figure 3.11 the adsorption isotherms for the metal ion Cr(III) with EDTA modified HP39, 200DF and SBA15 silica are shown. We used Cr(III) ion for our adsorption experiments mainly to compare the difference in adsorption behavior between divalent metal and a trivalent metal. As well as the metal ion Hg(II), Cr(III) also showed a very high adsorption capacity with the EDTA modified three types of silicas. Here also, the highest Cr(III) adsorption capacity is shown by HP39 silica among the three types of silicas used for adsorption experiments. The molar percentages adsorbed onto each silica are given in Table 3.6, showing the high affinity of Cr(III) towards the EDTA modified silica. But compared to the metal ion Hg(II), molar capacities are low in Cr(III). That means in contrast to the trivalent Cr(III), EDTA modified silica showing high adsorption capacities for the divalent metal ion Hg(II).

Figure 3.12 includes FTIR specrta observed for the EDTA modified silica after adsorbing metal ion Cr(III) at different concentrations. In this case we observed the expected trend in vibrational frequencies, that is the C=O frequencies of the Cr(III) EDTA modified silica complexes move into higher region when increasing the metal ion concentration. That means the Cr(III) EDTA modified silica metal complexes behave in the opposite way compared to the Hg(II) EDTA modified silica metal complexes in this sense. It is well known that in the Cr(III)-ethylenediaminetetraacetic complex a seven coordination geometry(Figure 3.13) exists, and according to the diagram Cr(III) metal coordinated with all of the carboxylic groups and two nitrogen atoms in ethylenediaminetetraacetic as well as with water molecules to satisfy the coordination number seven (Harris, 2007). So the same structures might be expected for the

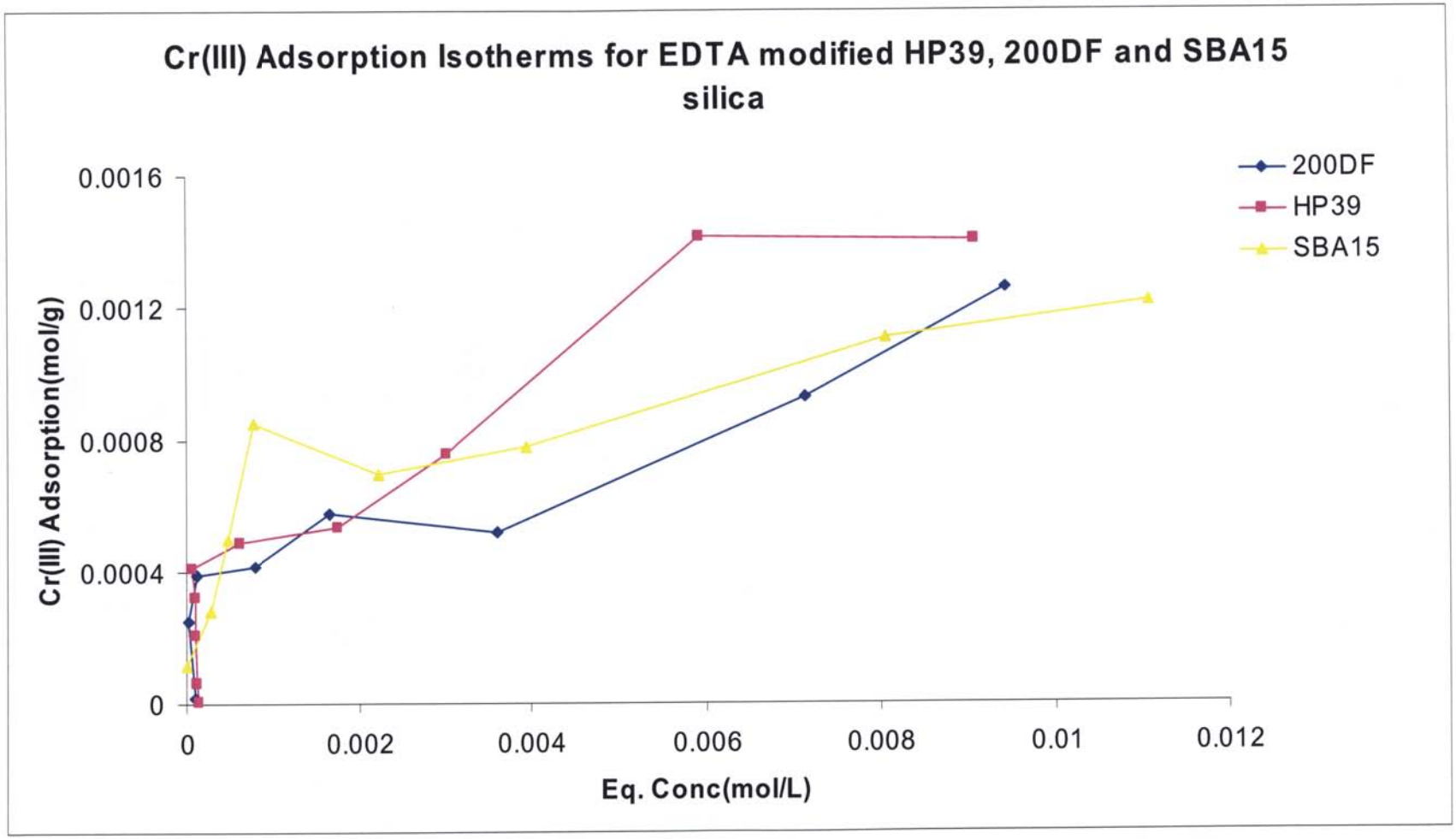

Figure 3.11 Cr(III) Adsorption Isotherm EDTA modified HP39, 200DF and SBA15 silica

Initial concentration of Cr(III) solution (ppm)	Molar percent adsorbed into HP39 silica	Molar percent adsorbed into 200DF silica	Molar percent adsorbed into SBA15 silica
7.31	7.82	30.1	100.0
32.6	83.0	98.3	55.5
56.4	94.2	89.0	57.0
94.8	67.0	57.0	58.2
160.9	43.2	46.3	28.0
255.2	38.4	26.4	19.8
491.4	37.3	24.6	14.6
654.5	27.9	24.9	12.1

Table 3.6 The percentages of Cr(III) adsorbed by each silica

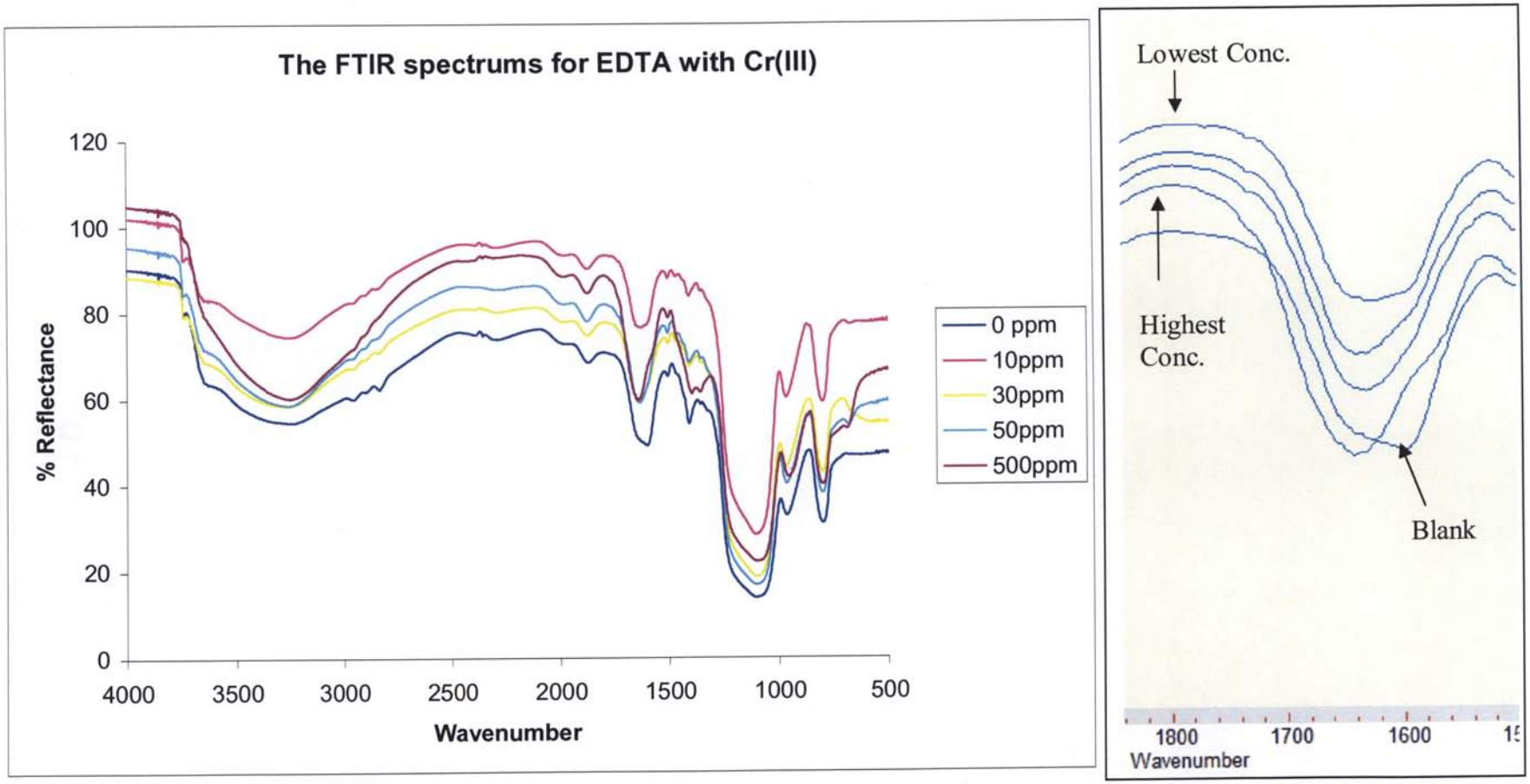

Figure 3.12 FTIR spectrums observed for the HP39 EDTA modified silica after adsorbing metal ion Cr(III) at different concentrations

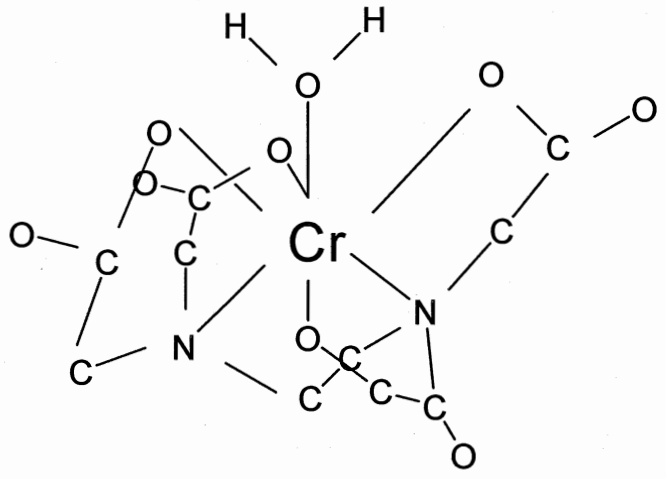

Figure 3.13 Seven coordinate geometry of Cr(III)-ethylenediaminetetraacetic complex

Cr(III) EDTA modified silica with one exception, that is for the missing carboxylic group for the Cr(III) EDTA modified silica complex compared to the Cr(III) ethylenediaminetetraacetic complex replaced by water molecule. To confirm this idea we performed a computational calculation using MM and UFF. For the computationally calculated structures for Cr(III) EDTA modified silica complexes, the minimum energy structure was more close to the expected Cr(III) ethylenediaminetetraacetic. The obtained structures after optimization for each molecule are shown in Figure 3.14 and their energies in Table 3.7. According to the obtained structures, the minimum energy structure, that is Cr(III)EDTA(H_2O), all carboxylic groups are coordinated with the metal ion. Therefore it is clear that the more electronegative atom pulls electron density from the carbonyl oxygen, decreasing the need for conjugation and thus increasing the stretching frequency. So C=O frequencies of the Cr(III) EDTA modified silica complexes move into the higher energy region with increasing metal ion concentration. In addition, now it is clear that Cr(III) EDTA modified silica metal complexes behave in an opposite way compared to the Hg(II) EDTA modified silica metal complexes, in the sense of carboxyl frequency shifts, mainly because of the differences in ionic radius and coordination number of two metals.

3.3.3 Sr(II) adsorption data and analysis

Next we chose to study metal ion Sr(II) with HP39, 200DF and SBA15 EDTA modified silica because radioactive isotopes of strontium metal ions are toxic to human as well as other aquatic living creatures, especially vertebrates. This metal ion is released in enormous amounts as nuclear waste. We didn't use the radioactive isotope for our

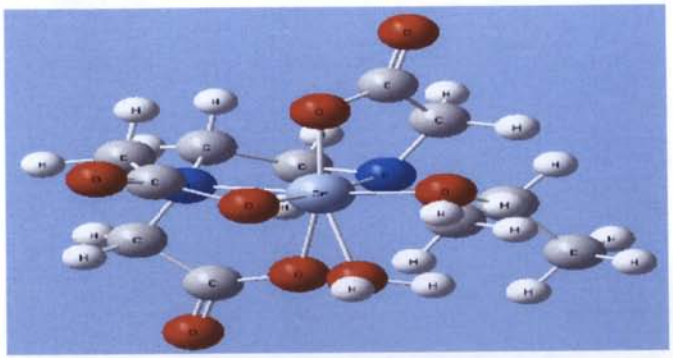

Cr(III)EDTA(H_2O)$_2$

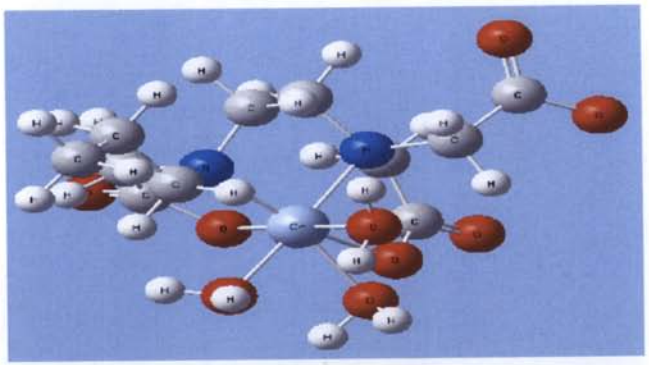

Cr(III)EDTA(H_2O)$_3$

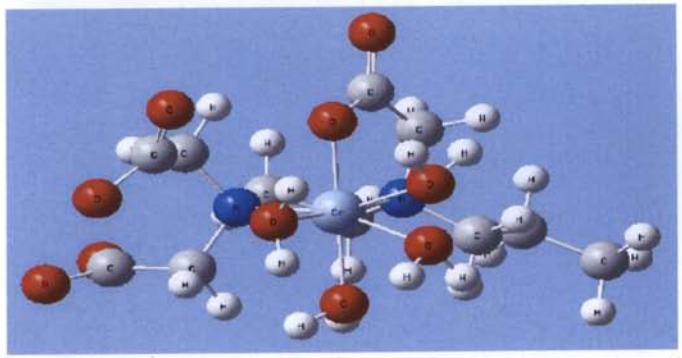

Cr(III)EDTA(H_2O)$_4$

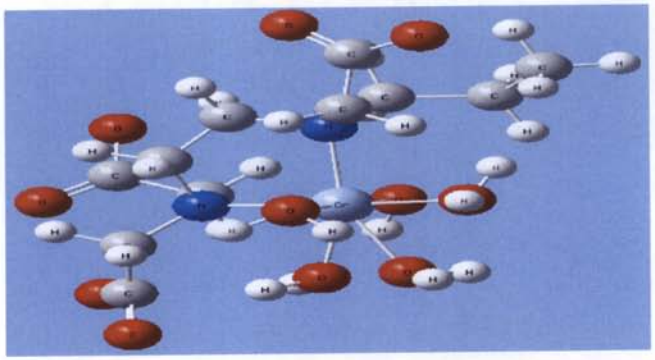

Cr(III)EDTA(H_2O)$_5$

Figure 3.14 Structures obtained after the geometry optimization of Cr(III) EDTA modified silica complexes

Complex	Minimum calculated energy (a.u)
$Cr(III)EDTA(H_2O)_2$	0.3130245
$Cr(III)EDTA(H_2O)_3$	0.31484907
$Cr(III)EDTA(H_2O)_4$	0.36431138
$Cr(III)EDTA(H_2O)_5$	0.46375651

Table 3.7 Calculated Energy values for each Cr(III) EDTA complex

experiments, but used non radioactive isotope because in both cases they should have nearly identical chemical properties, which will give rise to the same or similar adsorption results. Compared to the isotherms obtained for the metal ions Cr(III) and Hg(II), the Sr(II) adsorption isotherms have a nature of monolayer formation as indicated by there Langmuir behavior in Figure 3.15. Therefore these isotherms can be easily fit to the Langmuir equation. The obtained plots after fitting into the Langmuir equation are given in Figure 3.16. The obtained R squared values in Table 3.8 for these plots suggesting how well the regression line approximates real data points after fitted into the Langmuir equation. For all three plots R squared values are above the acceptable limit and fit well into the Langmuir equation. In addition calculated Γ_{max} values suggesting that, HP39 EDTA modified silica has the highest Sr(II) adsorption capacity among the three types of modified silica studied, and the lowest adsorption capacity is for 200DF silica. Further, for metal ion Sr(II), SBA15 EDTA modified silica also has a high adsorption capacity close to HP39 EDTA modified silica, both much improved over 200DF silica.

Figure 3.17 includes FTIR spectra observed for the HP39 EDTA modified silica after adsorbing metal ion Sr(II) at different concentrations. In this plot it can be observed that the C=O frequencies of the Sr(II) EDTA modified silica complexes move into a lower energy region with increasing metal ion concentration. Therefore Sr(II) EDTA complexes behave as Hg(II) EDTA modified silica complexes, when considering the carbonyl shift, with increasing metal ion concentration. As well as Hg(II) EDTA complexes, it is well known that Sr(II) can easily coordinate with carboxylic groups belongs to two EDTA molecules in Sr(II) EDTA metal complexes

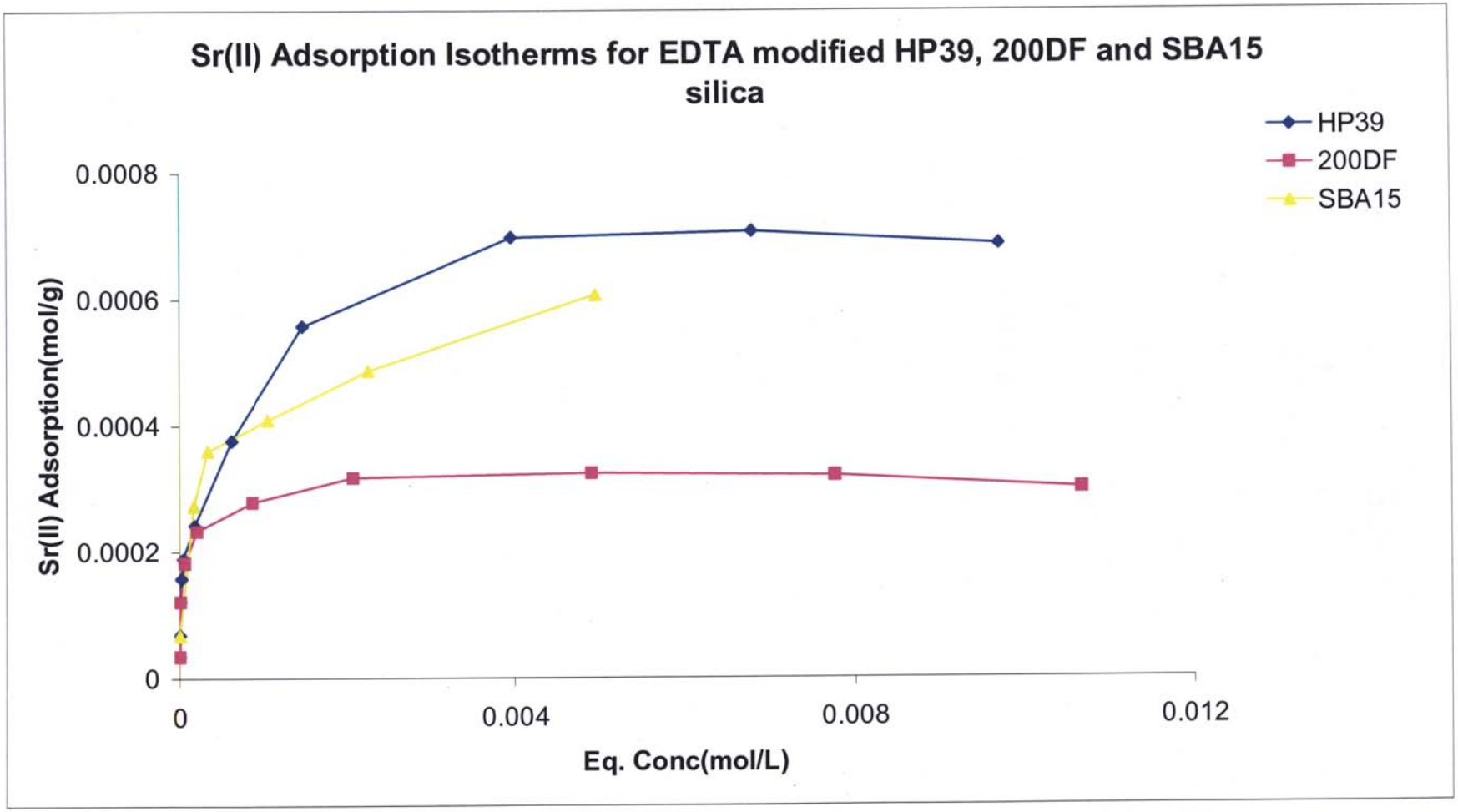

Figure 3.15 Sr(II) Adsorption Isotherm EDTA modified HP39, 200DF and SBA15 silica

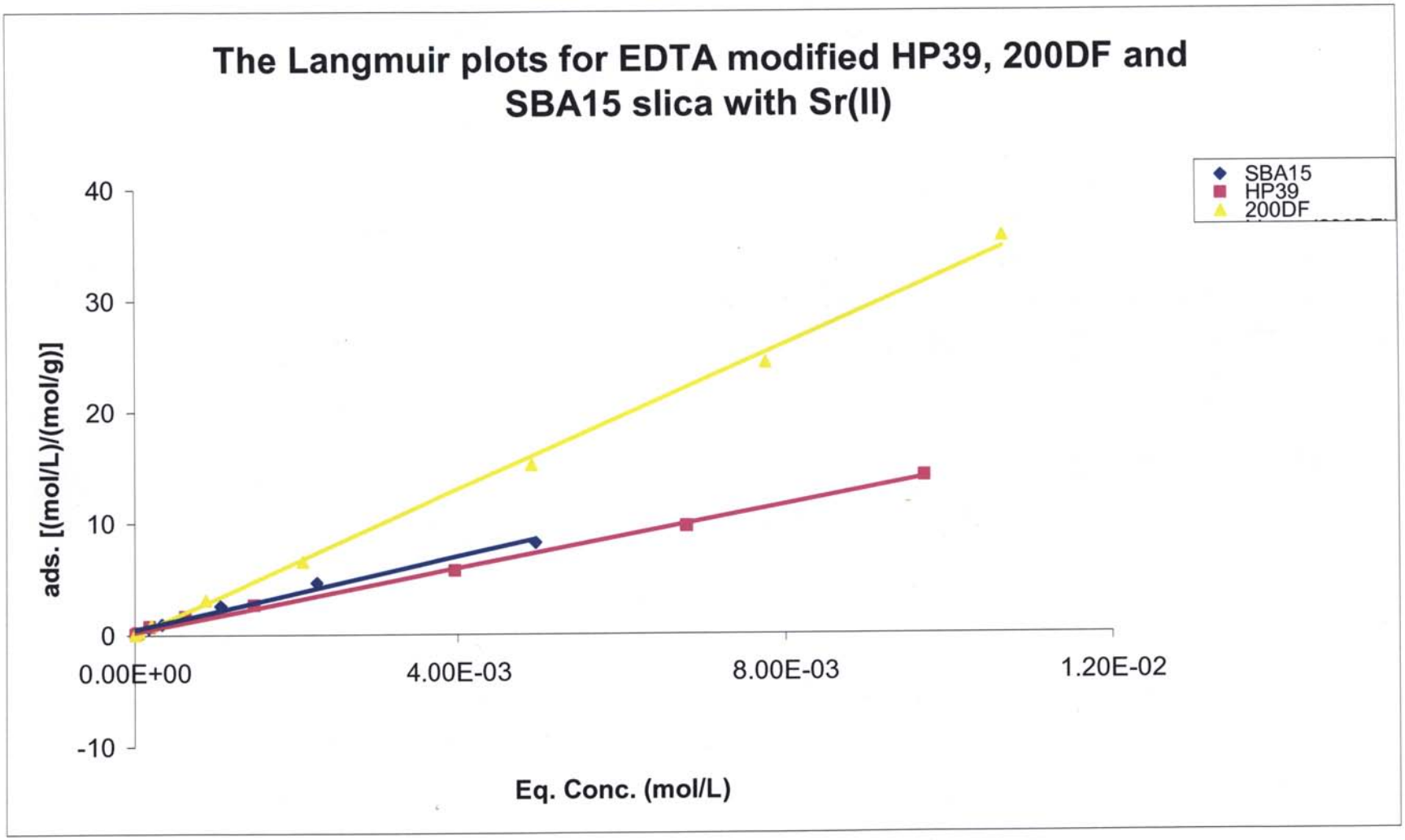

Figure 3.16 The langmuir plots for EDTA modified HP39, 200DF and SBA15 silica with Sr(II)

Silica Type	Modification group	Metal ion	R^2	Γ_{max} (mol/g)
HP39	EDTA	Sr(II)	0.9967	$7.050*10^{-4}$
200DF	EDTA	Sr(II)	0.9981	$3.073*10^{-4}$
SBA15	EDTA	Sr(II)	0.9842	$6.163*10^{-4}$

Table 3.8 Calculated Γ_{max} values and R^2 values for langmuir plots for EDTA modified HP39, 200DF and SBA15 silica with **Sr(II)**

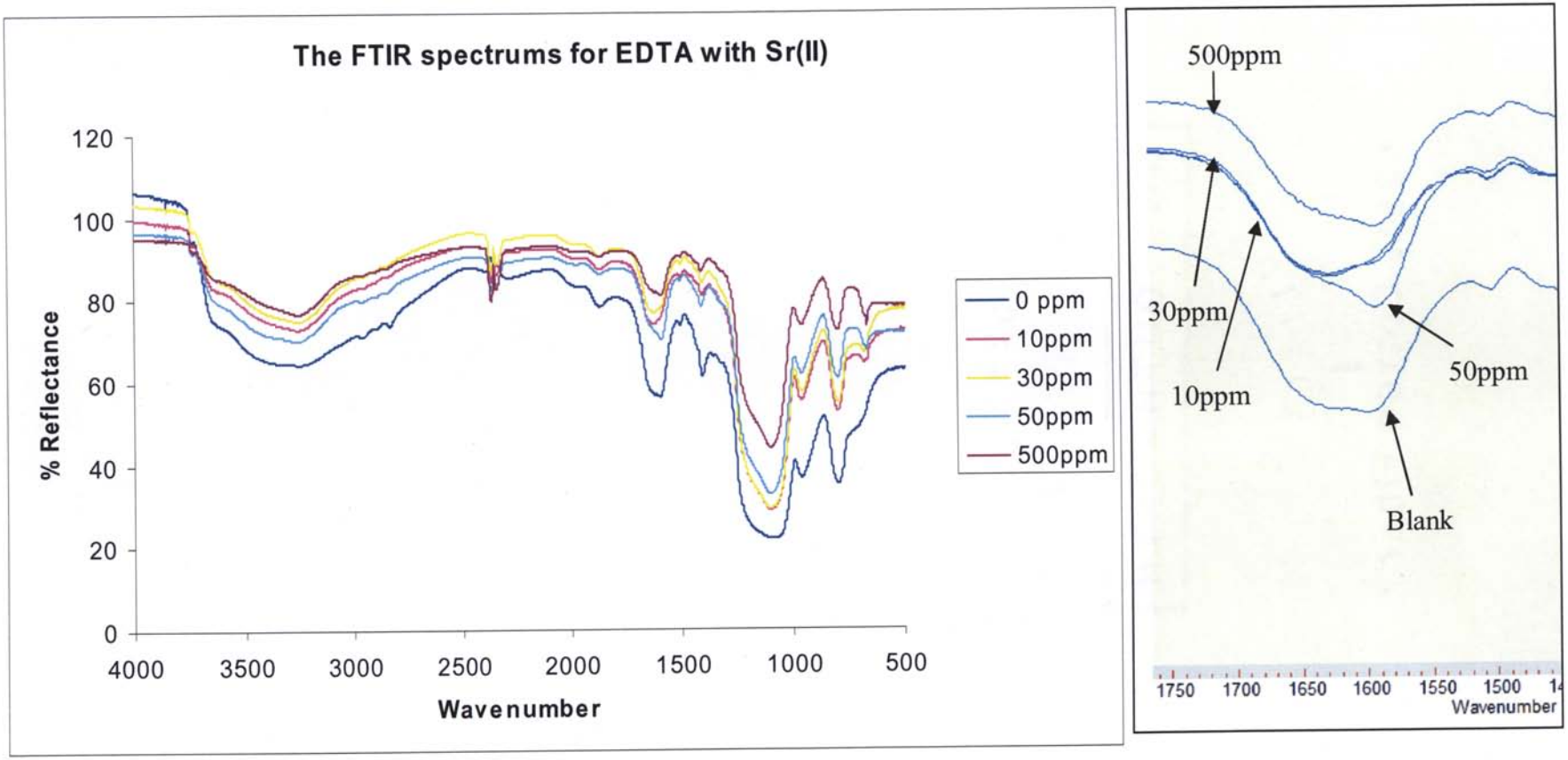

Figure 3.17 FTIR spectrums observed for the HP39 EDTA modified silica after adsorbing metal ion Sr(II) at different concentrations

(Polyakova, Poznyak, & Sergienko, 2009). Therefore Sr(II) EDTA modified silica complexes the same theory is possible as with Hg(II) and C=O frequencies of the these modified silica complexes move into lower region when increasing the metal ion concentration.

3.3.4 Adsorptive capacity of metal ions

Ethylenediaminetetraacetic acid (EDTA) forms strong complexes with most metal ions. Some of the formation constants for these metal ions with EDTA are given in Table 3.9. (Harris, 2007). Therefore we thought N-(triethoxysilylpropyl) ethylenediaminetriacetic acid silane modified silica will also show a good affinity for many metal ions. The only difference between these two molecules is the EDTA silane has three carboxylic group and EDTA molecule has four carboxylic groups at the reactive centers.

Therefore, we tried HP39 EDTA modified silica with five metal ions (Cu(II), Cd(II), Sr(II), Cr(III) and Hg(II)) for the adsorption experiments which is shown in the Figure 3.18. For most of the isotherms, adsorption behavior is complex when the metal ion concentrations are low. Further, for most of the metal ions, high molar adsorption percentages were observed at the range of concentrations we have studied. Therefore it is possible to use EDTA modified silica to adsorb different metal ions contaminated by the same water sample.

In addition, to check any structural changes that took place on the surface of the modified silica with increasing Cu(II) ion concentration, FTIR spectroscopy was done and the spectra are shown in the Figure 3.19. The vibrational frequencies, that is the C=O

Metal ion	Log K_f	Metal ion	Log K_f	Metal ion	Log K_f
Li^{+}	2.95	Mn^{2+}	13.89	VO_2^{+}	15.5
Na^{+}	1.86	Fe^{2+}	14.30	Ag^{+}	7.20
K^{+}	0.8	Co^{2+}	16.45	Tl^{+}	6.41
Be^{2+}	9.7	Ni^{2+}	18.4	Pd^{2+}	25.6[a]
Mg^{2+}	8.79	Cu^{2+}	18.78	Zn^{2+}	16.5
Ca^{2+}	10.65	Ti^{3+}	21.3	Cd^{2+}	16.5
Sr^{2+}	8.72	V^{3+}	25.9[a]	Hg^{2+}	21.5
Ba^{2+}	7.88	Cr^{3+}	23.4[a]	Sn^{2+}	18.3[b]
Ra^{2+}	7.4	Mn^{3+}	25.2	Pb^{2+}	18.0
Se^{3+}	23.1[a]	Fe^{3+}	25.1	Al^{3+}	16.4
Y^{3+}	18.08	Co^{3+}	41.4	Ga^{3+}	21.7
La^{3+}	15.36	Zr^{4+}	29.3	In^{3+}	24.9
V^{2+}	12.7[a]	Hf^{4+}	29.5	Tl^{3+}	35.3
Cr^{2+}	13.6[a]	VO^{2+}	18.7	Bi^{3+}	27.8[a]

a = 20 ^{O}C, ionic strength = 0.1 M b = 20 ^{O}C, ionic strength = 1.0 mol

Table 3.9 Stability constants of metal complexes with EDTA

(Source: A.E. Martell, R.M. Smith, and R.J. Motekitis, NIST critically selected stability constants of metal complexes, NIST standard reference database 46, Gaithersberg, MD 2001.)

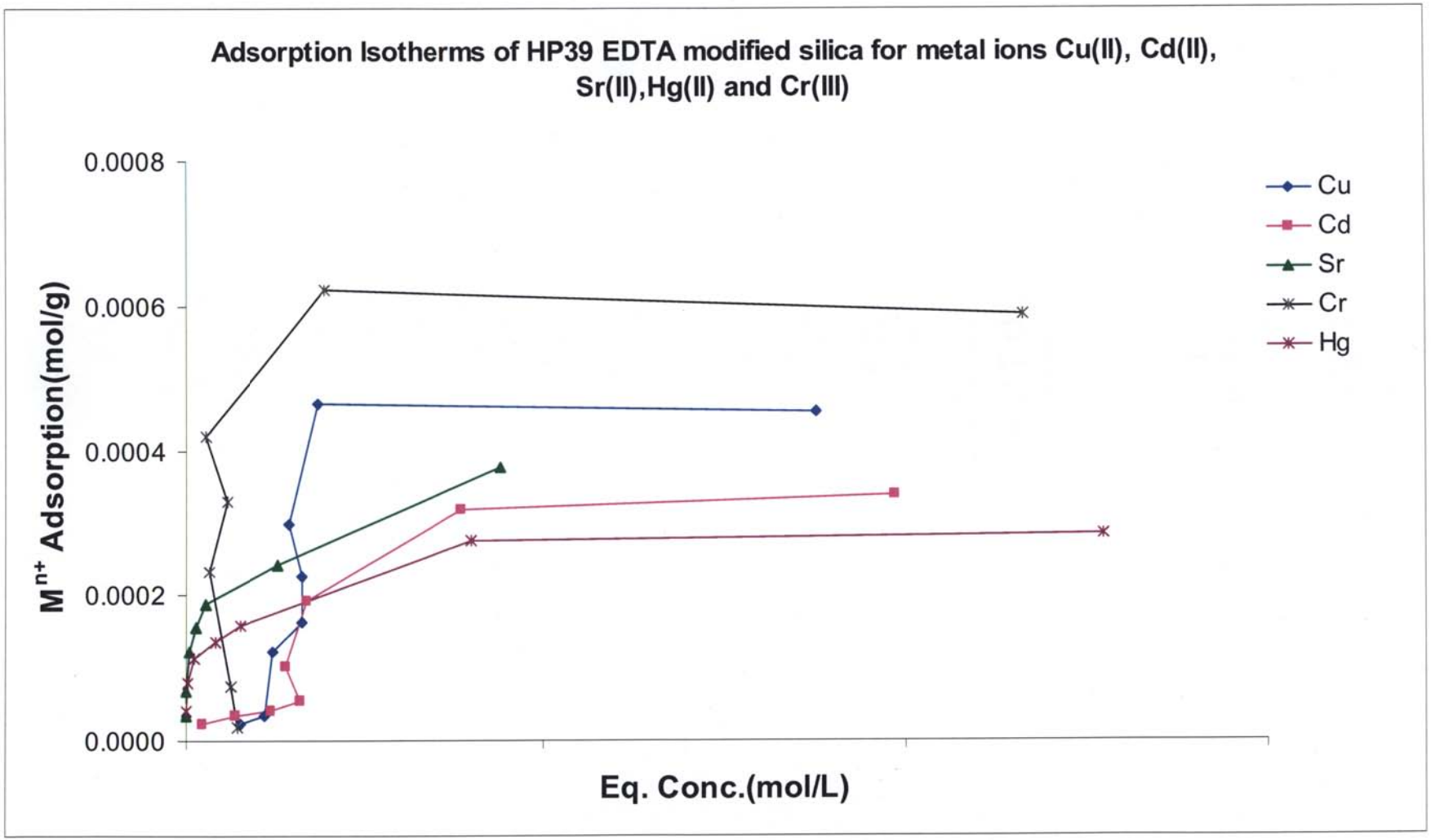

Figure 3.18 Adsorption Isotherms of HP39 EDTA modified silica for metal ions Cu(II), Cd(II), Sr(II), Hg(II) and Cr(III)

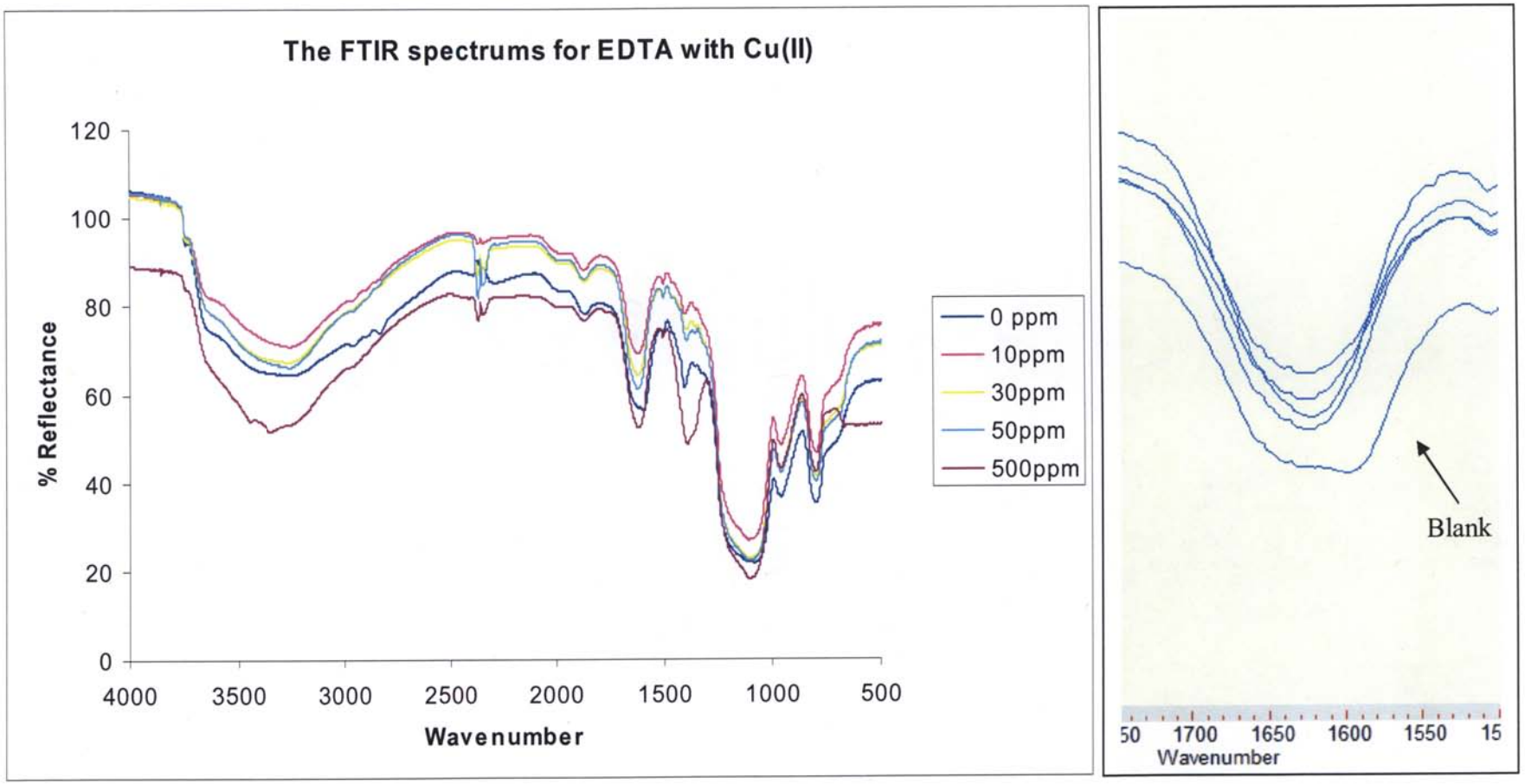

Figure 3.19 FTIR spectrums observed for the HP39 EDTA modified silica after adsorbing metal ion Cu(II) at different concentration.

frequencies of the Cu(II) EDTA modified silica complexes, show no shift as the metal ion concentration is increased. From this observation it is impossible to say that there is no structural change when metal ion concentration increased. But the frequency shift may be not in a detectable range.

3.3.5 pH dependence on adsorption studies at EDTA modified silica

In aqueous solutions, the presence of H^+ and OH^- species influences the degree of complexation in metal EDTA complexes. At low pH, H^+ species compete with the metal ions for the ligands and at high pH, OH^- species competes with the ligands, in the sense of coordination (McKetta, 1998). Therefore we suspect the same phenomenon can be possible for the EDTA modified silica. That is, the metal ion adsorption can depend on the pH of the solution.

So, pH dependency on the adsorption were studied using HP39 EDTA modified silica with metal ion Sr(II) and the observed adsorption isotherms were shown in Figure 3.20. According to the adsorption isotherms, metal ions with low concentrations showed a similar adsorption behavior at pH 5 and 9. At higher metal ion concentrations, the metal ion adsorption observed at pH 9 was slightly greater compared to the adsorption at pH 5, but not significantly. From these results we can concluded that, at pH 5 and 9 EDTA modified silica has almost same adsorption behavior and the adsorption is not dependent in the pH range studied.

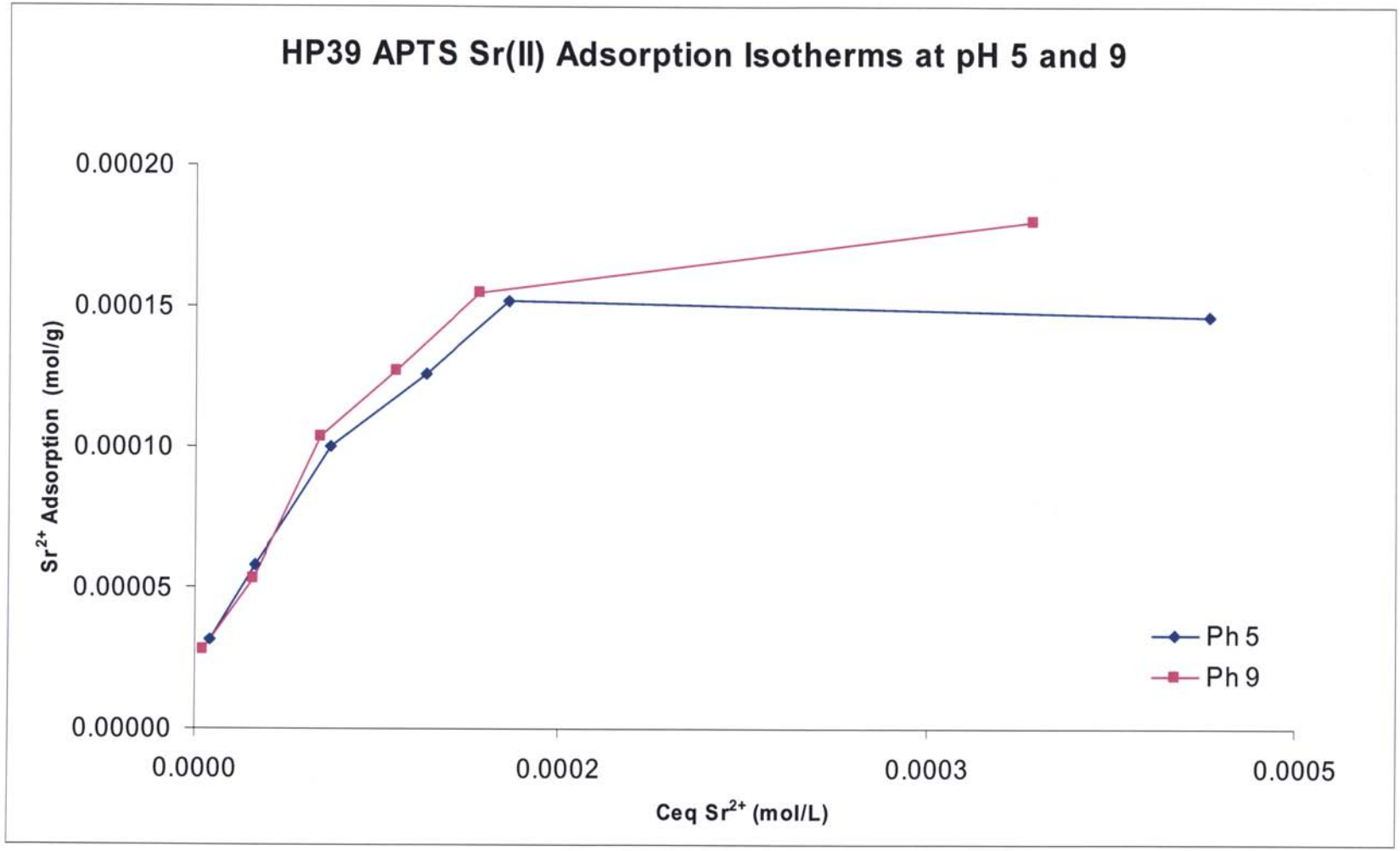

Figure 3.23 Adsorption Isotherms for HP39 APTS modified silica with metal ion Sr(II) at pH 5 and 9

3.3.6 Amino modified silica

Surface modification through various functional groups on silica and metal ion adsorption studies on those surfaces were highly studied during the past few decades. Our research group also has done many experiments under this category and amino modified silicas are one capable silica type as a metal ion remover (Ian P. Blitz, et al., 2007; I.P. Blitz, et al., 2006). Therefore we have done further studies on this modified silica type by using two metal ions, Cu(II) and Cd(II). For these experiments modified silica was prepared by using APTS, diamine and triamine organosilanes which has one, two and three amino groups respectively and structures shown in Table 3.10.

3.3.6.1 Cu(II) adsorption data and analysis

The adsorption isotherms observed for the metal ion Cu(II) with amino modified silica are shown in the Figure 3.21. According to the observed adsorption isotherms, at low concentrations diamine and triamine modified silica exhibit a complex adsorption behavior, while at high Cu(II) concentrations they showed a greater adsorption compared to the APTS. However, at low concentrations APTS modified silicas show superior adsorption behavior with Cu(II).

3.3.6.2 Cd(II) adsorption data and analysis

Cadmium poisoning can have a bad influence on health such as pregnancy, lactation, hormonal disorders, aging, calcium deficiency etc. Therefore removal of Cd metal ions from contaminated water is important to many animals as well as plants (Nogawa, et al., 2004). Previous studies indicated that a considerable adsorption capacity

Structure	Name/Acronym
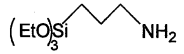	APTS 3-aminopropyltriethoxysilane
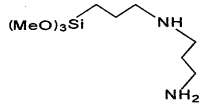	Diamino
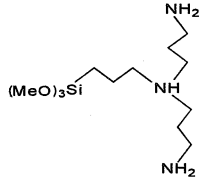	Triamino

Table 3.10 The structures of amino silanes used for modification

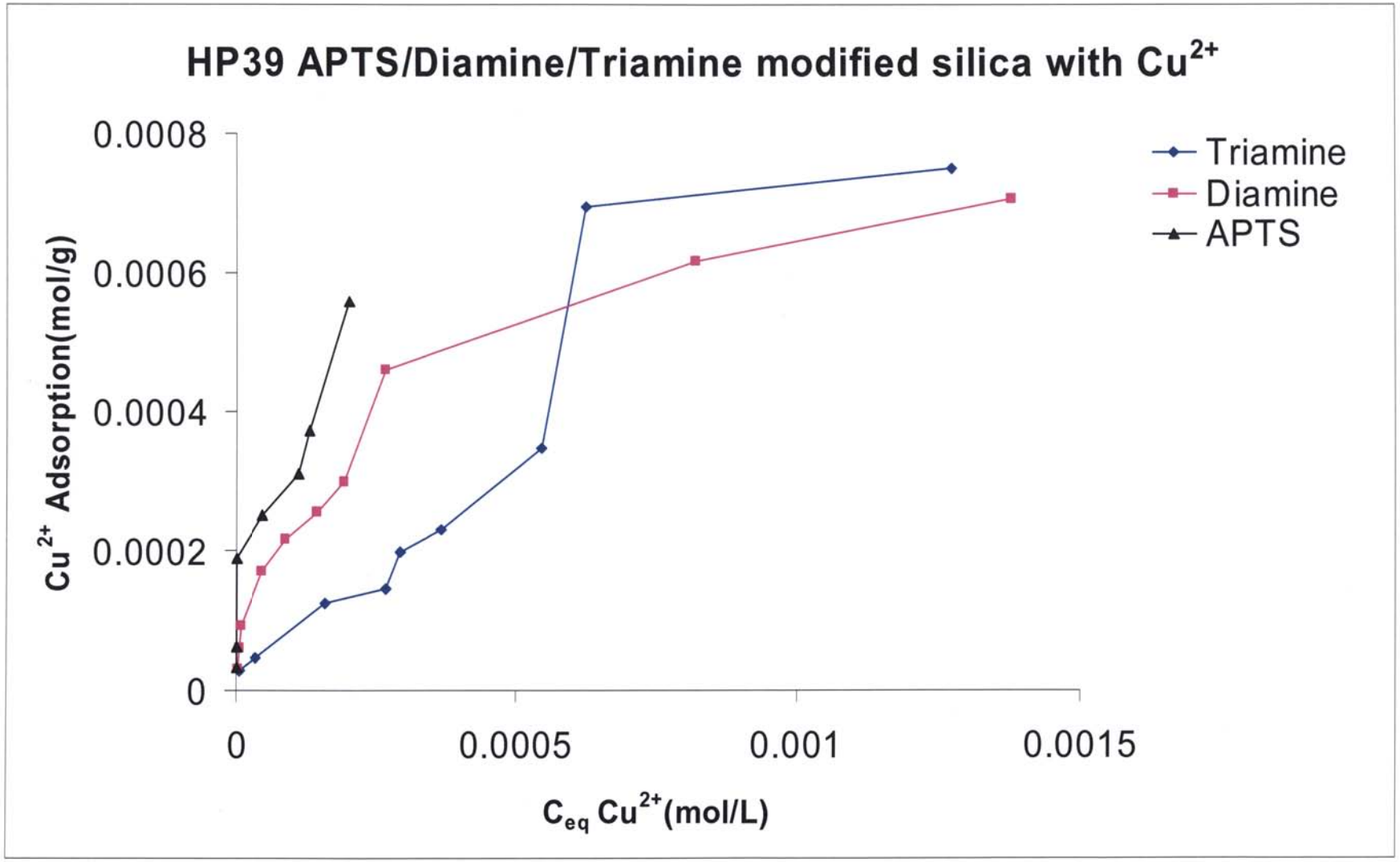

Figure 3.21 Adsorption Isotherm for HP39 amino modified APTS, diamine and triamine silica with metal ion Cu(II)

can be observed in Cu(II) with the amino modified silicas. Cd(II) metal ion has similar properties as Cu(II), because they are diagonal metals in the periodical table and both metals usually have the same oxidation number(+2). Therefore for Cd(II), we expected a similar adsorption capacity as in Cu(II), with the amino modified silicas.

The adsorption Isotherms observed for the HP39 amino modified silicas with metal ion Cd(II) is shown in the Figure 3.22. According to the adsorption isotherms observed, APTS, diamine and triamine have a similar adsorption behavior at low Cd(II) concentration. But diamine has comparatively higher metal ion adsorption than the APTS and triamine at high metal ion concentrations.

3.3.6.3 pH dependence on adsorption studies at amino modified silica

The solution pH dependency on the adsorption were studied of amino silicas by using HP39 APTS modified silica with metal ion Sr(II).The observed adsorption isotherms shown in figure 3.23. According to the adsorption isotherms, at lower concentrations at pH 5 and 9 APTS modified silicas has almost the same adsorption behavior. But at higher concentrations pH 9 solutions have higher adsorption. Therefore adsorption capacities of amino modified silica were almost independent of the pH range studied.

3.3.7 DPPS silica

DPPS modified silica was prepared by solid phase reduction of 3-(2,4-dinitrophenylamino)propyltriethoxysilane modified silica. Previously used amino modified silicas, which are APTS, diamine and triamine contains long carbon chains before the ligand group, which is the amine group. Therefore this type of carbon chain

will help to coordinate the metal ion with the ligand, by the proper orientation of the ligand. The main idea of preparing DPPS silica is that it contains immobile ligand groups, therefore NH_2 groups can't move freely, and it is fixed into a aromatic ring system structure as shown in the Figure 3.25. Therefore by using DPPS silica we can study how the mobility of the ligand groups will help for the metal ion adsorption.

The obtained adsorption isotherm for DPPS modified silica with metal ion Cu(II) is shown in Figure 3.24 with a comparison to the adsorption isotherms belonging to the APTS, Diamine and Triamine with metal ion Cu(II). According to the observed adsorption isotherms, it is clear that the DPPS modified silica has a low Cu(II) adsorption capacity compared to the other three amino modified silicas. From these results we can conclude that the mobility of the ligand groups can improve the increasing ability of adsorption capacity.

In addition, these types of compounds have another structural difference. That is, the electron donor ability of the ligand group to the metal is low compared to the normal chain ligands. The reason is, the electrons belong to the amine group are attracted toward the benzene ring. Therefore the electron donor ability of the ligand to metal gets comparatively weak and that can result in lower metal ion adsorption capacity. It is interesting to note that the strength of adsorption, seen as the slope of the isotherm at low concentrations, is still very high.

As mentioned before, DPPS modified silica was prepared by using solid phase reduction of 3-(2,4-dinitrophenylamino)propyltriethoxysilane modified silica, the structure is given under the Figure 3.26. By a comparison of the two adsorption isotherms of the two silica types, one can compare the adsorption behavior of a nitro group

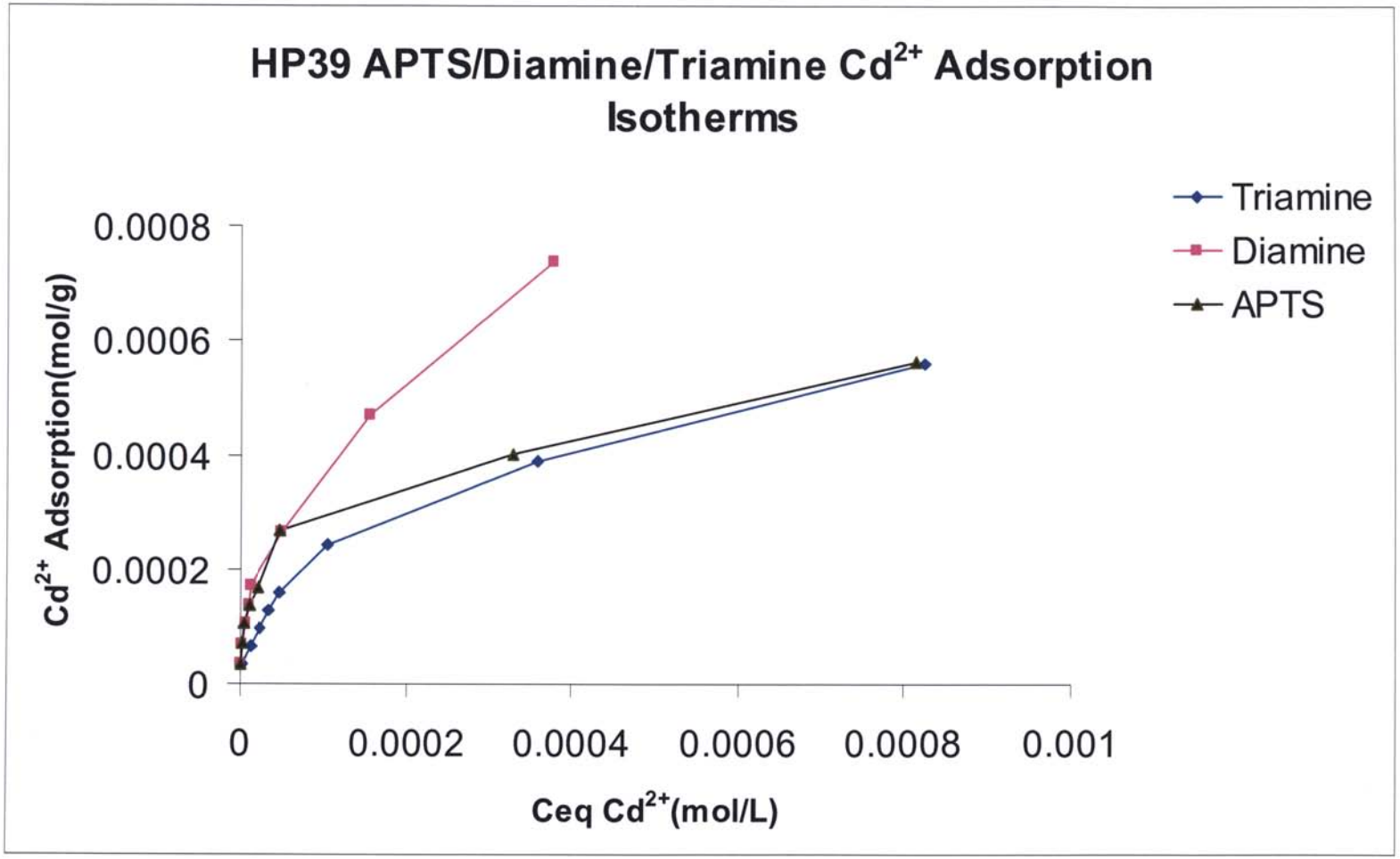

Figure 3.22 Adsorption Isotherm for HP39 amino modified APTS, diamine and triamine silica with metal ion Cd(II)

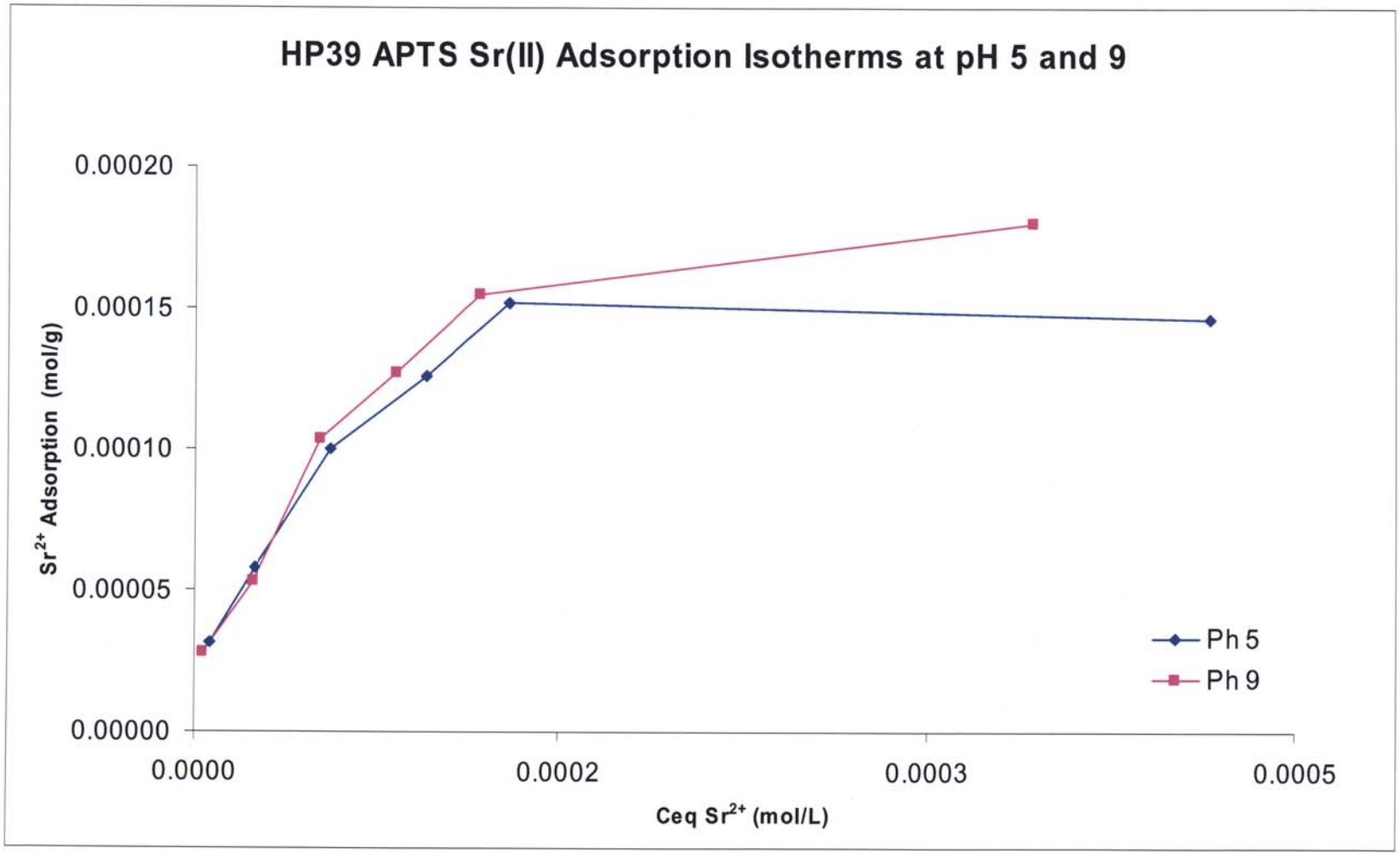

Figure 3.23 Adsorption Isotherms for HP39 APTS modified silica with metal ion Sr(II) at pH 5 and 9

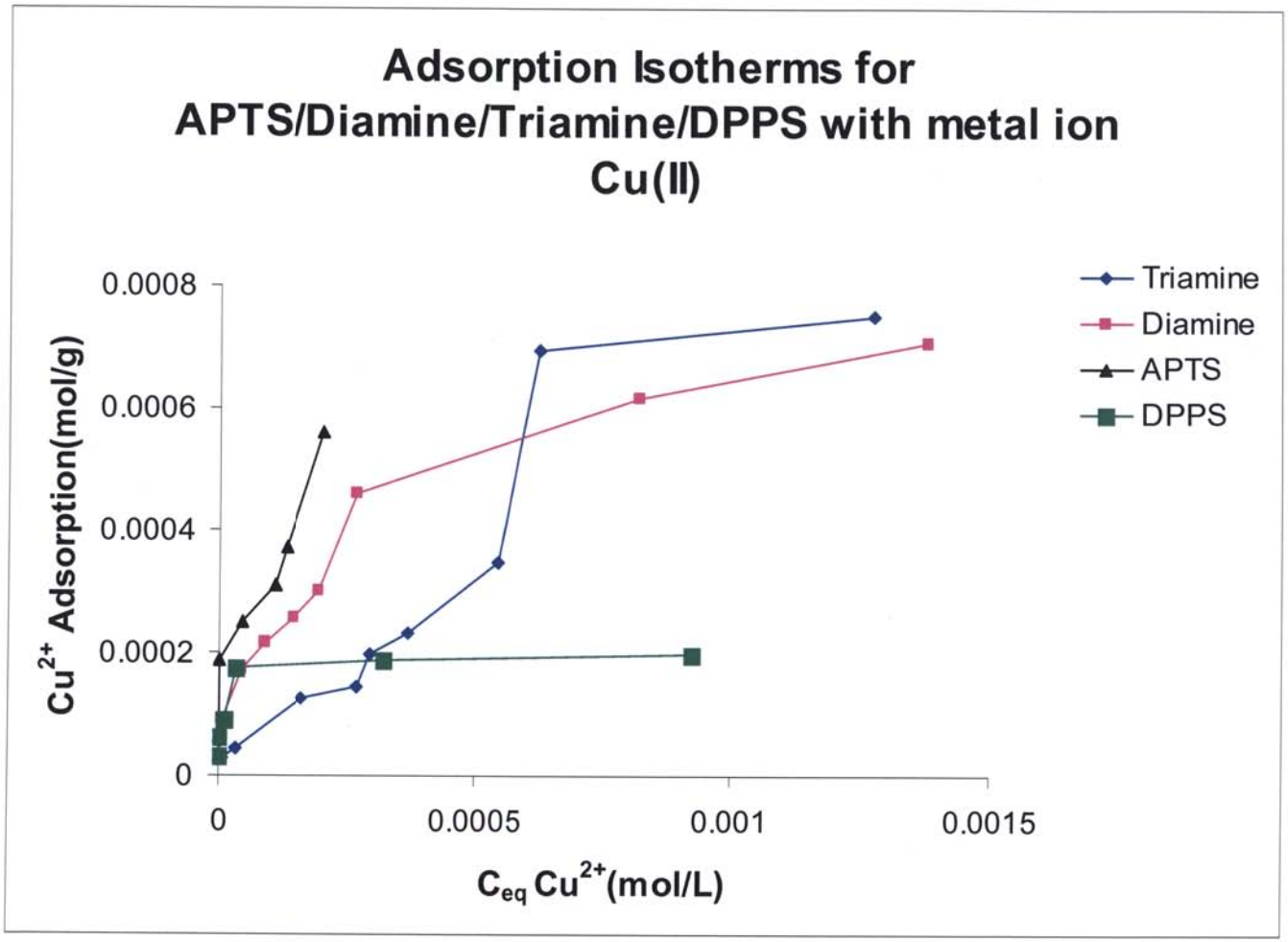

Figure 3.24 Adsorption Isotherm for DPPS silica in compared to APTS, Diamine and Triamine silica with metal ion Cu(II)

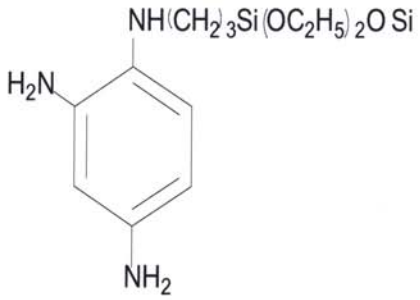

Figure 3.25 Structure of DPPS silica

compared to an amino group. The adsorption isotherms for 3-(2,4-dinitrophenylamino)propyltriethoxysilane modified silica and the DPPS silica with the metal ion Cu(II) are shown in the Figure 3.26. It was very clear from the adsorption isotherms that the amino modified silica has a higher adsorption capacity compared to the nitro modified silica. It appears as though the nitro modified silica is not at all successful in adsorbing Cu(II).

3.3.8 Phosphino modified silica

The phosphino modified silica was prepared by reacting HP39 silica with 2-(diphenylphosphino)ethyltriethoxysilane, in which the structure is shown in the Figure 3.29. This modified silica was prepared to compare the coordination ability of the phospeno ligand with other ligands that were used in these studies. The observed adsorption isotherm for phosphino modified silica with Cu(II) is shown in the Figure 3.28. By comparing the adsorption isotherms for the amino modified silica especially with APTS given at Figure 3.21, it is very clear that the phosphino modified silica has a low adsorption capacity.

3.4 Conclusion

Surface modification with EDTA organosilane provides materials which have high affinity and a large adsorption capacity for the adsorption of metal ions specially for the Hg(II) from aqueous solutions. In addition, EDTA modified silica has an ability to adsorb many metal ions and adsorption capacity is not depend on the pH range which used for this study. The FTIR frequency shift of EDTA metal complexes when increasing

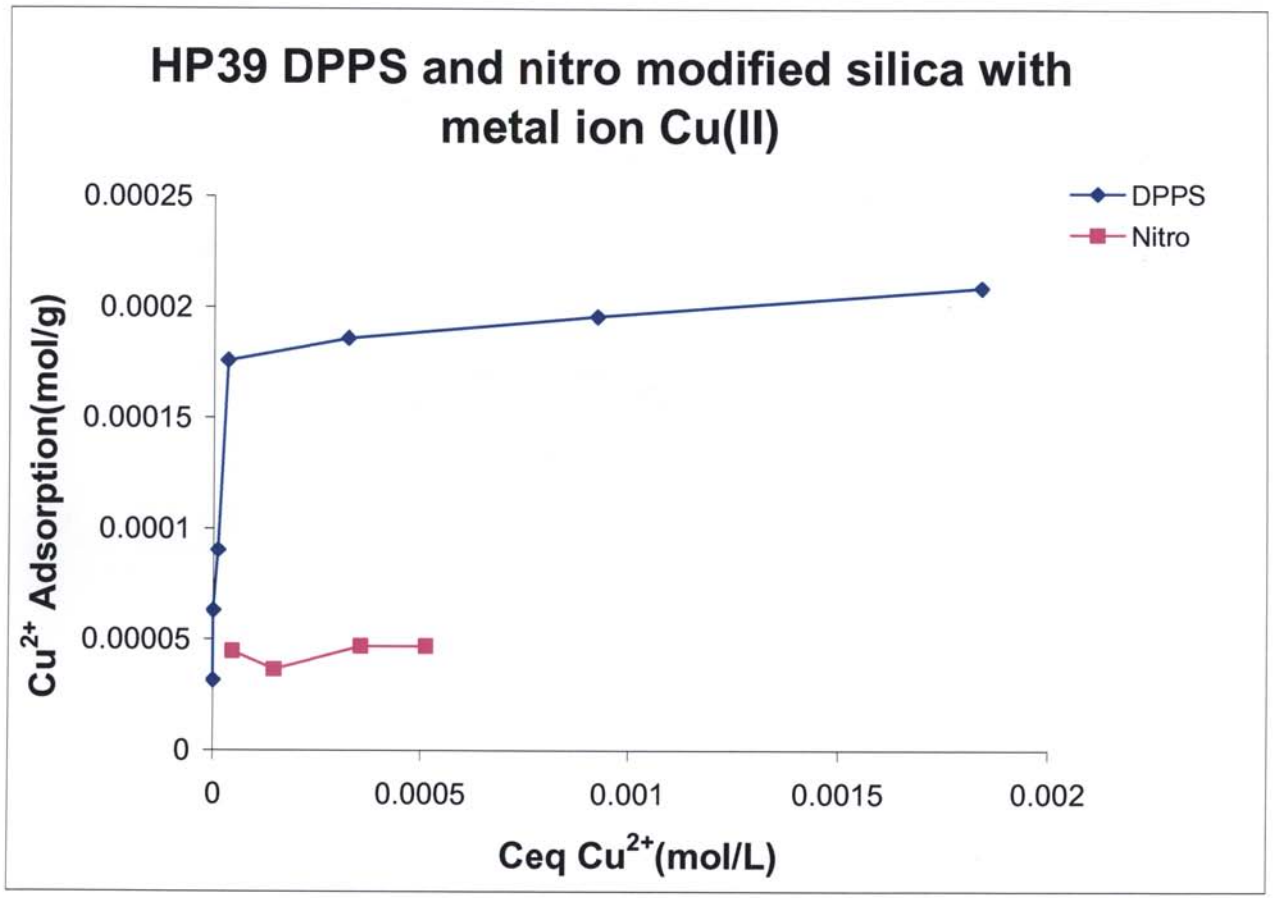

Figure 3.26 Adsorption Isotherm for DPPS silica in compared to 3-(2,4-dinitrophenylamino) nitro propyltriethoxysilane modified silica.

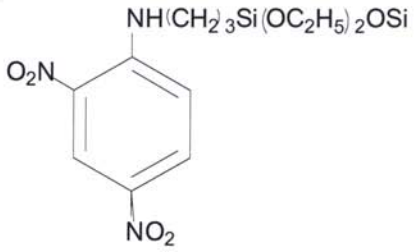

Figure 3.27 Structure of modified silica

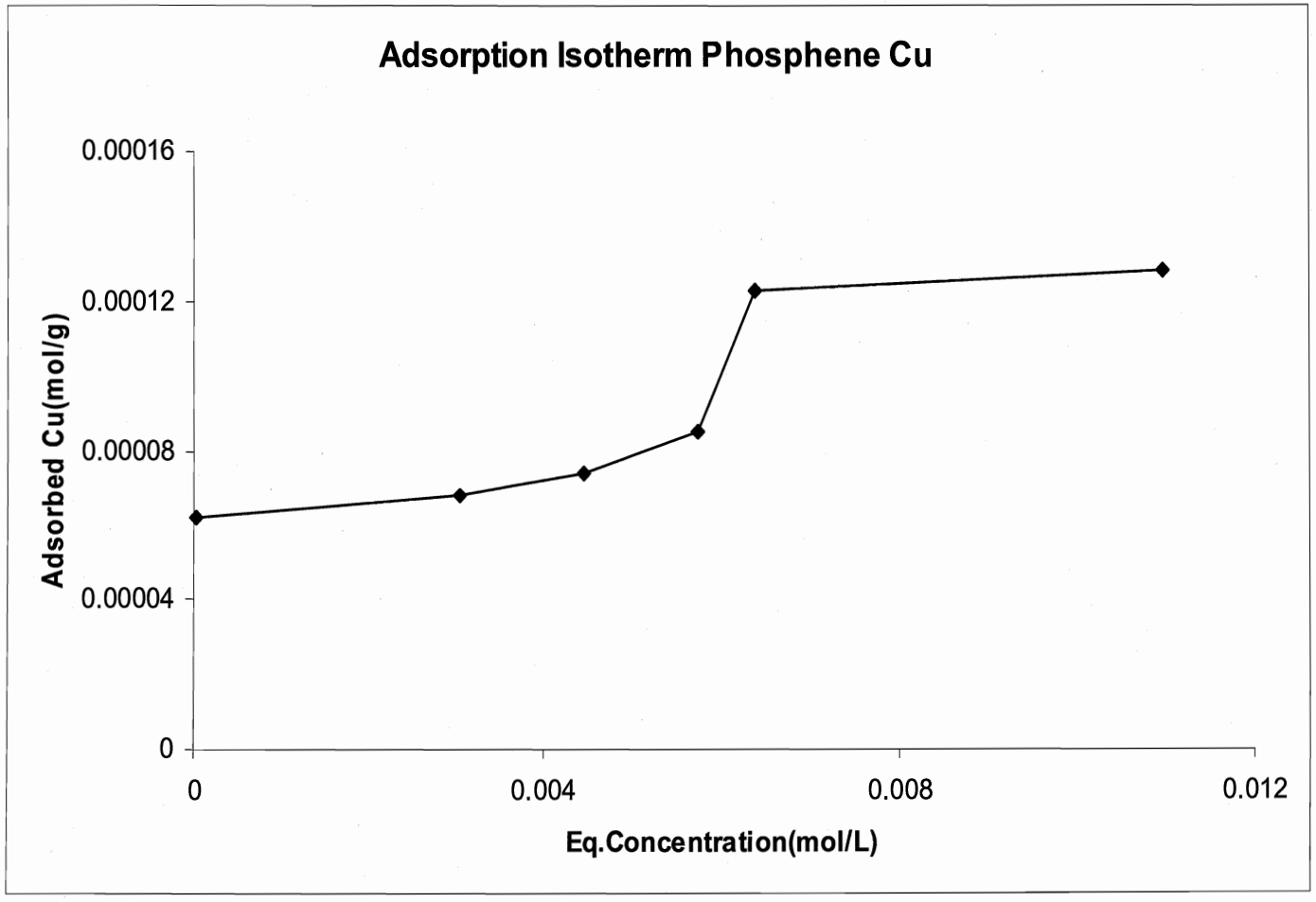

Figure 3.28 Adsorption Isotherm for 2-(diphenylphosphino)ethyltriethoxysilane modified silica with metal ion Cu(II) .

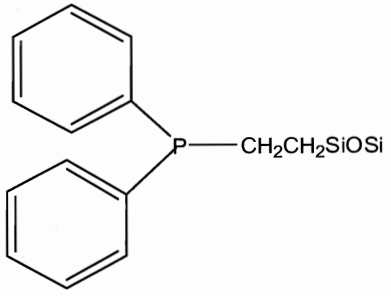

Figure 3.29 Structure of phospeno modified silica

metal ion concentration probed the metal ion - surface bonding interactions. The nature of the metal ligand interactions according to the ionic radius and the coordination number of the metal ion can be rationalized using simple computational calculations.

Amino modified silicas showed lower adsorption capacities compared to the EDTA modified silica. Immobility of the amino groups in DPPS silica further reduced the adsorption capacity. But the amino ligand has high affinity towards the Cu(II) compared to the nitro ligands. Similar to EDTA modified silica, the adsorption capacities of amino modified silica were independent of the pH range studied. Phosphino modified silica showed the least adsorption capacity.

3.5 Supplementary

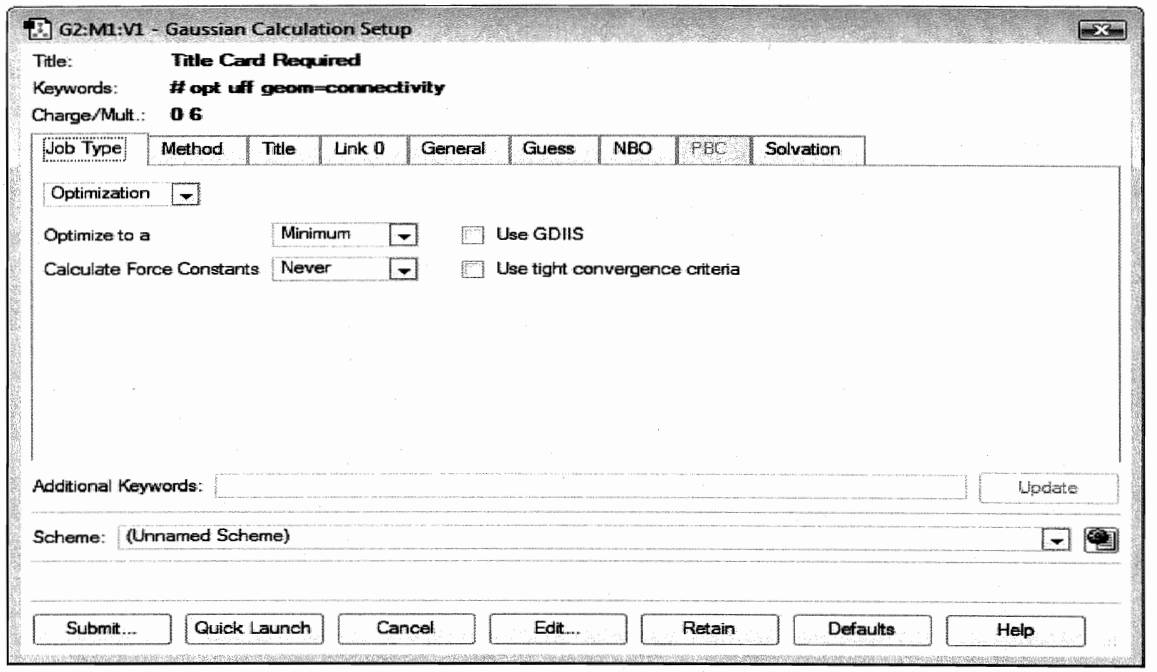

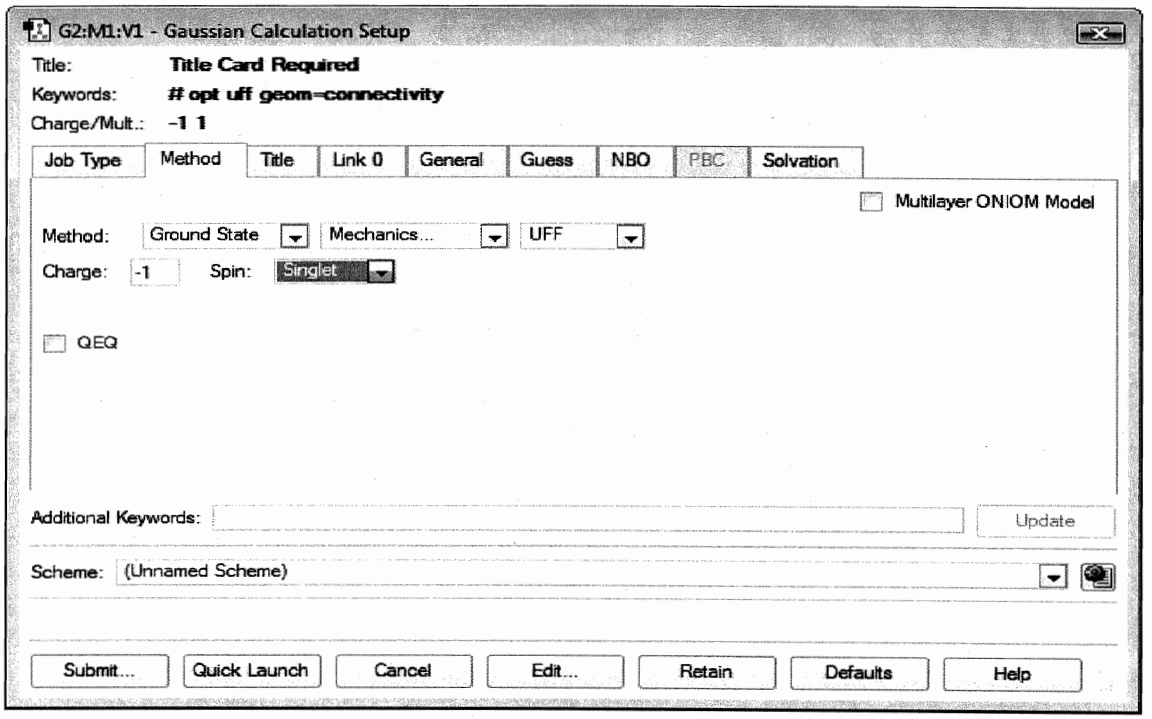

Diagram 3.30: Parameter setup for the geometry optimization in Hg(II) EDTA modified silica complexes

Initial Conc. (ppm)	Hg Adsorbed (mol/g)	Equ.Conc. (mol/L)
20.00	0.0000399	0.0000000
40.00	0.0000708	0.0000224
60.00	0.0001050	0.0000365
80.00	0.0001275	0.0000801
100.00	0.0001478	0.0001290
177.90	0.0002205	0.0003355
355.00	0.0002537	0.0011356
665.00	0.0003467	0.0024484
900.00	0.0004180	0.0034419
2600.90	0.0023667	0.0070496
4478.08	0.0036132	0.0132917

Table 3.11 Adsorption data of HP39 EDTA with Hg(II)

Initial Conc. (ppm)	Hg Adsorbed (mol/g)	Equ.Conc. (mol/L)
20.00	0.0000325	0.0000185
40.00	0.0000626	0.0000430
60.00	0.0000705	0.0001228
80.00	0.0000976	0.0001548
100.00	0.0001194	0.0002001
177.90	0.0001391	0.0005391
355.00	0.0001839	0.0013099
665.00	0.0002213	0.0027619
900.00	0.0002671	0.0038190
2938.90	0.0029843	0.0071906
4478.08	0.0029909	0.0148473

Table 3.12 Adsorption data of 200DF EDTA with Hg(II)

Initial Conc. (ppm)	Hg Adsorbed (mol/g)	Equ.Conc. (mol/L)
20.00	0.0000399	0.0000000
60.00	0.0000975	0.0000554
86.60	0.0001247	0.0001200
177.90	0.0001195	0.0005881
355.00	0.0000935	0.0015359
665.00	0.0006295	0.0017416
900.00	0.0009800	0.0020367
2600.90	0.0023839	0.0070065

Table 3.13 Adsorption data of SBA15 EDTA with Hg(II)

Initial Conc. (ppm)	Cr Adsorbed (mol/g)	Equ.Conc. (mol/L)
7.31	0.00000440	0.000130
14.30	0.00006228	0.000119
32.61	0.00020810	0.000107
46.83	0.00032027	0.000100
56.42	0.00040895	0.000063
94.82	0.00048844	0.000603
160.98	0.00053513	0.001758
255.16	0.00075452	0.003021
491.42	0.00141146	0.005922
654.51	0.00140321	0.009080

Table 3.14 Adsorption data of HP39 EDTA with Cr(III)

Initial Conc. (ppm)	Cr Adsorbed (mol/g)	Equ.Conc. (mol/L)
7.31	0.0000169	0.0000983
32.61	0.0002466	0.0000107
56.42	0.0003864	0.0001190
94.82	0.0004156	0.0007846
160.98	0.0005738	0.0016614
255.16	0.0005175	0.0036134
491.42	0.0009286	0.0071296
654.51	0.0012561	0.0094473

Table 3.15 Adsorption data of 200DF EDTA with Cr(III)

Initial Conc. (ppm)	Cr Adsorbed (mol/g)	Equ.Conc. (mol/L)
7.31	0.000112	0.000000
32.61	0.000278	0.000279
56.42	0.000495	0.000467
94.82	0.000849	0.000762
160.98	0.000694	0.002228
255.16	0.000779	0.003934
491.42	0.001107	0.008068
654.51	0.001218	0.011065

Table 3.16 Adsorption data of SBA15 EDTA with Cr(III)

Initial Conc. (ppm)	Sr Adsorbed (mol/g)	Equ.Conc. (mol/L)
7.41	0.00003	0.000000
14.82	0.00007	0.000000
26.85	0.00012	0.000005
35.89	0.00016	0.000018
44.58	0.00019	0.000039
68.46	0.00024	0.000178
136.22	0.00038	0.000617
250.00	0.00056	0.001462
500.00	0.00070	0.003964
750.00	0.00071	0.006794
1000.00	0.00069	0.009698

Table 3.17 Adsorption data of HP39 EDTA with Sr(II)

Initial Conc. (ppm)	Sr Adsorbed (mol/g)	Equ.Conc. (mol/L)
7.41	0.0000338	0.0000000
26.85	0.0001203	0.0000056
44.58	0.0001814	0.0000554
68.46	0.0002316	0.0002022
136.22	0.0002775	0.0008610
250.00	0.0003164	0.0020623
500.00	0.0003230	0.0048989
750.00	0.0003190	0.0077621
1000.00	0.0002990	0.0106654

Table 3.18 Adsorption data of 200DF EDTA with Sr(II)

Initial Conc. (ppm)	Sr Adsorbed (mol/g)	Equ.Conc. (mol/L)
7.41	0.0000672	0.00000053
44.58	0.0002719	0.00016886
68.46	0.0003592	0.00033238
136.22	0.0004082	0.00104452
250.00	0.0004859	0.00224588
500.00	0.0006060	0.00494894

Table 3.19 Adsorption data of SBA15 EDTA with Sr(II)

Initial Conc. (ppm)	Cd Adsorbed (mol/g)	Equ.Conc. (mol/L)
10.00	0.0000275	0.0000201
20.00	0.0000479	0.0000581
30.00	0.0000442	0.0001563
40.00	0.0000583	0.0002101
50.00	0.0000743	0.0002590
80.00	0.0002168	0.0001698
150.00	0.0003237	0.0005250
250.00	0.0003191	0.0014262
400.00	0.0004554	0.0024199

Table 3.20 Adsorption data of HP39 EDTA with Cd(II)

Initial Conc. (ppm)	Cu Adsorbed (mol/g)	Equ.Conc. (mol/L)
10.00	0.0000215	0.000104
15.00	0.0000335	0.000152
30.00	0.0001210	0.000170
40.00	0.0001614	0.000226
50.00	0.0002243	0.000226
60.00	0.0002980	0.000199
90.00	0.0004640	0.000256
150.00	0.0004540	0.001226
250.00	0.0007853	0.001971

Table 3.21 Adsorption data of HP39 EDTA with Cu(II)

Initial con.(ppm)	Cu(II) adsorbed(mol/g)	Equi. con.(mol/L)
5.00	0.0000315	0.0000000
10.00	0.0000630	0.0000000
30.00	0.0001888	0.0000000
40.00	0.0002500	0.0000463
50.00	0.0003103	0.0001103
60.00	0.0003724	0.0001316
90.00	0.0005584	0.0002035
150.00	0.0006005	0.0085928
200.00	0.0006533	0.0151399

Table 3.22 Adsorption data of HP39 APTS with Cu(II)

Initial con.(ppm)	Cu adsorbed(mol/g)	Equi. con.(mol/L)
5.00	0.0000302	0.00000329
10.00	0.0000607	0.00000554
15.00	0.0000911	0.00000834
30.00	0.0001709	0.00004488
40.00	0.0002163	0.00008872
50.00	0.0002563	0.00014604
60.00	0.0002996	0.00019521
90.00	0.0004589	0.00026903
150.00	0.0006153	0.0008223
200.00	0.0007066	0.00138084

Table 3.23 Adsorption data of HP39 Diamine Cu(II)

Initial con.(ppm)	Cu absorbed(mol/g)	Equi. con.(mol/L)
5.00	0.00000686	0.0000287
10.00	0.00003489	0.0000449
30.00	0.00015910	0.0001252
40.00	0.00026853	0.0001444
50.00	0.00029426	0.0001970
60.00	0.00036902	0.0002301
90.00	0.00054713	0.0003477
150.00	0.00062767	0.0006931
200.00	0.00127512	0.0007489

Table 3.24 Adsorption data of HP39 Triamine Cu(II)

Initial con.(ppm)	Cu absorbed(mol/g)	Equi. con.(mol/L)
10.00	0.00003558	0
20.00	0.00007047	0.000001744
30.00	0.00010483	0.000004804
40.00	0.00013803	0.000010764
50.00	0.00016858	0.000020336
80.00	0.00026628	0.000045983
150.00	0.00040192	0.000329594
200.00	0.00056406	0.000813862

Table 3.25 Adsorption data of HP39 APTS Cd(II)

Initial con.(ppm)	Cu absorbed(mol/g)	Equi. con.(mol/L)
10.00	0.0000355	0.000000213
20.00	0.00006997	0.000003007
30.00	0.00010441	0.000005853
40.00	0.00013766	0.00001168
50.00	0.00017274	0.000012952
80.00	0.00026494	0.000049319
150.00	0.00047096	0.000156997
250.00	0.00073819	0.000378525

Table 3.26 Adsorption data of HP39 Diamine Cd(II)

Initial con.(ppm)	Cd absorbed(mol/g)	Equi. con.(mol/L)
10.00	0.000000344	0.0000288
20.00	0.000000641	0.0001180
30.00	0.000000975	0.0002322
40.00	0.000001290	0.0003327
50.00	0.000001592	0.0004671
80.00	0.000002426	0.0010531
150.00	0.000003901	0.0035906
250.00	0.000005593	0.0082580

Table 3.27 Adsorption data of HP39 Triamine with Cd(II)

Metal ion	Calculated formation constant(log K_f)
Hg(II)	3.51
Sr(II)	3.79

Table 3.28 Calculated formation constants by Langmuir plots for HP39 EDTA (Log K_f for Hg(II) ethylenediaminetetraacetic is 21.5 and Sr(II) ethylenediaminetetraacetic is 8.72)

Silica type	No. of moles at high Hg(II) concentration	No. of moles at low Hg(II) concentration
HP39	22.99	2.66
SBA15	5.20	0.260

Table 3.29 Number of moles of Hg(II) adsorbed into each silica compared to the molar surface coverage calculated for the EDTA modified silica by nitrogen adsorption data.

3.6 Reference

1. Adams, W. J., Chapman, G. A., & Landis, W. G. (1988). *Aquatic toxicology and hazard assesment* (Vol. 10). Ann Arbor, MI.

2. Al-Oweini, R., & El-Rassy, H. (2009). Synthesis and characterization by FTIR spectroscopy of silica aerogels prepared using several Si(OR)4 and R"Si(OR')3 precursors. [doi: DOI: 10.1016/j.molstruc.2008.08.025]. *Journal of Molecular Structure, 919*(1-3), 140-145.

3. Alimarin, I. P., Fadeeva, V. I., Kudryavtsev, G. V., Loskutova, I. M., & Tikhomirova, T. I. (1987). Concentration, separation and determination of scandium, zirconium, hafnium and thorium with a silica-based sulphonic acid cation-exchanger. [doi: DOI: 10.1016/0039-9140(87)80013-9]. *Talanta, 34*(1), 103-110.

4. Arakaki, L. N. H., Nunes, L. M., Simoni, J. A., & Airoldi, C. (2000). Ethyleneimine Anchored on Thiol-Modified Silica Gel Surface--Adsorption of Divalent Cations and Calorimetric Data. [doi: DOI: 10.1006/jcis.2000.6842]. *Journal of Colloid and Interface Science, 228*(1), 46-51.

5. Asagba, S., & Obi, F. (2005). A comparative evaluation of the biological effects of environmental cadmium-contaminated control diet and laboratory-cadmium supplemented test diet. *BioMetals, 18*(2), 155-161.

6. Basu, B., Das, P., & Das, S. (2005). Transfer hydrogenation using recyclable polymer-supported formate (PSF): Efficient and chemoselective reduction of nitroarenes. [10.1007/s11030-005-8106-1]. *Molecular Diversity, 9*(4), 259-262.

7. Blitz, I. P., Blitz, J. P., Gun'ko, V. M., & Sheeran, D. J. (2007). Functionalized silicas: Structural characteristics and adsorption of Cu(II) and Pb(II). *Colloids and Surfaces A: Physicochemical and Engineering Aspects, 307*(1-3), 83-92.

8. Blitz, I. P., Blitz, J. P., V.M., G., & Sheeran, D. J. (2006). Functionalized surfaces: silica structure and metal ion adsorption behavior *surface chemistry in biomedical and environmental science* (pp. 337-348): Springer Netherland.

9. Bogus, lstrok, Buszewski, a., Jezierska, M., Miros, We, a., et al. (1998). Survey and Trends in the Preparation of Chemically Bonded Silica Phases for Liquid Chromatographic Analysis. *Journal of High Resolution Chromatography, 21*(5), 267-281.

10. Budiman, H., Fransiska, S. H. K., & Setiawan, A. H. (2009). Preparation of Silica Modified with 2-Mercaptoimidazole and its Sorption Properties of Chromium(III). *E-Journal of Chemistry, 6*(1), 141-150.

11. Bulut, Y., & Tez, Z. (2007). Removal of heavy metals from aqueous solution by sawdust adsorption. *Journal of Environmental Sciences, 19*(2), 160-166.

12. Casewit, C. J., Colwell, K. S., & Rappe, A. K. (1992). Application of a universal force field to organic molecules. [doi: 10.1021/ja00051a041]. *Journal of the American Chemical Society, 114*(25), 10035-10046.

13. Cestari, A. R., & Airoldi, C. (1997). Chemisorption on Thiol-Silicas: Divalent Cations as a Function of pH and Primary Amines on Thiol-Mercury Adsorbed. *Journal of Colloid and Interface Science, 195*(2), 338-342.

14. Davis, S. S. (1997). Biomédical applications of nanotechnology -- implications for drug targeting and gene therapy. [doi: DOI: 10.1016/S0167-7799(97)01036-6]. *Trends in Biotechnology, 15*(6), 217-224.

15. Denkhaus, E., Beck, F., Bueschler, P., Gerhard, R., & Golloch, A. (2001). Electrolytic hydride generation atomic absorption spectrometry for the determination of antimony, arsenic, selenium, and tin – mechanistic aspects and figures of merit. [10.1007/s002160100718]. *Fresenius' Journal of Analytical Chemistry, 370*(6), 735-743.

16. Deorkar, N. V., & Tavlarides, L. L. (1997). Zinc, Cadmium, and Lead Separation from Aqueous Streams Using Solid-Phase Extractants. [doi: 10.1021/ie960415m]. *Industrial & Engineering Chemistry Research, 36*(2), 399-406.

17. Duffus, J. H. (2002). "Heavy metals" a meaningless term? (IUPAC Technical Report). *Pure Appl. Chem., 74*(5), 793-807.

18. Esposito, F., Del Nobile, M. A., Mensitieri, G., & Astarita, G. (1996). A Generalized Form of the Langmuir Isotherm for Gas Adsorption in Glassy Polymers. [doi: 10.1021/ie950722c]. *Industrial & Engineering Chemistry Research, 35*(9), 2939-2945.

19. Frackelton, J. P., & Christensen, R. L. (1998). Mercury Poisoning and Its Potential Impact on Hormone Regulation and Aging: Preliminary Clinical Observations Using a New Therapeutic Approach. *Journal of Advancement in Medicine, 11*(1), 9-25.

20. Fuhrmann, G. F. (1996). Handbook of experimental pharmacology, volume 115. Toxicology of metals. Biochemical aspects : G.V.R Born, P. Cuatrescasas, D. Ganten, H. Merken, K.L. Melmon, Robert A. Goyer and M. George Cherian (Eds.) Springer-Verlag, Berlin, New York, 1995. 467 pages, 37 figures and 17 tables. Price: hardcover, DM 598.00; ISBN 3-540-58281-9. *Toxicology, 108*(1-2), 153-154.

21. Goyer, R. A. (1997). Toxic and essential metal interactions. *Annual Review of Nutrition, 17*(1), 37-50.

22. Gregg S.J., S. K. S. W. (1982). *Adsorption, Surface Area and Porosity* (second ed.). London: Academic press.

23. Grube, M., Muter, O., Strikauska, S., Gavare, M., & Limane, B. (2008). Application of FT-IR spectroscopy for control of the medium composition during the biodegradation of nitro aromatic compounds. [10.1007/s10295-008-0456-0]. *Journal of Industrial Microbiology and Biotechnology, 35*(11), 1545-1549.

24. Harris, D. C. (2007). *Quantitative Chemical Analysis* (Seventh Edition ed.). New York: W.H. Freeman and Company.

25. Hinchliffe, A. (2003). *Molecular modelling for beginners*. Chichester: British libarary cataloguing in publication data.

26. Hodgson, S. N. B., Shen, X., & Sale, F. R. (2000). Preparation of alkaline earth carbonates and oxides by the EDTA-gel process. [10.1023/A:1004826324526]. *Journal of Materials Science, 35*(21), 5275-5282.

27. Iler, R. K. (1978). *The Chemistry of Silica*. New york: Wiley-Interscience

28. Jal, P. K., Patel, S., & Mishra, B. K. (2004). Chemical modification of silica surface by immobilization of functional groups for extractive concentration of metal ions. [doi: DOI: 10.1016/j.talanta.2003.10.028]. *Talanta, 62*(5), 1005-1028.

29. Kruk, M., Jaroniec, M., Ko, C. H., & Ryoo, R. (2000). Characterization of the Porous Structure of SBA-15. [doi: 10.1021/cm000164e]. *Chemistry of Materials, 12*(7), 1961-1968.

30. Kumar, A., Rao, N. N., & Kaul, S. N. (2000). Alkali-treated straw and insoluble straw xanthate as low cost adsorbents for heavy metal removal - preparation, characterization and application. *Bioresource Technology, 71*(2), 133-142.

31. Kusiak, R. A., Ritchie, A. C., Springer, J., & Muller, J. (1993). Mortality from stomach cancer in Ontario miners. *Br J Ind Med, 50*(2), 117-126.

32. Lanigan, K. C., & Pidsosny, K. (2007). Reflectance FTIR spectroscopic analysis of metal complexation to EDTA and EDDS. [doi: DOI: 10.1016/j.vibspec.2007.03.003]. *Vibrational Spectroscopy, 45*(1), 2-9.

33. Lavrich, D. J., Wetterer, S. M., Bernasek, S. L., & Scoles, G. (1998). Physisorption and Chemisorption of Alkanethiols and Alkyl Sulfides on Au(111). [doi: 10.1021/jp980047v]. *The Journal of Physical Chemistry B, 102*(18), 3456-3465.

34. Lewinsky, A. A. (2007). *Hazardous Materials and Wastewater*. New York: Nova science publishers.

35. Martell, A. E., & Hancock, R. D. (1996). *Metal complexes in aquoeus solution.*

36. McKetta, J. J. (1998). *Encyclopedia of Chemical Processing and Design* (Vol. 64). New York: Marcel Dekker Inc.

37. Metian, M., Warnau, M., HÃ©douin, L., & Bustamante, P. (2009). Bioaccumulation of essential metals (Co, Mn and Zn) in the king scallop Pecten maximus: seawater, food and sediment exposures. *Marine Biology, 156*(10), 2063-2075.

38. Miledi, R. (1966). Strontium as a Substitute for Calcium in the Process of Transmitter Release at the Neuromuscular Junction. *Nature, 212*(5067), 1233-1234.

39. Narin, I., Soylak, M., Elçi, L., & Dogan, M. (2000). Determination of trace metal ions by AAS in natural water samples after preconcentration of pyrocatechol violet complexes on an activated carbon column. [doi: DOI: 10.1016/S0039-9140(00)00468-9]. *Talanta, 52*(6), 1041-1046.

40. Nogawa, K., Kobayashi, E., Okubo, Y., & Suwazono, Y. (2004). Environmental cadmium exposure, adverse effects and preventive measures in Japan. *BioMetals, 17*(5), 581-587.

41. O'Dell, B. L., & Sunde, R. A. (Eds.). (1997). *Handbook of nutritionally essential mineral elements*. New York: Marcel Dekker, Inc.

42. Ooya, T., & Yui, N. (1999). Synthesis of theophylline-polyrotaxane conjugates and their drug release via supramolecular dissociation. [doi: DOI: 10.1016/S0168-3659(98)00163-1]. *Journal of Controlled Release, 58*(3), 251-269.

43. Plueddemann, E. p. (1982). *Silane coupling agents*. New york: Plenum publishing corporation.

44. Polyakova, I., Poznyak, A., & Sergienko, V. (2009). Crystal and molecular structure of Sr2(Edta) · 5H2O, Sr2(H2 Edta)(HCO3)2 · 4H2O, and Sr2(H2 Edta)Cl2 · 5H2O strontium ethylenediaminetetraacetates. [10.1134/S1063774509020114]. *Crystallography Reports, 54*(2), 236-241.

45. Prado, A. G. S., & Airoldi, C. (2001). Adsorption, preconcentration and separation of cations on silica gel chemically modified with the herbicide 2,4-dichlorophenoxyacetic acid. *Analytica Chimica Acta, 432*(2), 201-211.

46. Prasad, R. N., Agrawal, M., & Sharma, M. (2003). MIXED LIGAND COMPLEXES OF ALKALINE EARTH METALS: PART-X. Mg(II), Ca(II), Sr(II) and Ba(II) COMPLEXES WITH 5-BROMOSALICYLALDEHYDE AND b-DIKETONES. *Journal of the Chilean Chemical Society, 48*, 1-5.

47. Raja, K., Hazarey, V., Peters, T., & Warnakulasuriya, S. (2007). Effect of areca nut on salivary copper concentration in chronic chewers. *BioMetals, 20*(1), 43-47.

48. Sarkar, A. R., Datta, P. K., & Sarkar, M. (1996). Sorption recovery of metal ions using silica gel modified with salicylaldoxime. [doi: DOI: 10.1016/0039-9140(96)01953-4]. *Talanta, 43*(11), 1857-1862.

49. Thomas G. Spiro, W. M. S. (1980). *Environmental science in perspective*. New york: State university of New York Press, Albany.

50. Tong, A., Akama, Y., & Tanaka, S. (1990). Selective preconcentration of Au(III), Pt(IV) and Pd(II) on silica gel modified with [gamma]-aminopropyltriethoxysilane. [doi: DOI: 10.1016/S0003-2670(00)82778-6]. *Analytica Chimica Acta, 230*, 179-181.

51. Vansant, E. F., Van der voot, P., & Vrancken, K. C. (1995). *Charachterization and chemical modification of silica surface* (1 ed. Vol. 93). Amsterdam: Elsevier.

52. Vuchkova, L., & Arpadjan, S. (1996). Behaviour of the dithiocarbamate complexes of arsenic, antimony, bismuth, mercury, lead, tin and selenium in methanol with a hydride generator. [doi: DOI: 10.1016/0039-9140(95)01780-1]. *Talanta, 43*(3), 479-486.

53. Wasiak, W., & Urbaniak, W. (1997). Chemically bonded chelates as selective complexing sorbents for gas chromatography V. Silica chemically modified by Cu(II) complexes via amino groups. [doi: DOI: 10.1016/S0021-9673(96)00683-8]. *Journal of Chromatography A, 757*(1-2), 137-143.

54. Yurieva, A., Poleshchuk, O., & Filimonov, V. (2008). Comparative analysis of a full-electron basis set and pseudopotential for the iodine atom in DFT quantum-chemical calculations of iodine-containing compounds. [10.1007/s10947-008-0073-9]. *Journal of Structural Chemistry, 49*(3), 548-552.

55. Zdravkov, B., Čermák, J., Šefara, M., & Janků, J. (2007). Pore classification in the characterization of porous materials: A perspective. [10.2478/s11532-007-0017-9]. *Central European Journal of Chemistry, 5*(2), 385-395.

56. Zejli, H., de Cisneros, J. L. H.-H., Naranjo-Rodriguez, I., Elbouhouti, H., Choukairi, M., Bouchta, D., et al. (2007). Electrochemical Analysis of Mercury Using a Kryptofix Carbon-Paste Electrode. *Analytical Letters, 40*(14), 2788-2798.

Chapter 4

Conclusion and future studies

The main purpose of our research project was to synthesize materials that have the ability to adsorb high amounts of metal ions. The main advantage of using silica as a base material is its high surface area. The large surface area of these materials results from their extremely porous nature. As a result of these surface modification, pores on the nanometer scale can get physically plugged resulting in a severe reduction in surface area. This defeats the purpose of using these materials for high capacity. So we have used this new method to perform surface modification reactions which results in less loss of porosity than that has been previously described for such materials. So in our research project we achieved one of the primary goals.

The second goal is to create multiple sites for heavy metal adsorption for each molecule that is used for the surface modification reaction. We have used a molecule which has a high affinity for many metal ions, at high heavy metal concentrations in water solutions, adsorbs one metal per surface molecule. This results in a material which can actually bind its weight in mercury; i.e., for each gram of material approximately one gram of mercury can be removed from a water solution. This adsorption capacity is greater than any material that we are aware of.

Diffuse reflectance FTIR spectrometry shows changes after metal adsorption indicated specific metal - organosilane interactions are responsible for the adsorption of metal ions. The theoretical computational calculations were not inconsistence with this logic. But still we don't have any experimental evident to support this.

The quality of the computationally calculated structures must be improved. The reason is the molecular mechanics calculations we used to optimized the Hg(II) EDTA complexes, not gave the experimental N-M-N bond angles, which is much larger compared to the obtained bond angles, that is 88.60° (Arthur E martell, 1996). Threfore as an improvement, calculations by using density functional theory (DFT) , B3LYP method and DGDZVP basis set would be a starting point. As advantages B3LYP DFT method in a DGDZVP gives full-electron basis and generally characterized by smaller computing times (Yurieva, Poleshchuk, & Filimonov, 2008).